FINAL REPORT ~ FHWA-OK-14-15

EVALUATION OF PERFORMANCE OF ASPHALT PAVEMENTS CONSTRUCTED USING INTELLIGENT COMPACTION TECHNIQUES

Sesh Commuri, Ph.D.

Syed Imran

School of Electrical and Computer Engineering

Musharraf Zaman, Ph.D., P.E.

Manic Barman, Ph.D.

Moeen Nazari

School of Civil Engineering and Environmental Science

College of Engineering

The University of Oklahoma

October 2014

EVALUATION OF PERFORMANCE OF ASPHALT PAVEMENTS CONSTRUCTED USING INTELLIGENT COMPACTION TECHNIQUES

FINAL REPORT ~ FHWA-OK-14-15
ODOT SP&R ITEM NUMBER 2246

Submitted to:

John R. Bowman, P.E.
Director of Capital Programs
Oklahoma Department of Transportation
200 N.E. 21st Street, Oklahoma City, OK 73105

Prepared by:

Dr. Sesh Commuri
Dr. Musharraf Zaman
Dr. Manik Barman
Moeen Nazari
Syed Imran
College of Engineering, The University of Oklahoma, Norman, OK 73019

Submitted by:

Office of Research Services
201 David L. Boren Blvd, The University of Oklahoma, Norman, OK 73019

October 2014

TECHNICAL REPORT DOCUMENTATION PAGE

16. ABSTRACT

The long-term performance of asphalt pavements depends on the quality of the subgrade and asphalt layers. Intelligent compaction methods continuously monitor the modulus/stiffness of subgrade and asphalt layers during compaction process and have been proposed for ensuring uniform compaction. The use of the Intelligent Compaction Analyzer (ICA) developed at the University of Oklahoma in Norman, OK in determining the subgrade modulus and asphalt layer density/dynamic modulus during construction was addressed in this project. Several case studies were conducted to demonstrate the application of the ICA in real-time estimation of compaction quality. Results from these case studies show that the ICA was able to estimate the modulus of the stabilized subgrade with accuracy suitable for the control of compaction quality. Similarly, the ICA was found to accurately estimate the density/dynamic modulus of asphalt layers during construction of asphalt pavements. Project results demonstrate that the ICA was helpful in identifying and remediating the under-compacted regions in stabilized subgrades as well as asphalt layers. It was also found that the average subgrade modulus, average asphalt layer density/dynamic modulus, and overall uniformity of compaction could be improved with the use of the ICA.

SI* (MODERN METRIC) CONVERSION FACTORS

APPROXIMATE CONVERSIONS TO SI UNITS

SYMBOL	WHEN YOU KNOW	MULTIPLY BY	TO FIND	SYMBOL
LENGTH				
in	inches	25.4	millimeters	mm
ft	feet	0.305	Meters	m
yd	yards	0.914	Meters	m
mi	miles	1.61	kilometers	km
AREA				
in^2	square inches	645.2	square millimeters	mm^2
ft^2	square feet	0.093	square meters	m^2
yd^2	square yard	0.836	square meters	m^2
ac	acres	0.405	hectares	ha
mi^2	square miles	2.59	square kilometers	km^2
VOLUME				
fl oz	fluid ounces	29.57	milliliters	mL
gal	gallons	3.785	Liters	L
ft^3	cubic feet	0.028	cubic meters	m^3
yd^3	cubic yards	0.765	cubic meters	m^3
NOTE: volumes greater than 1000 L shall be shown in m^3				
MASS				
oz	ounces	28.35	Grams	g
lb	pounds	0.454	kilograms	kg
T	short tons (2000 lb)	0.907	mega grams (or "metric ton")	Mg (or "t")
TEMPERATURE (exact degrees)				
^{o}F	Fahrenheit	5 (F-32)/9 or (F-32)/1.8	Celsius	^{o}C
ILLUMINATION				
fc	foot-candles	10.76	Lux	lx
fl	foot-Lamberts	3.426	candela/m^2	cd/m^2
FORCE and PRESSURE or STRESS				
lbf	poundforce	4.45	newtons	N
lbf/in^2	poundforce per square inch	6.89	kilopascals	kPa

APPROXIMATE CONVERSIONS FROM SI UNITS				
SYMBOL	**WHEN YOU KNOW**	**MULTIPLY BY**	**TO FIND**	**SYMBOL**
LENGTH				
mm	millimeters	0.039	inches	in
m	meters	3.28	Feet	ft
m	meters	1.09	yards	yd
km	kilometers	0.621	miles	mi
AREA				
mm^2	square millimeters	0.0016	square inches	in^2
m^2	square meters	10.764	square feet	ft^2
m^2	square meters	1.195	square yards	yd^2
ha	hectares	2.47	acres	ac
km^2	square kilometers	0.386	square miles	mi^2
VOLUME				
mL	milliliters	0.034	fluid ounces	fl oz
L	liters	0.264	gallons	gal
m^3	cubic meters	35.314	cubic feet	ft^3
m^3	cubic meters	1.307	cubic yards	yd^3
MASS				
g	grams	0.035	ounces	oz
kg	kilograms	2.202	pounds	lb
Mg (or "t")	megagrams (or "metric ton")	1.103	short tons (2000 lb)	T
TEMPERATURE (exact degrees)				
ºC	Celsius	1.8C+32	Fahrenheit	ºF
ILLUMINATION				
lx	lux	0.0929	foot-candles	fc
cd/m^2	candela/m^2	0.2919	foot-Lamberts	fl
FORCE and PRESSURE or STRESS				
N	newtons	0.225	poundforce	lbf
kPa	kilopascals	0.145	poundforce per square inch	lbf/in^2

*SI is the symbol for the International System of Units. Appropriate rounding should be made to comply with Section 4 of ASTM E380.

LIST OF ACRONYMS

1) CKD – Cement kiln dust

2) DCP – Dynamic cone penetrometer

3) FWD – Falling weight deflectometer

4) ICA – Intelligent Compaction Analyzer

5) LL – Liquid limit

6) MDD - Maximum dry density obtained by standard Proctor test

7) M_f – FWD modulus

8) M_{f-0} – FWD modulus after 0 day of curing

9) M_{f-7} – FWD modulus after 7 days of curing

10) M_{f-28} – FWD modulus after 28 days of curing

11) M_i – ICA modulus

12) M_r – Resilient modulus

13) M_{r-0} – Resilient modulus after 0 days of curing

14) M_{r-7} – Resilient modulus after 7 days of curing

15) M_{r-28} – Resilient modulus after 28 days of curing

16) NDG – Nuclear density gauge

17) ODOT– Oklahoma Department of Transportation

18) OkTC – Oklahoma Transportation Center

19) OMC – Optimum moisture content

20) PI – Plasticity index

21) PL – Plastic limit

22) PQI – Pavement quality indicator

23) γ_{dmax} – Maximum dry density obtained by standard Proctor test

24) σ_d – Deviotoric stress

25) σ_3 – Confining pressure

TABLE OF CONTENTS

LIST OF FIGURES

LIST OF TABLES

EXECUTIVE SUMMARY

Long-term performance of asphalt pavements depends on the quality of the supporting subgrade, among other factors. A well designed and compacted subgrade would drain well, have high strength, and have adequate load bearing capacity to support the pavement layers. Preparation of subgrade for an asphalt pavement typically requires stabilization of soil using cementitious additives such as Cement Kiln Dust (CKD), fly-ash and lime, and subsequent compaction using vibratory rollers. Quality control during preparation of subgrade is usually limited to taking spot readings of density and moisture content using a Nuclear Density Gauge (NDG). In some instances, Dynamic Cone Penetration (DCP), Falling Weight Deflectometer (FWD) or similar tests are conducted to determine the quality of compaction of the compacted subgrade. These tests, however, need additional time and money and often do not adequately reveal deficiencies in the preparation of the site. Intelligent Compaction (IC) techniques have been proposed to continuously monitor the quality of compaction of the subgrade during the compaction process and to alter the machine parameters to ensure uniform compaction. These technologies are gaining popularity due to their ability to estimate the level of compaction of pavement layers continuously during construction.

The Intelligent Compaction Analyzer (ICA) was developed at the University of Oklahoma. This tool was initially developed to estimate the density of asphalt pavements in real-time during construction. During 2008-2012, the ICA was demonstrated during the construction of asphalt pavements at several sites across the country. The application of the ICA was also extended to estimate the stiffness of asphalt pavements during compaction. The application of the ICA to study the level of compaction of stabilized subgrades was investigated during 2010-2012.

The ICA is based on the hypothesis that the vibratory roller and the underlying pavement form a coupled system whose response during compaction is influenced by the stiffness of the pavement layers. During field compaction, the ICA is first trained to recognize the vibration patterns and the trained ICA is then calibrated to convert these patterns into a numerical value indicative of the density/modulus of the layers being compacted. In previous projects (Commuri et al. 2013, Barman et al., 2013; Singh et al., 2011; and Commuri, 2010), the ICA was used to determine the quality of compaction of stabilized subgrade as well as asphalt layers during construction. The ICA was capable of generating as-built maps providing information on coverage and quality of compaction of the constructed pavement. While the use of the ICA in estimating the quality of compaction of asphalt layers and stabilized subgrade was investigated, its use in improving the quality of compaction was not studied. Several case studies are considered in the current project to demonstrate the use of compaction quality parameters (density and dynamic modulus for the asphalt layer(s), and density and modulus for stabilized subgrade), estimated in real-time by the ICA, to improve the quality of asphalt layers and stabilized subgrades during construction.

Specifically, six case studies were undertaken in the current project to demonstrate the following: (i) ability of the ICA to estimate the density/modulus of stabilized subgrade and asphalt layers, and (ii) use the estimated density/modulus to identify and remediate inadequately compacted areas. In the first two case studies, in which the Intelligent Compaction was demonstrated on the two CKD-stabilized subgrades, Intelligent Compaction data were used to refine the method for estimating the ICA modulus (M_i) (Barman et al. 2014) in real-time. The ICA modulus is the modulus estimated from the ICA vibration data and is comparable to the laboratory resilient modulus (M_r) of subgrade. The ICA modulus is equivalent to the laboratory subgrade M_r when the stress state in the M_r test is equivalent to the stress state existing in the field. This refined method was then implemented in Case Studies 3 and 4 to demonstrate the

use of the ICA in improving the quality of compaction of CKD-stabilized subgrades. In Case Study 3, the use of the ICA in improving the compaction quality of CKD-stabilized subgrade was demonstrated during the reconstruction and widening of I-35 near the intersection of I-35 and Main Street in Norman, Oklahoma. In Case Study 4, the use of the ICA in monitoring compaction quality was demonstrated during the extension of the I-35 service Road from the Kohl's shopping center to NW 24th Avenue in Norman, Oklahoma.

In both Case Studies 3 and 4, a smooth steel drum vibratory roller equipped with the ICA was used for proof rolling the CKD-stabilized subgrades that were previously compacted using a sheep-foot roller. The compaction quality of the CKD-stabilized subgrade was recorded continuously in terms of M_i during the proof rolling process. Several test locations were marked on the compacted subgrade; the moisture content and dry density were recorded using a NDG. The method developed in Case Studies 1 and 2 was used to estimate the M_i values at the selected test locations. The respective GPS coordinates of the test locations were used to determine the M_i values at these locations. A comparison was made between M_i and M_r of the representative CKD-stabilized soil. It was found that the ICA can estimate the subgrade modulus with an accuracy suitable for quality control purposes in the field. As-built maps developed using the M_i values were used to identify areas with inadequate compaction. Remedial rolling was performed at these locations to investigate whether the level of compaction of the CKD-stabilized subgrade can be improved, and the compacted CKD-stabilized subgrade be made more uniform.

In the last two Case Studies, the use of the ICA in improving the quality of compaction of asphalt layers was demonstrated. The ICA was installed on a dual steel drum vibratory roller and calibrated to estimate the density of asphalt layers. During the compaction process, the ICA-estimated density was recorded continuously for each roller pass. After the compaction of

the stretch, test locations were marked on the compacted asphalt layer and the density was recorded at these locations using a NDG. Cores were then extracted from these test locations and their density was measured in the laboratory. A comparison was made between the ICA-estimated density and the core density. It was seen that the ICA can estimate the density with an accuracy suitable for quality control in the field. As was done in the previous case, after the stretch was compacted, the as-built map generated by the ICA was used to identify under-compacted areas. Remedial rolling was carried out on these areas; cores were extracted for determining core density at those test locations. A comparison between the core densities and ICA-estimated densities shows that the overall density improved as a result of the remedial rolling. Further, the variance of these densities about their mean was smaller than the variance observed during the traditional compaction process.

The following are the key results from the six case studies concluded in this project:

1. The current study was limited to the installation of the ICA on a smooth steel drum vibratory roller. It was found that the sensors and the computational hardware of the ICA used to estimate the density of asphalt layers could also be used for compaction of stabilized subgrade without significant modifications. The ICA software, on the other hand, had to be modified to account for differences in the calibration method for the stabilized subgrade and the analysis of the vibration data.

2. Regression models were developed for estimation of resilient modulus for a given soil and stabilizing agent using laboratory data from resilient modulus tests conducted according to the AASHTO T 307 test method. Given the soil type and stabilizing agent, these models can estimate the resilient modulus of the stabilized soil for a given dry density and moisture content. It was found that these regression models can predict the

resilient modulus with less than 20% error ($R^2 > 0.81$). These regression models provide a way to compare the M_i with M_r values.

3. The regression model noted under Item 2 was used to calibrate the ICA. NDG readings were taken at different test locations after the proof rolling of the compacted subgrade. Moisture content and density obtained from the NDG readings were then used to estimate field equivalent resilient modulus. A comparison between the M_i and field equivalent M_r obtained from the regression models demonstrated that the ICA was able to estimate moduli of the compacted stabilized subgrade with an acceptable level of accuracy ($R^2 > 0.60$).

4. As-built maps generated during the compaction of CKD-stabilized subgrades were used to identify areas where the M_i values were lower than the rest of the compacted subgrade. In Case Study 3, two such areas were identified on the subgrade that was initially compacted with the traditional procedure. Immediately after the traditional compaction, NDG tests were performed at three random locations on each of these two areas. Subsequently, two remedial passes were provided on those two areas with the smooth drum roller that was used for the proof rolling. Following the remedial compaction, it was found that the average M_i improved from 202 MPa to 212 MPa. Further, the standard deviation M_i decreased from 12 MPa to 9 MPa. This shows that the use of the ICA resulted in an improvement in the subgrade modulus and at the same time the quality of compaction of the subgrade became more uniform.

5. The ICA was able to estimate the density of asphalt layers with an accuracy level suitable for quality control purposes during construction. It was found that the ICA was able to estimate the asphalt layer density within 0.7% of core density (in terms of percentage of maximum theoretical density (MTD)) in over 99% of test locations.

6. The as-built map generated by the ICA was used to identify under-compacted areas during compaction in Case Studies 5 and 6. Remedial rolling on these areas increased the average density by 0.4% of MTD with a corresponding decrease in standard deviation from 0.6% to 0.4% of MTD. This shows that the use of the ICA enabled the roller operator to improve both the level and the uniformity of compaction as compared to that which could be achieved with the traditional rolling.

Future Works and Recommendations

The case studies carried out in the current project demonstrate the advantage of obtaining reliable and accurate estimates of the quality of compaction in real-time during the construction of the pavements. Such estimates can not only provide real-time feedback of the quality of compaction to the roller operator, but can also be used to identify and remediate under-compacted regions and thereby improve the overall quality of compaction of both stabilized subgrades and asphalt layers. In the coming year, extensive contractor-led testing is planned to independently validate the use of ICA in improving the quality of pavement layers during construction.

Some of the problems encountered during the study are:

1) Difficulty in coordinating field test schedules with construction schedules as IC is not a requirement in the project specifications.

2) Selection of number of test locations is constrained by project schedules and weather conditions.

3) Availability of construction sites that meet project requirements such as layer thickness and length of the pavement for demonstration is an ongoing challenge.

4) Verification of the impact of IC-based construction on the performance of pavements is hard to ascertain unless the entire pavement is constructed using IC techniques and evaluated periodically.

6) Contractors and pavement professionals are still unclear on the functionality and benefits of IC techniques. Lack of information about specifications and incentives for implementation of IC is also a limiting factor in the early adoption of the technology.

Based on the experience gained from the current study, the following recommendations are made for studying the performance of ICA in greater detail and to further the early acceptance of Intelligent Compaction methods:

1) The necessary specification or a special provision shall be developed for Intelligent Compaction of both the stabilized subgrades and asphalt layers;

2) Intelligent Compaction shall be considered as a requirement in the bidding of the work;

3) Workshops and training programs shall be conducted for providing necessary training to the construction crews;

4) ICA technology shall be demonstrated on more construction sites varying with soil type, additive type and asphalt layer property to study the influence of these parameters on the ICA-estimated compaction quality parameters (ICA modulus of subgrade, density of subgrade, density of asphalt layer, dynamic modulus of asphalt layer);

5) Research studies shall be carried out to study the long-term benefits of the Intelligent Compaction;

6) The closed-loop control of vibratory compactors during Intelligent Compaction of subgrade and asphalt layers shall be considered in future projects.

The research team is working with ODOT and contractors to identify additional sites for demonstrating the ICA technology. In follow up work that is currently being pursued, the research team is assisting ODOT in the preparation and implementation of the IC specifications. The extension of the ICA to compaction of subgrades with lime and fly-ash additives, compaction of cohesive soils, compaction of granular aggregate bases, and closed-loop control of vibratory compactors during Intelligent Compaction of soils and asphalt pavements are topics planned for future projects.

1. INTRODUCTION

Improving the quality of asphalt pavements during construction can greatly enhance their performance and longevity. Lack of adequate tools to determine the quality of compaction of the entire pavement in a non-destructive manner is a limiting factor in the construction of long lasting roads. Tools that can estimate the quality of compaction in real-time can help avoid over/under-compaction during construction. Construction of high quality roads can help minimize pavement distresses such as rutting, cracking, and other forms of distresses, and improve the long-term performance of the pavement.

In recent years, several equipment manufacturers have proposed Intelligent Compaction (IC) as a means of achieving uniformity in compaction of subgrades and asphalt layers (FHWA, 2009). Over the last decade, the Principal Investigators (PIs) of the current project have developed the Intelligent Asphalt Compaction Analyzer (IACA) technology to estimate quality of compaction of asphalt pavements during construction (Commuri et al., 2011; Commuri, 2010; Commuri and Zaman, 2009 and 2008). In collaboration with industry partners, the use of this technology was demonstrated in estimating the density (Commuri et al., 2011; Commuri 2010) and dynamic modulus[1] ($|E^*|$) (Singh et al., 2011) of asphalt layers in several construction projects. During 2010-2012, this technology was extended to estimate the density[2] and modulus of stabilized subgrades during construction (Barman et al. 2014; Imran et al. 2014; Barman et

---

[1] In this report, "modulus" is used as an indicator of "stiffness." The stiffness of the compacted layer is a function of its modulus and cross-sectional properties.

[2] In this report, "density", which is more commonly used in the literature, is used instead of "unit weight".

al., 2013). The extended technology is called Intelligent Compaction Analyzer (ICA). This terminology is used in this report.

During 2008-2012, the ICA was demonstrated to estimate the quality of compaction of asphalt layers (density and dynamic modulus) and stabilized subgrade (density and ICA modulus (M_i)) in real-time during construction. The ICA modulus is the subgrade modulus estimated by the ICA and is comparable to the resilient modulus obtained from laboratory test data. The ICA modulus is equivalent to the laboratory resilient modulus when the state of stress in the M_r test is equivalent to the state of stress in the field. As-built maps showing the compaction quality parameters (density/dynamic modulus/ICA modulus) were developed in real-time. However, these compaction quality parameters were not employed in improving the quality of construction. In the current project, the aim was to demonstrate the use of the compaction quality parameters available in real-time to identify and remediate inadequately compacted regions or regions of stabilized subgrades and asphalt layers.

1.1. INTELLIGENT COMPACTION TECHNOLOGY

Intelligent Compaction (IC) techniques are based on the hypothesis that the roller and the pavement form a coupled system whose response to vibratory compaction is influenced by the properties of the layers being compacted. In the compaction process, the stiffness of the underlying layer(s) increases and as a consequence, the vibration patterns experienced by the roller change. The amplitude and frequency of these vibrations, therefore, can be used to measure the properties of the layer (asphalt, soil, aggregate, etc.) being compacted. Sandstrom (1998) utilized the frequency and amplitude of vibration of the roller to compute the shear modulus and a "plastic" parameter of subgrade. These values were then used to adjust the velocity, frequency and amplitude of the roller for optimal compaction of the subgrade. Thurner (1978) and Minchin (1999) estimated the degree of compaction by comparing the amplitude of

the fundamental frequency of vibration of the roller with the amplitudes of its harmonics. By relating the ratio of the second harmonic of the vibratory signal to the amplitude of the third harmonic, Minchin (1999) was able to predict the compacted density with 80% accuracy, in some cases. Swanson et al. (2000) tried to correlate the properties of asphalt mix and site characteristics with variations seen in the vibratory responses of a compactor. Jaselskis (1998), on the other hand, measured the density of asphalt layer by a completely different approach using microwave signals. In that research, Jaselskis (1998) transmitted a microwave signal through the asphalt layer and estimated its density based on the transmission characteristics of the wave. While the above techniques have been successful in demonstrating the feasibility of the respective approaches, they have not been able to overcome some of the inherent limitations of the methods pertaining to commercial applications.

In general, the Intelligent Compaction technology possesses the following benefits on the overall quality of the pavements (Chang, 2011; Maupin, 2007; Zambrano et al., 2006; Camargo et al., 2006; Peterson and Petersen, 2006; White et al., 2006; Petersen, 2005; Briaud and Seo, 2003):

(i) A complete coverage of the compaction area;

(ii) Uniform compaction;

(iii) Reduced construction cost;

(iv) Reduced life-cycle cost by increasing the service life of the pavement;

(v) Improved management and control of the compaction process;

(vi) As-built map of the compaction quality parameter(s) for the constructed pavement; and

(vii) Stored information for later use in forensic analysis and pavement management.

1.2. UNIVERSITY OF OKLAHOMA INTELLIGENT COMPACTION ANALYZER (ICA)

The ICA is based on the hypothesis that the vibratory roller and the underlying pavement layers form a mechanically coupled system. The response of the roller is determined by the frequency of the vibratory motors and the natural vibratory modes of the coupled system. The vibration of the roller varies with the stiffness of the underlying pavement layer(s). The vibration spectra of the roller can, therefore, be used to estimate the stiffness of the pavement layer(s). The ICA is mounted on a vibratory roller and is equipped with a measurement system that can continuously monitor and record the compaction level of the layer(s) underneath. A GPS-based documentation system is installed for continuous recording of the spatial location of the roller. A user-interface is incorporated to display the real-time operational parameters such as compaction level, temperature of pavement, number of roller pass, direction of roller, GPS location of the roller, and a color coded as-built map showing the compaction level at each location.

Figure 1.1 shows a vibratory roller equipped with the ICA technology. The functional modules of the ICA are shown in Figure 1.2. The sensor module (SM) in the ICA consists of accelerometer(s) for measuring the vibrations of the roller. A user-interface for specifying the amplitude and frequency of the vibration motors and for recording the soil type is also a part of the SM. The feature extraction (FE) module computes the Fast Fourier Transform of the input signal and extracts the features corresponding to vibrations at different salient frequencies. The Neural Network (NN) classifier is a multi-layer Neural Network that is trained to classify the extracted features so that each class represents a vibration pattern specific to a pre-specified level of compaction. The Compaction Analyzer (CA) then post-processes the output of the NN and estimates the compaction level parameters (density/dynamic modulus/ICA modulus) in real-

time. Further details on the components of the ICA and its installation procedure are covered in the User Manual as provided in Appendix.
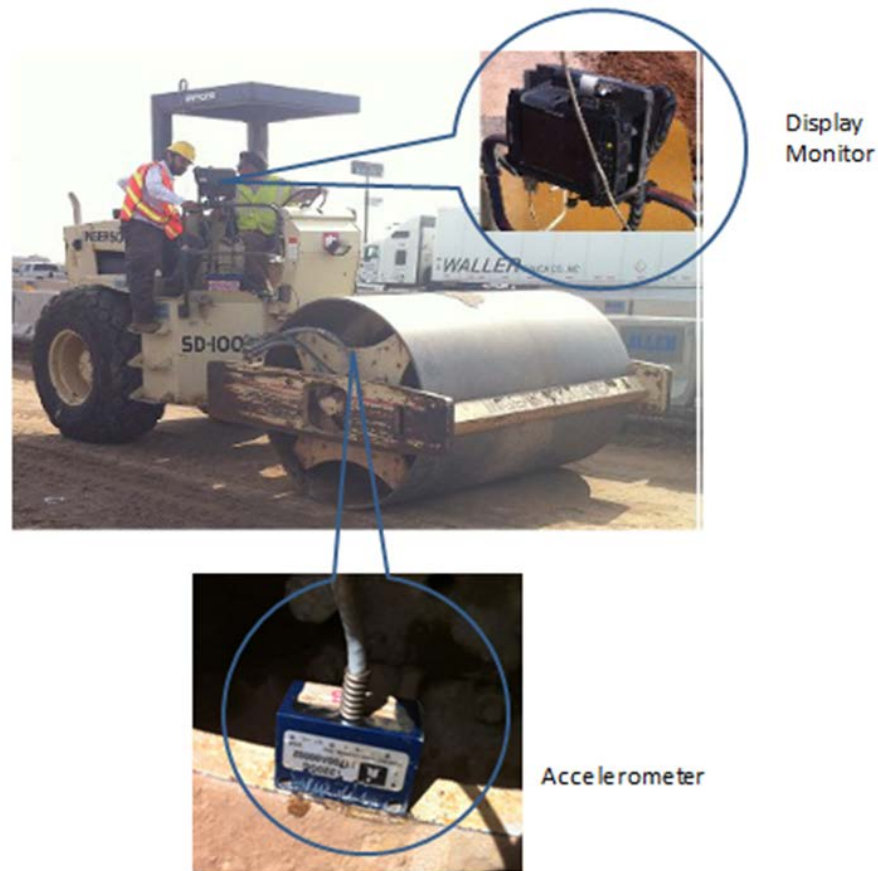
Figure 1.1. A vibratory roller equipped with the ICA technology in operation.
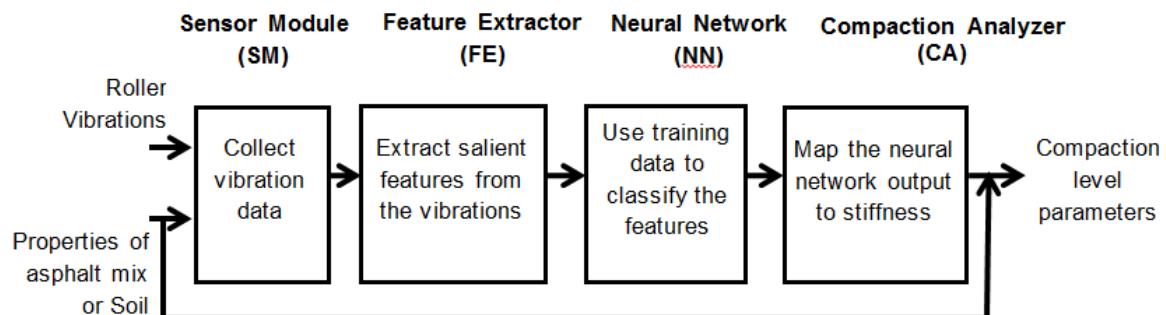
Figure 1.2. Flowchart of modules involved in estimation of compaction parameters by the ICA.

1.3. GOALS AND OBJECTIVES

The main goal of this project was to demonstrate the use of the ICA in improving the quality of compaction of stabilized subgrades and asphalt layers during construction. The ICA technology was developed at the University of Oklahoma and its use in estimating compaction quality parameters (density/dynamic modulus/ICA modulus) in real-time was demonstrated in several field projects. The goal of the present study is to investigate the use of this technology in identifying and remediating under-compacted regions during construction of stabilized subgrades and asphalt layers. In this report, this particular compaction procedure, in which the ICA measurements are recorded and monitored throughout the compaction process, under-compacted regions are identified using the as-built maps and then remediated with additional roller passes, is referred to as the ICA compaction procedure.

The specific objectives of the current project are listed below:

1. Demonstrate the ability of the ICA to estimate the density and/or modulus of stabilized subgrades in real-time;

2. Utilize the as-built map of density and/or ICA modulus to manually adjust the roller path to improve the quality of compaction of stabilized subgrades;

3. Demonstrate the ability of the ICA to estimate the density and/or dynamic modulus of asphalt layers in real-time;

4. Utilize the as-built map of density and/or dynamic modulus to manually adjust the roller path to improve the compaction quality of asphalt layer(s);

5. Compare the improvement in quality of compaction obtained through the use of the ICA with that obtained by conventional compaction techniques for both stabilized subgrades and asphalt layers;

6. Study the effect of improved quality on the performance of the pavement over a period of one year from its construction.

1.4. STUDY TASKS

In order to achieve the stated goals and objectives, the ICA technology was demonstrated at four different sites under the current study. Among these four sites, two sites involved compaction of CKD-stabilized subgrades and the other two sites involved compaction of asphalt layers. The following tasks were planned for the CKD-stabilized subgrades and the asphalt layers.

A. Compaction of CKD-stabilized subgrades

1. Identification of construction sites;
2. Characterization of natural subgrade soil and CKD-stabilized soil (mixture of soil and CKD) mixes;
3. Conducting resilient modulus test;
4. Development of regression models for resilient modulus of CKD-stabilized soil;
5. Calibration of the ICA for compaction of the CKD-stabilized subgrade;
6. ICA measurements;
7. Identification and remediation of under-compacted regions;
8. Validation of the ICA-estimated compaction parameters (density and ICA modulus); and
9. Improvement of compaction quality by the use of the ICA.

B. Compaction of asphalt layers

1. Identification of construction sites;

2. Characterization of asphalt mixes;

3. Calibration of the ICA for compaction of asphalt layers;

4. ICA measurements;

5. Identification and remediation of under-compacted regions;

6. Validation of the ICA-estimated compaction parameters (density and dynamic modulus);

7. Improvement of compaction quality by the use of the ICA; and

8. Periodic evaluation of the pavements constructed in Year I.

2. METHODOLOGY FOR SUBGRADE COMPACTION WORK

During subgrade compaction, the quality control is usually performed by monitoring moisture content and dry density at selected locations. In some cases, additional tests such as Dynamic Cone Penetrometer (DCP) and Falling Weight Deflectometer (FWD) are performed at randomly selected locations to check the quality of compacted subgrade. However, randomly selected locations do not adequately represent the quality of the entire compacted subgrade, and may leave under-compacted region(s). In order to design a long lasting pavement, Mechanistic-Empirical Pavement Design Guide (MEPDG) (ARA 2004) recommends the use of resilient modulus (M_r) for characterizing the subgrade. However, this property is seldom evaluated during the compaction of subgrade. Therefore, it remains uncertain if the design M_r is achieved during the construction process. The current project investigates the feasibility of using the ICA in estimating the level of compaction in terms of both compacted density and ICA modulus.

During the first six months of the project, the research team developed a methodology for evaluating the ICA modulus of stabilized subgrades during compaction. Field and laboratory test results from two previously completed projects (Commuri et al., 2013) were used to develop this methodology. This methodology was then used to evaluate the ability of the ICA in estimating the M_i throughout the remaining duration of the project. The following sections discuss various tasks performed for compaction of stabilized subgrades.

2.1. IDENTIFICATION OF SITES

Early identification of suitable sites is necessary to verify its suitability for the demonstration of ICA's capability in real-time measurement of compaction quality. Establishing proper communication with the contractor and the project crew is also essential for coordination of on-

site activities. Accessibility of the site is another important consideration as it can impede the research team's ability to carry out the demonstration and conduct validation tests. The research team worked closely with the ODOT, Oklahoma Asphalt Pavement Association and soil and asphalt contractors such as Silver Star Construction Company and Haskel-Lemon Construction Company for identification of project sites.

2.2. CHARACTERIZATION OF NATURAL AND STABILIZED SUBGRADE SOILS

Once the site was identified, the research team coordinated with the construction company to obtain the construction schedule. The construction schedules were used to plan the demonstration activities. After the site was prepared and the existing soil layer was graded during the construction process, bulk soil was collected and brought to the OU Broce Laboratory at the University of Oklahoma. The stabilizing agent used in the construction (CKD) was also collected. The processed soil was mixed with the additive to replicate the composition of the stabilized soil used in the field. Tests were conducted to determine particle size distribution (ASTM D6913), Atterberg's limits (ASTM D4318) and moisture–density relationship (ASTM D698) for the characterization of both natural and stabilized soils.

2.3. RESILIENT MODULUS TEST ON THE STABILIZED SOIL

Resilient modulus tests were conducted on the stabilized soil mix as per AASHTO T307-99. Resilient modulus tests were condcuted at different moisture contents and dry densities so that the variations of these two parameters in the field are covered. Resilient modulus tests were conducted at 15 different combinations of stress states (deviatoric stress and confining pressure). The test data were used to develop regression models. These models were used to calibrate and validate the ICA modulus.

2.4. REGRESSION MODELS FOR RESILIENT MODULUS

A comparitive analysis between the ICA modulus and other measurements taken on a compacted subgrade requires the knowledge of the level of compaction at each location on the subgrade. Since conventional spot tests do not reveal the level of compaction and tests such as FWD may be time-consuming and expensive, regression models were first developed to relate moisture content and dry density, obtained from spot tests using a NDG, to the resilient modulus of stabilized soils determined from laboratory tests assuming conditions similar to those observed in the field. The state of stress in the subgrade under the roller is not easily measureable and is beyond the scope of the current project. Therefore, the state of stress was assumed based on the data in literature (Mooney and Reinhart, 2009).

2.5. CALIBRATION OF THE ICA

The ICA measures and analyses the roller vibrations to provide continuous, real-time estimates of subgrade modulus during compaction. Therefore, the ICA has to be calibrated for the specfic roller and for the field conditions before it can be used to estimate the modulus of the subgrade. In the current project, this calibration was carried out on a 10-meter long test stretch. The calibration was carried out during the proof rolling of this stretch. The subgrade was initially compacted by a pad-foot roller and then by a smooth drum vibratory roller equipped with the ICA. According to general calibration procedure, several readings were taken using the NDG prior to proof rolling, to determine the initial and the target M_r. The vibrations and the spatial locations of the roller were recorded during the proof rolling process. A preliminary calibration was performed using the vibration measurements and the initial and target M_r values. After proof rolling of the calibration stretch by the smooth drum vibratory roller, dry densities and moisture contents were measured by an NDG at three selected locations, 3 meters apart, along

the centerline of the lane being compacted. The moisture contents and dry densities measured at these three points were used to compute the resilient moduli at these points. The final calibration was done by comparing the estimated and the measured moduli at the three test locations (similar to the process described in the ICA User Guide in Appendix).

2.6. ICA MEASUREMENTS

The calibrated ICA was used to record compaction data such as spatial location and vibrations of the roller, the speed and operational settings of the roller, and the ICA modulus of the subgrade during the entire proof rolling of the subgrade. Degree of compactions were also recorded whenever it was required. The degree of compaction is the ratio of the dry density measured at a point (γ_d) to the maximum dry density (γ_{dmax}), obtained by the standard Proctor test. The data was geo-referenced using the GPS coordinates of the roller collected during the compaction process. The ICA utilities were used to study the roller path, M_i achieved during each pass, and the overall stiffness achieved for each stretch. The as-built maps were used to determine under-compacted regions for remedial rolling.

2.7. IDENTIFICATION AND REMEDIATION OF UNDER-COMPACTED REGIONS

One of the key objectives of the current project is to evaluate the ability of the ICA to identify under-compacted regions during the proof rolling process in the traditional compaction procedure. In order to identify the under-compacted regions with the traditional compaction procedure, the roller operator initially followed the compaction process that is normally used. During the traditional compaction process, the compaction level was monitored by the ICA in real-time, and the under-compacted regions were identified. The under-compacted regions were the regions where the M_i values were significantly lower than the average M_i observed on the entire stretch. After the completion of the traditional compaction procedure, as-built maps were

generated to determine the location of the under-compacted regions. The GPS coordinates of these locations were used to plan additional roller passes to improve the level of compaction. Remedial rolling was performed at these locations until target M_i values were achieved and the variations of the M_i on the entire compacted subgrade became low.

2.8. VALIDATION OF THE ICA-ESTIMATED COMPACTION LEVEL

The ICA-estimated compaction levels were validated by comparing them with the compaction levels measured by spot-test devices such as NDG, DCP and FWD. In this project, NDG measurements (moisture contents and dry densities) were recorded right after the traditional compaction. NDG readings were taken at randomly selected locations along the compacted subgrade. The NDG measurements were also taken in the vicinity of the areas that were initailly identified as under-compacted regions. In such regions, NDG measurements were taken before and after the remedial compaction.

DCP and FWD testing were conducted on the finished subgrade when feasible for validating the ICA-estimated compaction levels. The test locations were selected at random on the compacted subgrade and their GPS coordinates were recorded. The recorded GPS coordinates were then used to determine the corresponding M_i values at these locations. While the DCP test was conducted on the same day of the subgrade compaction, FWD test was usually conducted at a later date depending on the availability of the FWD. The validation of the M_i values was performed by comparing the M_i values with the M_r, FWD moduli (M_f) and DCP indices.

3. CASE STUDY 1: SUBGRADE COMPACTION (60TH STREET)

3.1. IDENTIFICATION OF SITE

The ability of the ICA in estimating the density and ICA modulus of a subgrade was studied during the construction of a 3.4-kilometer (2.127-mile) long full-depth asphalt pavement on 60th Street, Norman, OK. This stretch is located between Tecumseh Road and Franklin Road in north-west Norman. The subgrade soil was stabilized by mixing 10% CKD to a depth of 202 mm (8 inches). A smooth drum vibratory roller was used for proof rolling. This roller is a single smooth drum roller. The base layer over the subgrade was constructed with two separate asphalt layers. The thickness of each layer was 90 mm (3.5 inch). The first layer was constructed using a S3 mix with P G64-22 OK binder. The second layer was also constructed using a S3 mix with PG 76-28 OK binder. The surface course was a 51-mm (2-inch) thick layer comprising of a S4 mix with PG 76-28 OK binder. The construction at this site was carried out by Silver Star Construction, Moore, OK between May, 2012 and June, 2012.

3.2. CHARACTERIZATION OF NATURAL AND STABILIZED SUBGRADE SOILS

Bulk subgrade soil (unstabilized) and CKD samples were collected from the construction site. The liquid limit (LL), plastic limit (PL) and plasticity index (PI) of the subgrade soil were found to be 23%, 19% and 4%, respectively. Based on the Unified Soil Classification System (USCS), it was classified as a CL-ML soil. As per the AASHTO classification, it was an A-4 soil. The optimum moisture content (OMC) and the maximum dry density (γ_{dmax}) of the CKD-stablized

mix were found as 4.6% and 17.3 kN/m^3, respectively. RESILIENT MODULUS TEST ON STABILIZED SOIL

Resilient modulus tests were performed on five specimens. Test specimens were prepared by mixing processed subgrade soil with 10% CKD, by weight of the soil. The test parameters were selected so as to closely replicate typical moisture contents and dry density range observed in the field. Table 3.1 lists the moisture content and degree of compaction for each of the five compacted specimens.

In accordance with the AASHTO T307-99 specifications, each specimen was tested with 15 different combinations of deviatoric stresses (σ_d) (13.78, 27.56, 41.34, 55.12 and 68.9 kPa) and confining pressures (σ_3) (13.78. 27.56 and 41.34 kPa). Specimens were tested at both 0- and 28-day curing periods. In this report, the M_r at 0- and 28-day curing periods are referred to as M_{r-0} and M_{r-28}, respectively.

Table 3.1. Moisture content, dry density and degree of compaction values for the five resilient modulus test specimens for the 60th Street project.

Specimen No.	Moisture content (%)	Dry density (kN/m^3)	Degree of compaction (% of γ_{dmax})	k_1, k_2 and k_3 based on M_{r-0}		
				k_1	k_2	k_3
1	12.1	17.26	98	6511.07	0.082	-0.154
2	12.4	17.12	97	5830.80	0.091	-0.194
3	12.1	17.20	97	6310.23	0.082	-0.163
4	14.7	17.43	99	5926.52	0.173	-0.257
5	14.8	17.56	99	6346.92	0.177	-0.241

3.3. REGRESSION MODELS FOR RESILIENT MODULUS

Regression models were developed based on the laboratory resilient modulus test results as a function of moisture content (M_c), dry density (γ_d) and stress state (σ_d and σ_3). A comprehensive discussion on the procedure for the M_r regression models can be found in Commuri et al. (2013). Regression models were developed using 80% of the test data. These

data were randomly selected. The developed models were then validated using the remaining 20% of the test data.

A number of models are available in the literature for predicting M_r (AASHTO 1993). The following model (AASHTO 1993) was used to predict M_r in this study.

$$M_r = k_1 p_a \left(\frac{\theta}{p_a}\right)^{k_2} \left(\frac{\sigma_d}{p_a}\right)^{k_3} \tag{3.1}$$

where k_1, k_2 and k_3 are regression coefficients; p_a is the atmospheric pressure; θ is the bulk stress (sum of the principal stresses) and σ_d is the deviatoric stress.

Since the coefficients (k_1, k_2 and k_3) are functions of M_c and γ_d and are different for different specimens, one regression model was developed for each of these coefficients so that these can be derived for any appropriate combinations of M_c and γ_d. The k_1, k_2 and k_3 coefficients (Table 3.1) were backcalculated using the Minitab® numerical analysis tool. M_{r-0}, M_c, γ_d and the applied stress state of each specimen were utilized to backcalculate these coefficients. The regression models are given in Equations 3.2 to 3.4.

$$k_1 = -53060.478 - 482.317(M_c) + 3790.046(\gamma_d)$$
$$\tag{3.2}$$

$$k_2 = -0.467 + 0.034(M_c) + 0.008(\gamma_d)$$
$$\tag{3.3}$$

$$k_3 = -2.553 - 0.052(M_c) + 0.175(\gamma_d)$$
$$\tag{3.4}$$
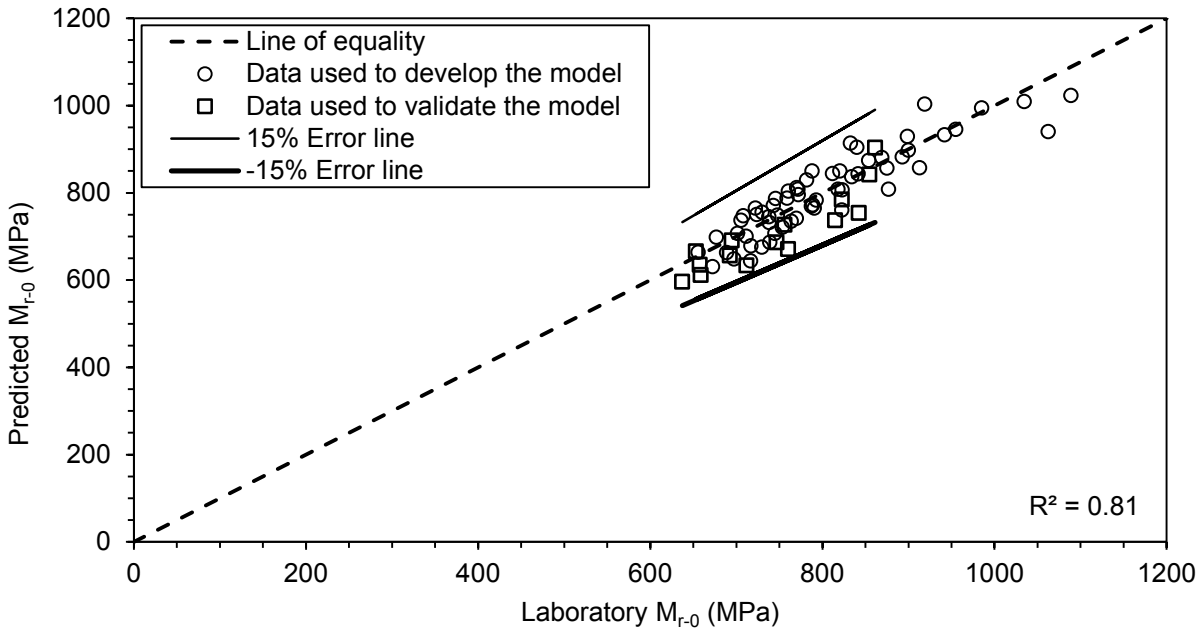
Figure 3.1. Comparison between laboratory and predicted M_{r-0} values.

Figure 3.1 shows a comparison between the laboratory and predicted M_{r-0} values. The resilient modulus data (80%) used to develop the model as well the rest of the data (20%) used to validate the model are both included in the figure. It is seen that the predictability of the models is quite good ($R^2 = 0.81$ for the data used to validate the model). Further, the model can predict the M_{r-0} within a ±15% error limit.

3.4. CALIBRATION OF THE ICA

During the field work, the ICA was calibrated first following the standard calibration procedure described in Commuri et al. (2013). Figure 3.2 shows a schematic of locations of different test points in the 60th Street project. The three calibration points (Points 1 to 3 in Figure 3.2) are located on the south-bound 60th Street near the intersection of 60th Street and West Rock Creek Road. Moisture contents and dry densities were measured at these locations. A preliminary

17

calibration of the ICA was performed using the vibration measurements and the NDG-measured degree of compaction values.

After resilient modulus tests and development of the regression model, the moisture contents and dry densities measured at the calibration points were used to compute the M_{r-0} at the three selected points. The stress state of the soil was assumed according to the procedure by Mooney and Rinehart (2009). The magnitude of the vertical normal stress was approximately 100 kPa, while the stresses in the transverse and longitudinal directions were approximately 25 to 40 kPa. These values led to a deviatoric stress between 60 and 75 kPa. Hence, in the estimation of field resilient modulus, the deviatoric, confined and bulk stresses were assumed as 69, 41 and 192 kPa, respectively. This stress state was similar to that of the last sequence in the resilient modulus test, i.e. σ_d = 68.9 kPa and σ_3 = 41.34 kPa.
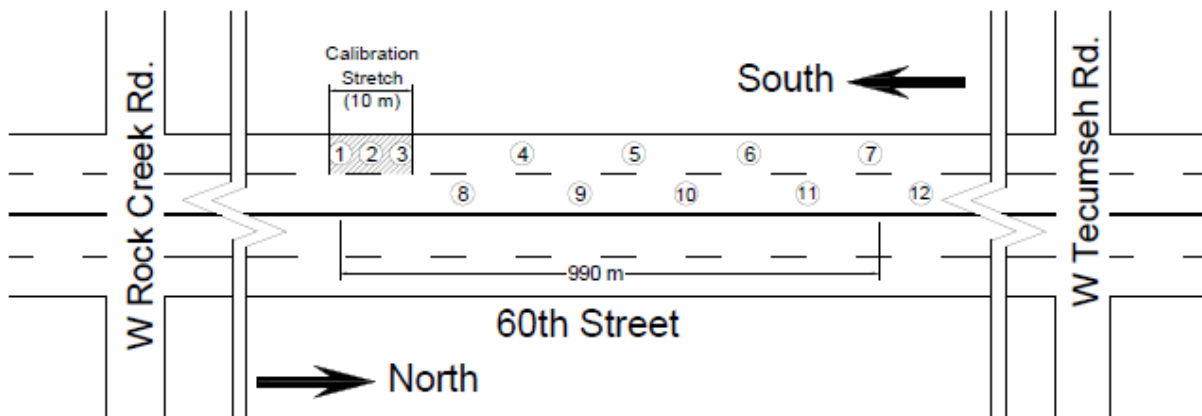
Figure 3.2. Schematic of different test points at the 60th Street project.

3.5. ICA MEASUREMENTS

After the preliminary calibration, the ICA was used to record the vibration data and GPS coordinates during the proof rolling of the remaining sections of the south-bound 60th Street.

These vibration data and the GPS readings were processed in real-time to estimate the degree of compaction.

3.6. VALIDATION OF THE ICA-ESTIMATED COMPACTION LEVEL

After proof rolling of the entire stretch, nine additional test locations on the compacted subgrade were selected at random (Points 4 through 12) and properly referenced for validating the ICA modulus. An NDG was used to measure moisture content and dry density at each of these locations. At this site, the study was limited to the verification of the regression models and the ICA-estimated modulus. Consequently, identification or remediation of under-compacted regions was not pursued at this site.

The degree of compaction at each test location was determined using the laboratory determined γ_{dmax} for CKD-stabilized soil (i.e., 17.3 kN/m^3) and the dry density measured using a NDG. The measured field moisture content, dry density and degree of compaction at each of the twelve test locations are presented in Table 3.2. It can be seen that the degree of compaction ranged from 96 to 101.7%, while the moisture content ranged from 12.3 to 17.1%. It should be noted here that the OMC of CKD-stabilized soil was determined as 14.6%, but the measured field moisture contents at some test locations were above the OMC while it was below the OMC at other test locations. Table 3.3 presents the estimated resilient modulus at 12 test points on the compacted subgrade.

Table 3.2 Field measured moisture content, dry density and degree of compactions at the twelve test points.

Test point	Moisture content (%)	Dry density (kN/m^3)	Degree of compaction (% of γ_{dmax})
1	14.2	16.6	96.0
2	13.2	16.8	97.1
3	12.3	17.6	101.7
4	13.2	17.2	99.4
5	13.9	16.9	97.7
6	13.8	16.7	96.5
7	15.1	17.3	100.0
8	13.7	17.0	98.3
9	16.0	17.1	98.8
10	16.7	16.9	97.7
11	17.1	16.6	96.0
12	15.1	17.1	98.8

Table 3.3. ICA-estimated moduli (M_i) at the twelve test points.

Test point	ICA modulus, M_i (MPa)
1	429
2	453
3	408
4	344
5	312
6	228
7	314
8	420
9	380
10	374
11	334
12	363

At this site, the ICA modulus values were validated by comparing them with the FWD modulus values. FWD test was performed at each of the 12 test points 28 days after the compaction of the subgrade. As the asphalt layers were already laid by then, FWD tests were performed on top of the asphalt surface layer. The FWD deflection values and the thicknesses (measured from cores) of different layers were used to backcalculate the asphalt layer moduli and subgrade resilient moduli at these locations. Outliers reflecting unreasonably low/high

moduli were observed at test locations 2, 4, and 8 and were excluded from the analysis. Since the FWD moduli (M_{f-28}) were obtained at 28 days, the values were converted to an equivalent 0-day FWD moduli (M_{f-0}). It may be noted here that all the samples that were tested for resilient modulus were tested both at 0-day and 28-day curing periods. A relationship between the M_{r-0} and M_{r-28} was then developed as described by Commuri et al. (2013). It was assumed that the relationship between M_{f-0} and M_{f-28} is similar to the relationship between the M_{r-0} and M_{r-28}. Table 3.4 presents the M_{f-0} and M_{f-28} values at the nine test points.

Table 3.4 FWD moduli at selected test points.

Test point	M_{f-0} (MPa)	M_{f-28} (MPa)
1	451	1384
3	519	1707
5	358	993
6	174	380
7	333	894
9	391	1125
10	363	1012
11	244	586
12	246	593
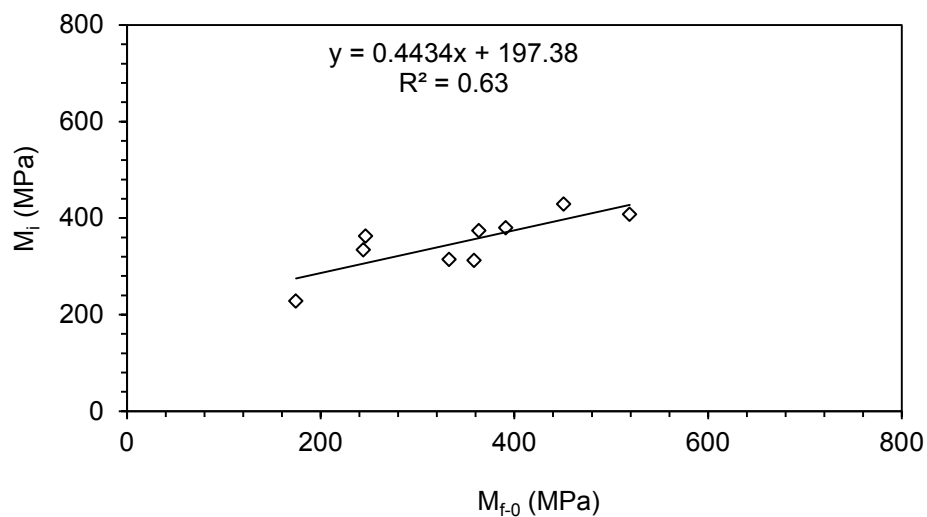
Figure 3.3. Correlation between M_{f-0} and M_i for the 60th Street project.

A comparison between the $M_{f\text{-}0}$ and M_i is shown in Figure 3.3. A reasonably good correlation ($R^2 = 0.63$) between $M_{f\text{-}0}$ and M_i can be seen. It is evident that the ICA can predict the subgrade resilient modulus with a reasonable accuracy.

4. CASE STUDY 2: SUBGRADE COMPACTION (APPLE VALLEY PROJECT)

4.1. IDENTIFICATION OF SITE

This site was located at Apple Valley, Edmond, OK. Two lanes of a 1.126-meter (0.7-mile) long stretch of East Hefner Road were constructed in this project. The road was constructed with a full-depth asphalt pavement. The subgrade was stabilized by mixing 10% CKD to a depth of 304.8 mm (12 inches). The base layer was constructed in two separate layers. Each layer was 76.5 mm (3 inches) thick and consisted of an S3 mix prepared with a PG 70-28 OK binder. The surface course was a 50.8 mm (2 inches) thick asphalt layer consisting of a S4 mix prepared with a PG70-28OK mix. The construction at this site was carried out by Haskell Lemon Construction Company, Oklahoma City, OK on September, 2011.

4.2. CHARACTERIZATION OF NATURAL AND STABILIZED SUBGRADE SOILS

The subgrade soil was silty sand, SM-type according to the USCS classification and A-2-4 as per AASHTO classification. The OMC and γ_{dmax} of the CKD-stabilized soil were 12.7 % and 18.3kN/m^3, respectively.

4.3. RESILIENT MODULUS TEST ON THE STABILIZED SOIL

In this project, six M_r specimens were tested. The M_c, γ_d and degree of compaction for the six specimens are given in Table 4.1. The degree of compactions achieved in these six specimens varied between 97 and 100%. The combinations of deviatoric stresses and confining pressures were kept similar to that of the 60th Street project, discussed in Section 3. M_r tests were conducted after at 0-day and 28-day curing periods. For two specimens (Numbers 5 and 6 in

Table 4.1), the test results were outliers when tested after 0-day curing period. Therefore, these M_{r-0} values were not used for developing the regression models. These values were used indeveloping the correlation between the M_{r-0} and M_{r-28} values.

Table 4.1 Moisture content, dry density and degree of compaction values for the six resilient modulus specimens.

Specimen No.	Moisture content (%)	Dry density (kN/m^3)	Degree of compaction (% of γ_{dmax})	k_1, k_2 and k_3 based on M_{r-28}		
				k_1	k_2	k_3
1	10.8	18.1	97.3	43609.1	0	-0.0327
2	10.8	18.3	98.3	43347.8	0.04376	-0.07368
3	10.6	18.3	98.1	39877.5	0	-0.1692
4	12.6	18.5	99.2	37817.5	0.045445	-0.05661
5	12.8	18.3	98.1	41754	0.100398	0.014232
6	11.4	18.6	99.9	41798.9	0.050764	-0.12664

4.4. REGRESSION MODELS FOR RESILIENT MODULUS

The M_r regression models were developed using the M_{r-28} values. The coefficients k_1, k_2 and k_3 (Table 4.1) were determined following the procedure similar to that of the West 60th Street project, but using the 28-day M_r values. The regression model is given in Equations 4.1 to 4.3.

$$k_1 = 127792.503 - 835.980(M_c) - 4183.115(\gamma_d) \tag{4.1}$$

$$k_2 = -0.880 + 0.035(M_c) + 0.028(\gamma_d) \tag{4.2}$$

$$k_3 = 3.662 + 0.055(M_c) - 0.238(\gamma_d) \tag{4.3}$$

Figure 4.1. shows the predictability of the developed regression models. It is seen that these models can predict the resilient modulus with good accuracy (error less than ± 20%). Further, the predicted modulus has good correlations with experimentally obtained values (R^2 = 0.84).
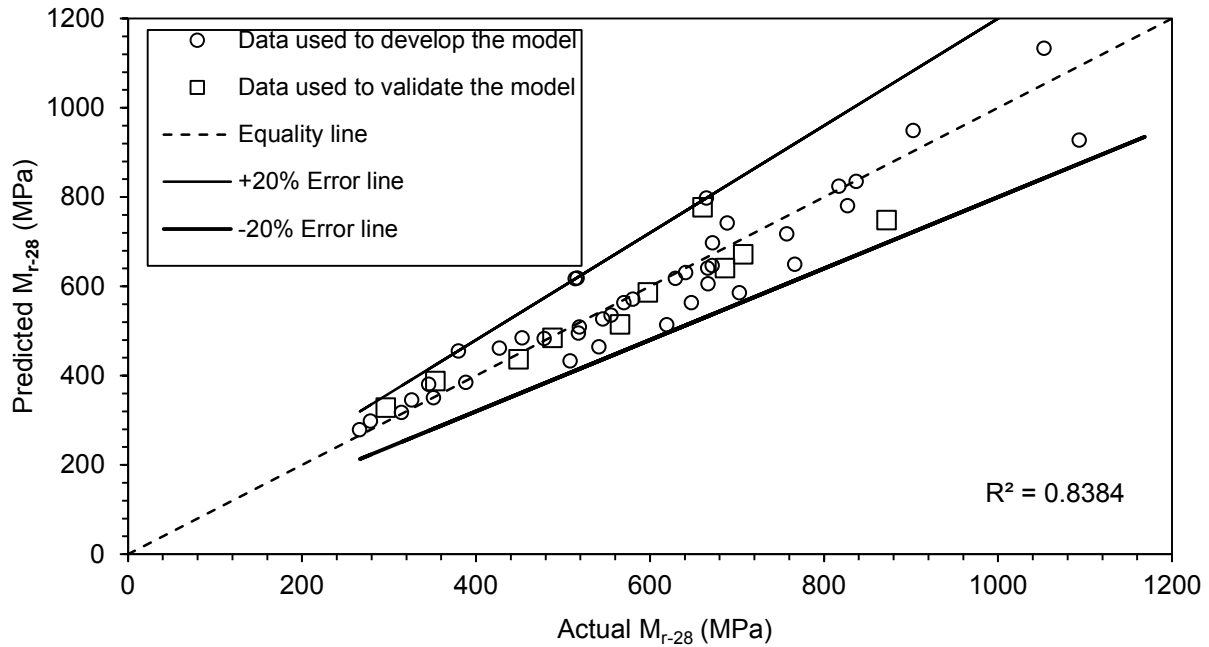
Figure 4.1.Predictability of the regression models for M_r.

4.5. CALIBRATION OF THE ICA

The calibration procedure for the ICA in this project was similar to the procedure used in the 60th Street project (Section 6.5). Three calibration points were selected on a 9.14 m (30 ft) long stretch on the west bound East Hefner Road, as shown in Figure 4.2.
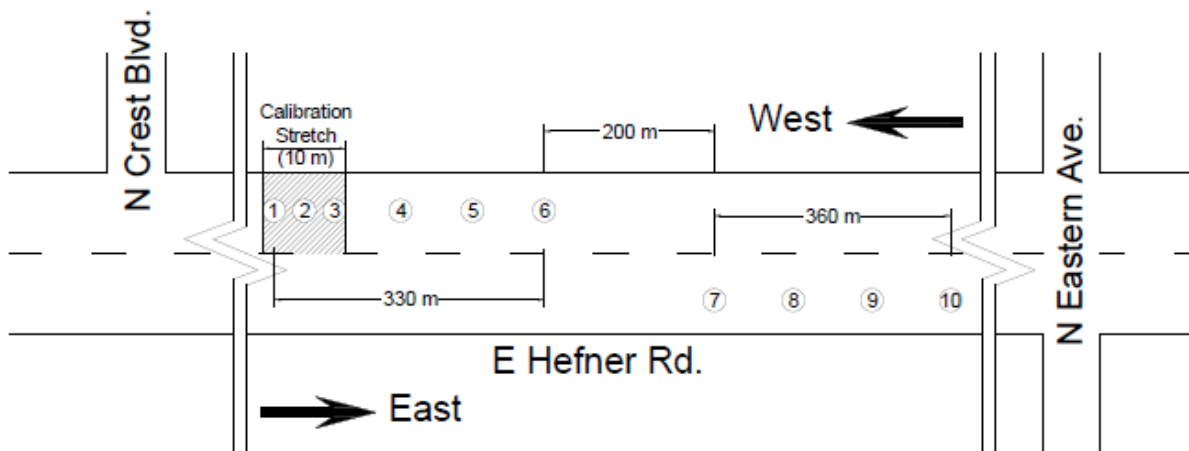
Figure 4.2. Location of different test points in Apple Valley project.

25

4.6. VALIDATION OF ICA-ESTIMATED COMPACTION LEVEL

Validation of M_i was performed by comparing the M_i values with the M_{r-0} values. In order to obtain M_{r-0} values, moisture contents and dry densities were first measured at seven randomly selected test points on the subgrade after the proof rolling was completed (Figure 4.2). The regression models developed in Section 4.5 were then used to predict M_{r-0} values at these test points.

Figure 4.3 shows the relationship between the M_i and M_{r-0}. The correlation is good with $R^2 = 0.60$. It is encouraging that the ICA can predict the subgrade resilient modulus with reasonable accuracy.
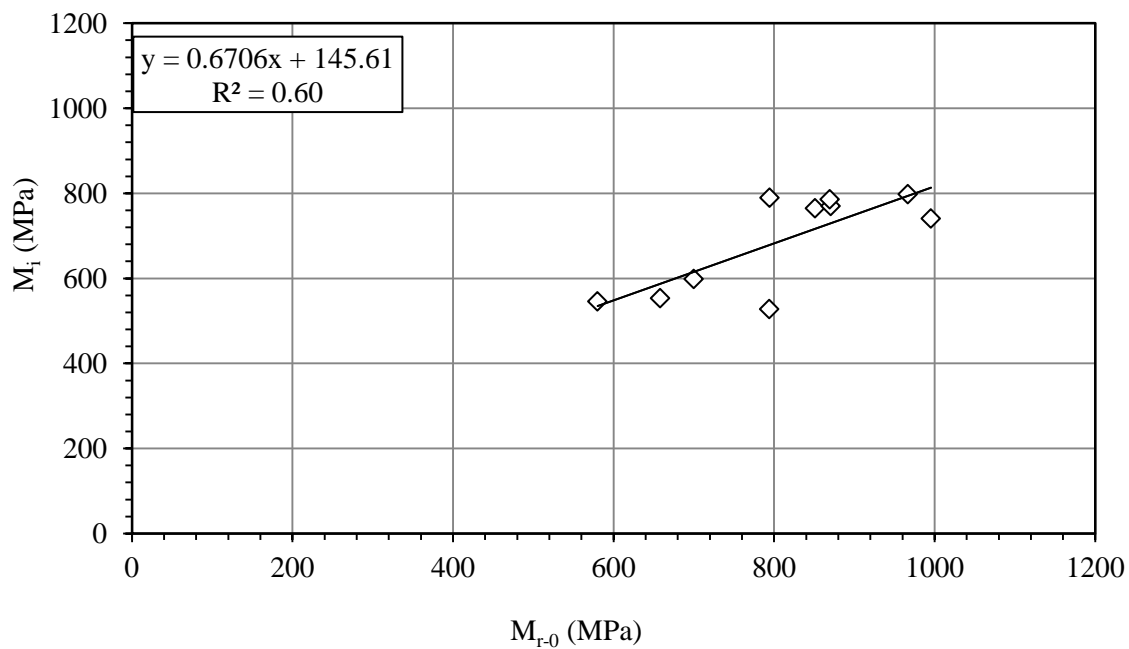
Figure 4.3. Correlation between the M_i and M_{r-0}.

5. CASE STUDY 3: SUBGRADE COMPACTION (I-35 PROJECT)

5.1. IDENTIFICATION OF SITE

The ability of the ICA to estimate resilient modulus of a stabilized subgrade during compaction was studied during the construction of a 640-meter (2100-ft) long full-depth asphalt pavement on the north-bound section of I-35 near Main St., Norman, OK(Figure 5.1). The construction at this site was carried out by Allen Construction, Oklahoma City, OK between April, 2013 and August, 2013.

The subgrade soil was stabilized by mixing 12% CKD to a depth of 202 mm (8 inches). Figure 5.2 shows a photographic view of mixing of CKD with the natural subgrade soil. Subgrade compaction was initially performed with a pad-foot roller and then by a single drum smooth vibratory roller. The ICA was installed on the vibratory roller, which was used for the proof rolling. The subgrade compaction work was performed on two separate 396-meter long (1300-feet) sections adjacent to each other. These sections are referred to as Test Section 1 and Test Section 2. Test Section 1 was compacted using a traditional compaction procedure, i.e., ICA measurements were taken and monitored throughout the compaction but under-compacted regions were neither identified nor remedied. The ICA compaction procedure was followed on Test Section 2. The ICA measurements were recorded and monitored throughout the compaction process, and under-compacted regions were identified as well. Under-compacted regions were then compacted using additional roller passes.

27
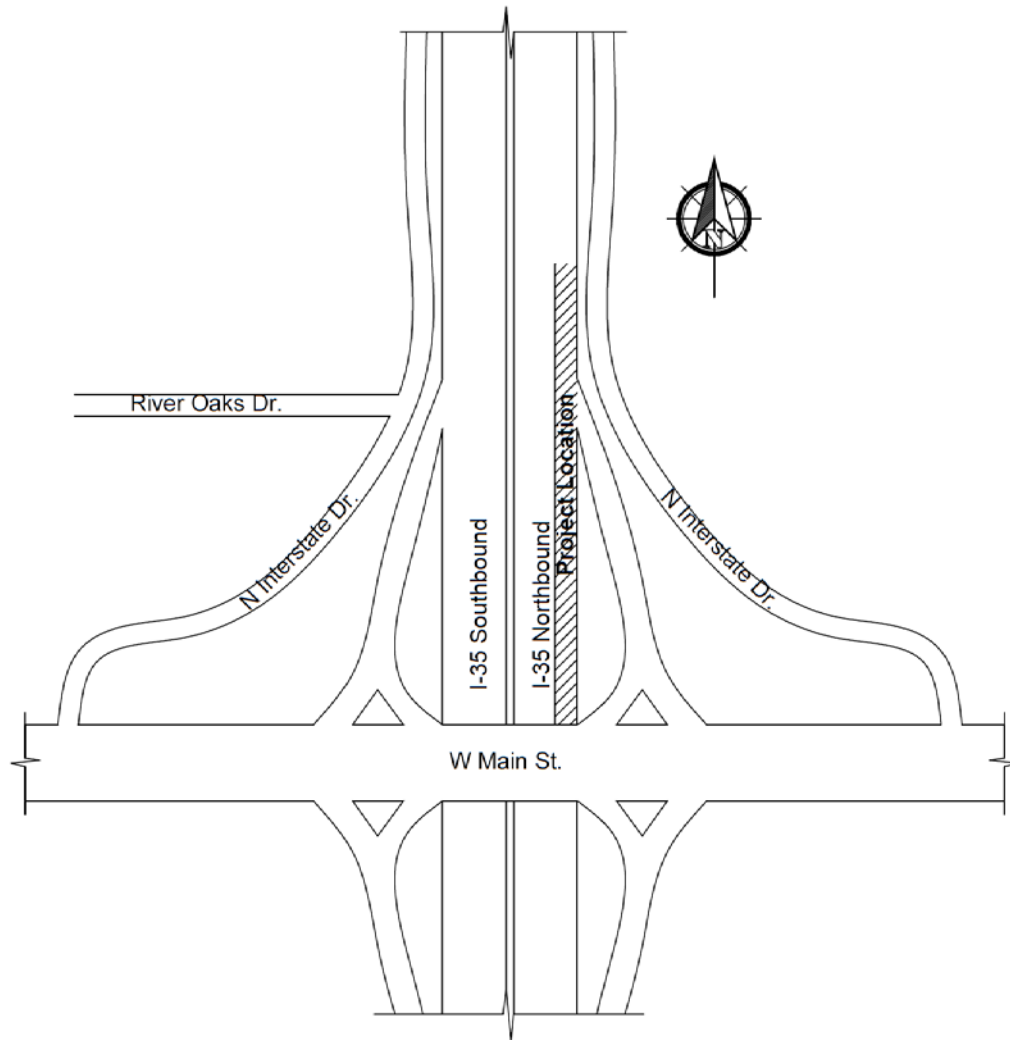
Figure 5.1. Location of the I-35 Project site.

Figure 5.2. Mixing of CKD with soil at the I-35 project in Norman, OK.

5.2. CHARACTERIZATION OF NATURAL AND STABILIZED SUBGRADE SOILS

Bulk soil and CKD samples were collected from the construction site during the subgrade compaction. Figure 5.3 demonstrates the particle distribution of the collected soil. Atterberg's limits test showed that the LL and PI of the natural subgrade soil are of 25% and 9, respectively. The soil was classified as CL (low plastisity clay), according to the USCS classification system. According the AASHTO soil classification, the subgrade soil type is A-4. The moisture-density content relationship for the CKD-stabilized soil, obtained through the standard Proctor test, can be seen in Figure 5.4. The OMC and γ_{dmax} of the stabilized soil were found as 14.8% and 17.3 kN/m^3, respectively.
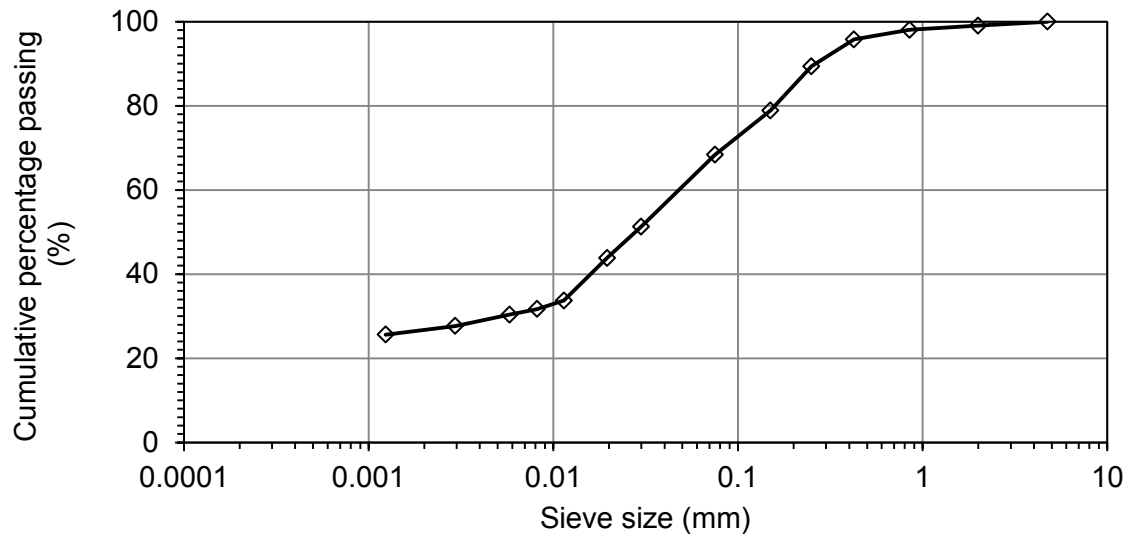
Figure 5.3. Particle size distribution of natural subgrade soil.
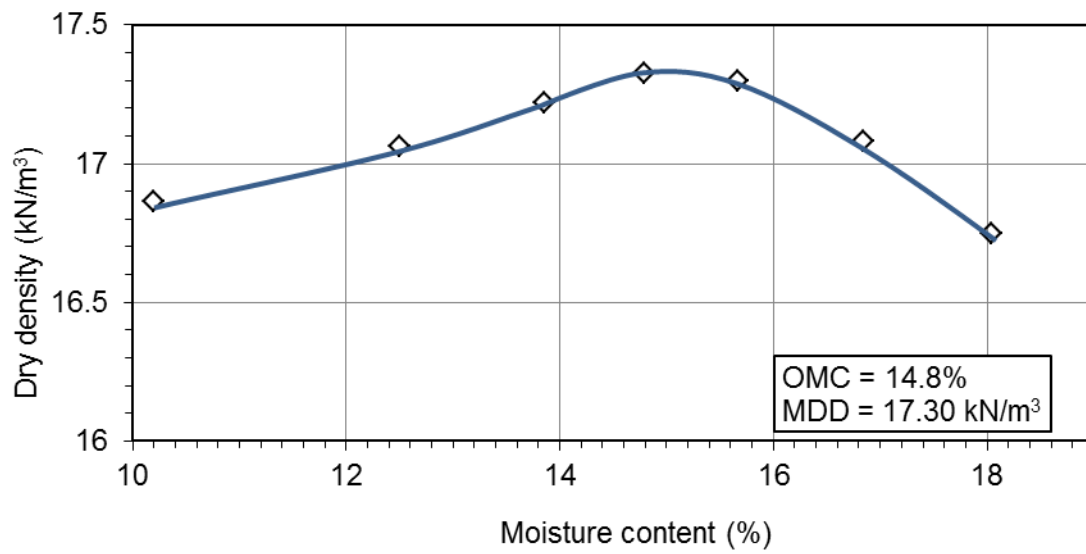
Figure 5.4. Proctor test results for CKD-stabilized soil.

5.3. CALIBRATION OF THE ICA

A preliminary calibration of the ICA was performed on a 10-m (33-ft) long stretch in Section 1 as shown in Figure 5.5. NDG measured densities and moisture contents were recorded at three selected locations (C1 to C3 in Figure 5.5). The NDG readings were taken both before and after the compaction by the smooth drum vibratory roller. Changes in project schedule prevented completion of resilient modulus test in the laboratory prior to field compaction. Therefore, the initial and target modulus values were estimated using previously developed regression models and the NDG readings (moisture contents and dry densities). The modulus values were then used to perform raw calibration of the ICA as specified in the IACA User Guide, as provided in Appendix. The calibration parameters were adjusted later on after the completion of the resilient modulus tests and development of regression models for this project site.

Table 5.1 presents dry densities and moisture contents for the three calibration points. It was observed that the NDG measured density at test locations C2 and C3 increased after the compaction by the smooth drum vibratory roller, whereas it remained virtually unchanged at test location C1.

Table 5.1. NDG measurements in calibration stretch.

Test points	Before compaction by smooth drum vibrator		After compaction by smooth drum vibrator	
	Dry density (kN/m^3)	Moisture content (%)	Dry density (kN/m^3)	Moisture content (%)
C1	16.51	16.8	16.45	17.9
C2	16.12	17.1	16.40	18.2
C3	15.82	19.4	16.23	18.2
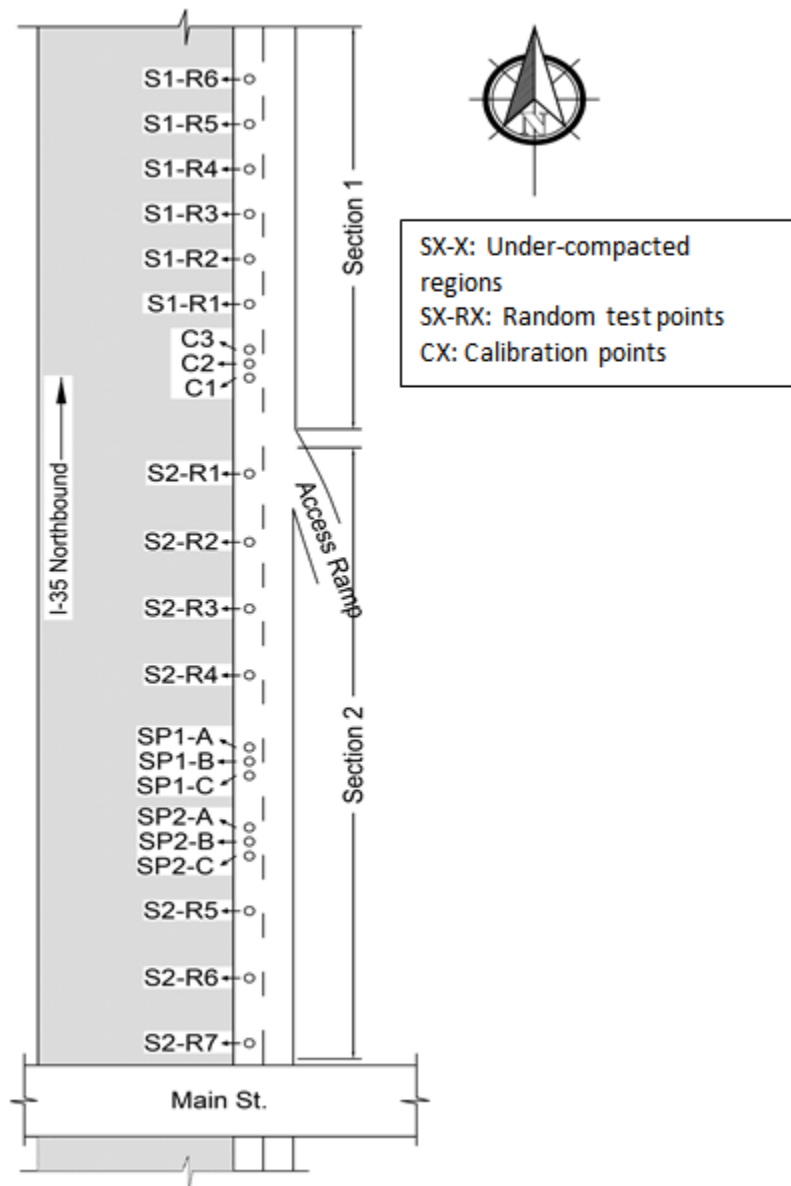
Figure 5.5. Locations of different test points for the I-35 project.

5.4. COLLECTION OF ICA MEASUREMENTS

After preliminary calibration was performed, ICA measurements were taken during the compaction of Test Section 1. Figure 5.6 shows collection of ICA measurements during proof rolling. Six random points (R1 to R6) were marked on Test Section 1 and the NDG measurements were taken after the compaction. The GPS readings of these locations were also recorded. Table 5.2 shows the dry density and moisture content at each of the test locations. It may be noted that accurate geo-referenced ICA measurements could not be recorded on the Point 'S1-R4' due to loss of satellite connection in the GPS unit of the ICA system. Hence, the ICA modulus could not be determined at this test location.

Figure 5.6. ICA compaction in progress.

In Test Section 2, seven additional test points were selected at random. NDG (Figure 5.7) and GPS readings were taken at these locations at the end of the entire compaction process. The densities and moisture contents measured at those points are given in Table 5.3.

33

Table 5.2. NDG readings in six randomly selected test points on Test Section 1.

Test points	Dry density (kN/m^3)	Moisture content (%)
S1-R1	15.36	16.8
S1-R2	15.68	16.1
S1-R3	16.09	16.3
S1-R4	15.14	17.6
S1-R5	15.85	17.8
S1-R6	16.31	16.8

Figure 5.7. Moisture content and dry density measurements with NDG test.

Table 5.3. NDG readings at seven randomly selected points on Test Section 2.

Test points	Dry density (kN/m^3)	Moisture content (%)
S2-R1	15.41	15.5
S2-R2	16.37	15.3
S2-R3	16.78	16.4
S2-R4	17.20	15.2
S2-R5	16.68	15.3
S2-R6	15.77	16.8
S2-R7	16.59	15.7

5.5. IDENTIFICATION AND REMEDIATION OF UNDER-COMPACTED REGIONS

In Test Section 2, the emphasis was given on identifying the under-compacted regions and remediating them through additional compaction. Test Section 2 was initially compacted using traditional rolling process similar to that employed on Test Section 1. Immediately following the compaction, the as-built map generated by the ICA was used to determine under-compacted regions if any. Two regions were identified as under-compacted, SP1 and SP2 in Figure 5.5. NDG tests performed at three different points (1-m apart) at each of these two under-compacted regions (SP1-A, SP1-B, SP1-C on SP1 and SP2-A, SP2-B, SP2-C on SP2). The roller operator was then requested to perform additional passes on the identified under-compacted regions in order to improve the level of compaction. NDG readings were taken again at those six points after the remedial passes. The vibration data and NDG readings taken before and after the remedial passes were compared to determine the improvement achieved. Table 5.4 presents a comparison of the NDG readings taken before and after the additional passes. It can be seen that the density of the under-compacted regions increased with the additional passes, as expected. The standard deviation of the dry density measurements also decreased slightly, indicating a more uniform compaction.

It may be mentioned that a good level of compaction was already achieved throughout the entire length in Test Section 2 during the traditional compaction process. The under-compacted regions identified by the ICA were not significantly below the target compaction level. Therefore, while resilient modulus values for regions SP1 and SP2 increased, the improvement was not significant. However, this demonstration showed the ability of the ICA in identifying the under-compacted regions and the feasibility of improving the level of compaction by applying remedial passes during the construction of subgrade. The improvement in resilient modulus values is presented later in this Chapter.

Table 5.4.Comparison of densities and moisture contents between the traditional and the ICA compaction.

Test points	Traditional compaction		ICA compaction	
	Dry density (kN/m^3)	Moisture content (%)	Dry density (kN/m^3)	Moisture content (%)
SP1-A	15.98	16.4	16.07	15.9
SP1-B	16.12	15.6	16.16	17
SP1-C	15.63	17.9	16.20	15.8
SP2-A	16.29	15.4	16.48	17.4
SP2-B	16.32	15.9	16.40	16
SP3-C	16.26	16.1	16.32	15.6
Average	16.10	-	16.22	-
Std. dev.	0.24	-	0.14	-
COV	1.49%	-	0.87%	-

Note: Std. dev. = Standard deviation; COV- Coefficient of variation

5.6. RESILIENT MODULUS TEST ON THE STABILIZED SOIL

Resilient modulus tests were conducted on specimens for five different combinations of moisture contents and dry densities. These combinations were selected based on the magnitudes of dry densities and moisture contents measured at test locations on Test Section 1 and Test Section 2 (Table 5.2, Table 5.3 and Table 5.5). The range of moisture content and dry density measured in the field can be seen in Figure 5.8. The moisture-density relationship for the stabilized soil is also depicted in Figure 5.8 to help characterize the variability of field measured moisture and dry density with respect to OMC and γ_{dmax}. Table 5.5 shows the target moisture content and degree of compactions for each of the five combinations. These five combinations were selected so that a reasonable range of field moisture and dry density combinations could be studied in the laboratory. Three specimens were prepared for each combination and the resulting 15 specimens were tested with 15 different combinations of stress of states. The same test procedure, as described in Section 2, was used here.

The resilient modulus tests were conducted immediately after the compaction of the specimen (i.e., 0-day curing period) to simulate the conditions on the day of compaction in the field. Resilient modulus tests were also performed after curing specimens for 28 days after compaction.
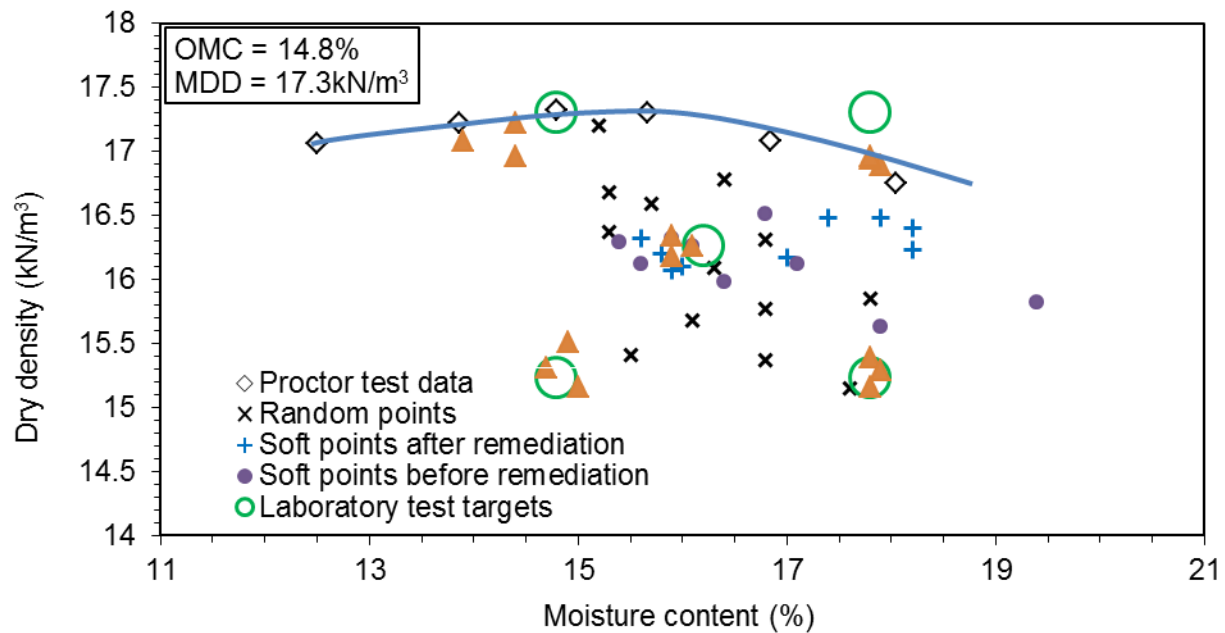
Figure 5.8. Comparison of field measured moisture contents and dry densities with moisture contents and dry densities of the M_r test specimens.

Table 5.5. Description of selected combinations of moisture contents and dry densities for M_r test.

Combination #	Combination designation	Moisture content (%)	Degree of compaction (% of γ_{dmax})
Comb. 1	I-35-R-C1-14.8-100	14.8	100
Comb. 2	I-35-R-C2-14.8-88	14.8	88
Comb. 3	I-35-R-C3-16.2-94	16.2	94
Comb. 4	I-35-R-C4-17.8-88	17.8	88
Comb. 5	I-35-R-C5-17.8	17.8	Max. possible

Note: I-35: Interstate 35, R- Resilient modulus, C- combination, 14.8- moisture content, 100- degree of compaction.

Table 5.6. Actual moisture contents, dry densities and degree of compaction of the M_r test specimens.

Combination designation	Specimen code	Moisture content (%)	Dry density (kN/m^3)	Degree of compaction (%)
I-35-R-C1-14.8-100	1	13.9	17.1	98.8
	2	14.4	17.2	99.5
	3	14.4	17.0	98.0
I-35-R-C2-14.8-88	1	14.7	15.3	88.5
	2	15.0	15.2	87.6
	3	14.9	15.5	89.6
I-35-R-C3-16.2-94	1	15.9	16.3	94.5
	2	16.1	16.3	94.0
	3	15.9	16.2	93.5
I-35-R-C4-17.8-88	1	17.8	15.4	89.0
	2	17.8	15.2	87.6
	3	17.8	15.3	88.4
I-35-R-C5-17.8-100	1	17.9	16.9	97.6
	2	17.8	16.9	97.9
	3	17.8	17.0	98.0

5.7. REGRESSION MODELS FOR RESILIENT MODULUS

M_r regression models were developed using M_{r-0} values following the procedure described in Section 2. The developed regression models are given in Equations 5.1 to 5.3.

$$k_1 = -4653.4 - 309.0(M_c) + 706.5(\gamma_d) \tag{5.1}$$

$$k_2 = -0.232 + 0.045(M_c) - 0.023(\gamma_d) \tag{5.2}$$

$$k_3 = -0.057 - 0.043(M_c) + 0.033(\gamma_d) \tag{5.3}$$

Figure 5.9 shows the predictability of the developed regression models. The eighty percent resilient modulus data used to develop the model and the remaining 20% data used for validation are included in Figure 5.9. It can be seen that the predictability of the models is excellent with a R^2 = 0.90 (for the data used to validate the model). Also, the model could predict the resilient moduli within ± 25% error limit.
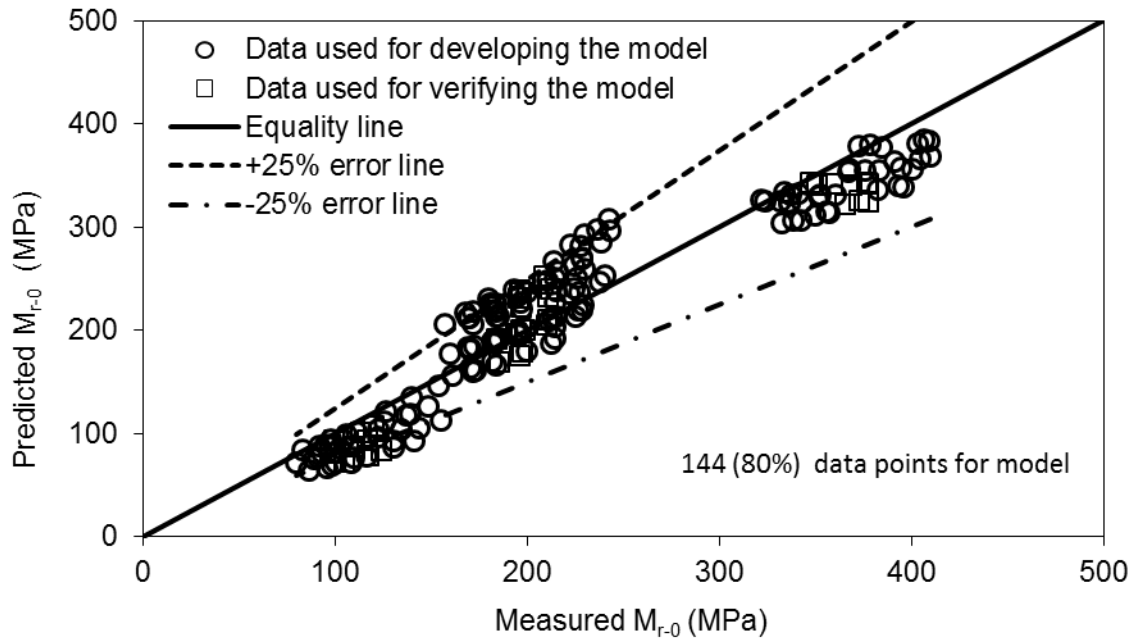
Figure 5.9. Predictability of the developed M_r models for the I-35 project.

5.8. VALIDATION OF ICA-ESTIMATED COMPACTION LEVEL

Figure 5.10 shows the relationship between the ICA-estimated modulus M_i and laboratory predicted modulus M_{r-0} (obtained using regression models in Equations 5.9 - 5.11). It can be seen from Figure 5.10 that the ICA-estimated modulus values are accurate within 25% of the modulus estimated using laboratory test procedure and correlate well with the M_r values of similar soil specimen tested in the laboratory (R^2 = 0.62).
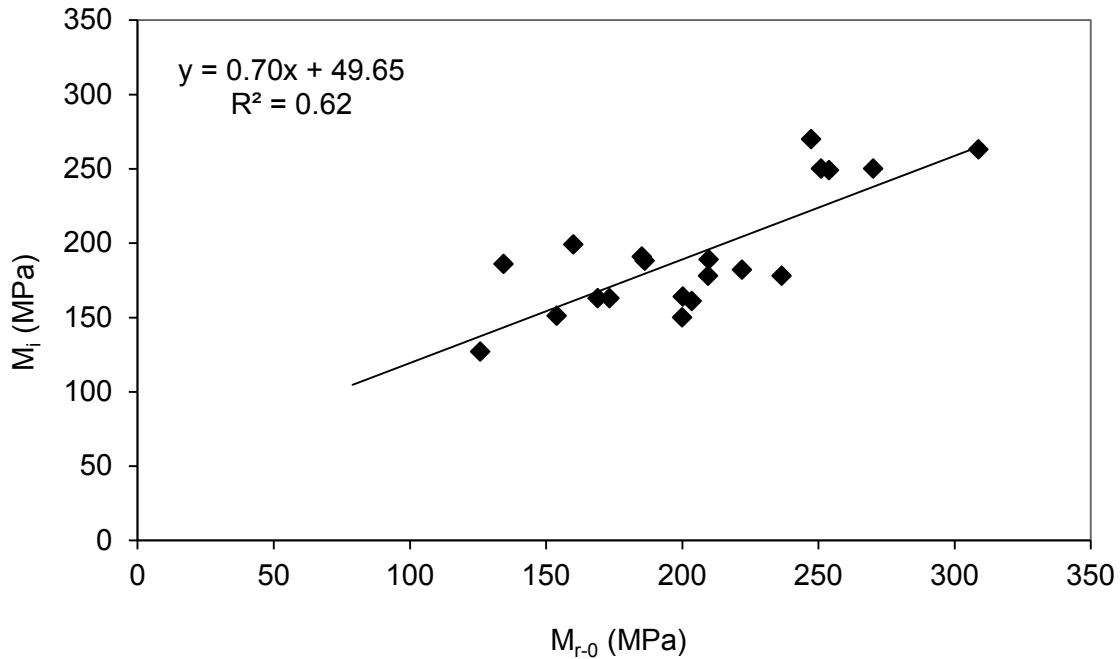
Figure 5.10. Relationship between M_i and M_{r-0}.

5.9. IMPROVEMENT IN THE RESILIENT MODULUS AFTER THE REMEDIAL COMPACTION

As mentioned before, two under-compacted regions, SP1 and SP2 were identified in Test Section 2 and additional compaction was provided using the same steel drum roller. Figure 5.11 presents the M_i values before and after the remedial passes at six test points on the two under-compacted regions. It can be seen that the average M_i at those six points increased from 163 MPa to 180 MPa. More importantly, the standard deviation of estimated modulus at these locations decreased from 12 MPa to 8.3 MPa, thereby indicating a more uniform compaction of the subgrade layer. The error bars in the graph also indicate that the stiffness of the subgrade achieved during the ICA compaction was significantly higher and more uniform than that achieved through traditional compaction.
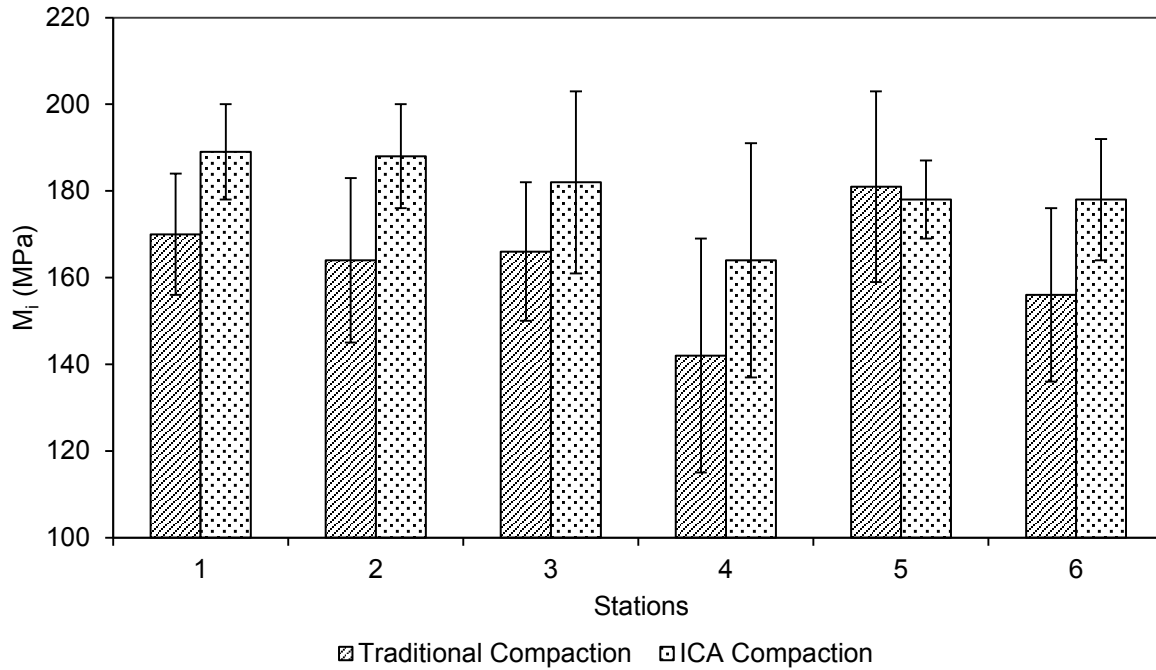
Figure 5.11. Improvement in ICA modulus (M_i) with the remedial compaction.

5.10. RELATIONSHIP BETWEEN THE M_{r-0} AND M_{r-28}

A regression model was developed to correlate the resilient moduli values for two different curing periods (0-day and 28-day). Figure 5.12 shows the correlation between the M_{r-0} and M_{r-28}. It may be mentioned that when CKD-stabilized subgrade is used in the pavement construction, the resilient modulus at 28-day curing period is important information from the mechanistic pavement design point of view. A correlation between M_{r-0} and M_{r-28} can be used to verify if the ICA can be used to predict the ICA modulus at 28-day curing period during the construction of the subgrade itself. The following equation presents the relationship between the M_{r-0} and M_{r-28} values.

$$x = -2.4612\frac{M_c}{OMC} + 13.4185\frac{\gamma_d}{\gamma_{\mathrm{dmax}}} - 0.0152861(M_{r-0}) \tag{5.4}$$

where,

x = the ratio of M_{r-28} to M_{r-0}; other variables were previously mentioned. The coefficient of determination, R^2, for the correlations is found to be excellent (R^2 = 0.94).The M_{r-28} values were intended for a comparison of the ICA-estimated modulus with the modulus backcalculated from FWD tests. Unfortunately, the site was not accessible to the FWD trailer and the comparison could not be carried out, as previously planned.
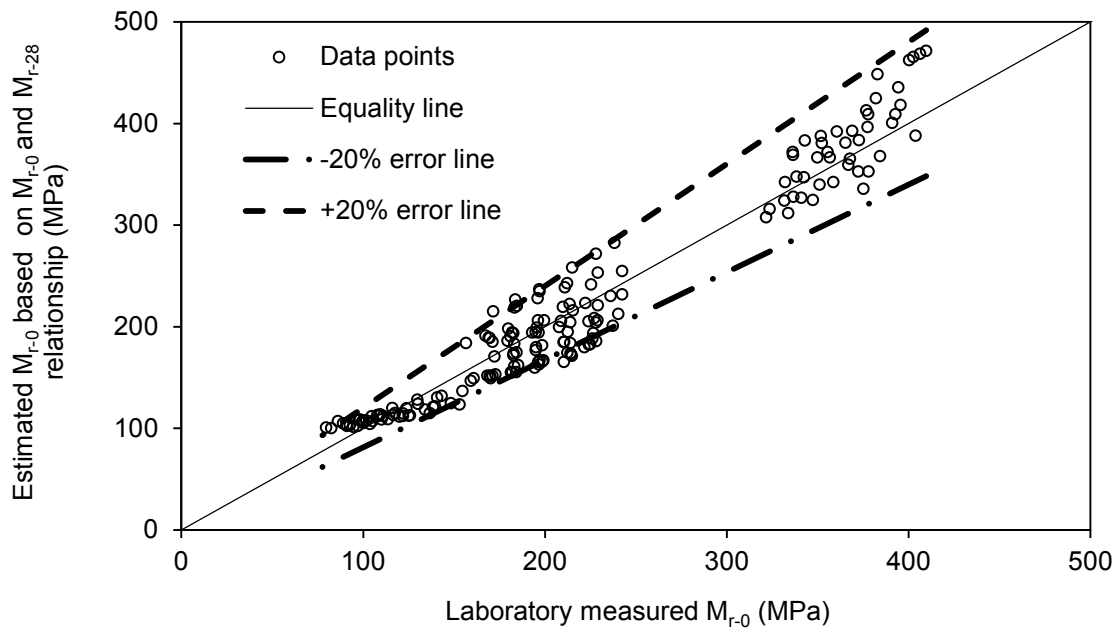
Figure 5.12. Predictability of the regression model developed for relating the M_{r-0} and M_{r-28}.

42

6. CASE STUDY 4: SUBGRADE COMPACTION (I-35 SERVICE ROAD)

6.1. IDENTIFICATION OF SITE

The Intelligent Compaction was demonstrated on a 300-m long stretch on the I-35 Service Road. This site is located at the University Park area of North-West Norman, Oklahoma. The location of the site is shown in Figure 6.1. The north-bound I-35 Service Road is being extended from the Kohl's store to NW 24th Avenue. This Service Road is located on the east side of the I-35, and it connects I-35 to NW 24th Avenue. The ICA technology was used during the construction of the stabilized subgrade. This project comprised of one east-west stretch and one north-south stretch. The construction at this site was carried out by Silver Star Construction Company, Moore, OK on August, 2014.

The natural subgrade soil was highly plastic clay. Therefore, the subgrade was pre-treated by adding 3% quick lime. The average moisture content of the soil during the mixing of quick lime was 22%. The 'quick lime' is referred to as 'lime' in this report. The lime-treated soil was subsequently stabilized by mixing 12% CKD to a depth of 202 mm (8 inches) after a 14-day curing period, under ambient conditions.

The subgrade soil was compacted using both traditional and the ICA compaction procedures at different sections, as shown in Figure 6.2. Traditional compaction was performed in Sections A and C, whereas, Sections B and D were compacted following the ICA compaction procedure. In all the sections, the subgrade was initially compacted by a pad-foot roller. The proof rolling was performed using a single smooth drum vibratory roller. The ICA measurements were taken during the proof rolling. In Sections B and D, under-compacted regions were identified and remediated. NDG measurements were taken both before and after remedial

passes. The ICA-estimated densities and moduli were validated by conducting DCP and FWD

tests, in addition to the NDG tests.
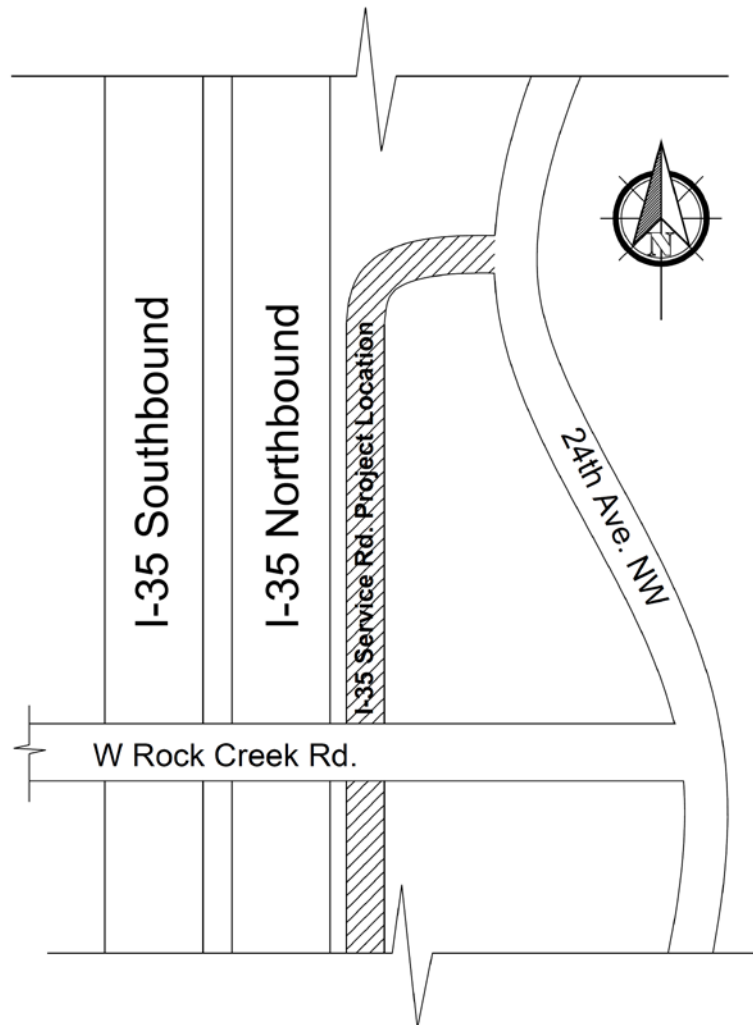
Figure 6.1. Location of the I-35 Service Road project site.
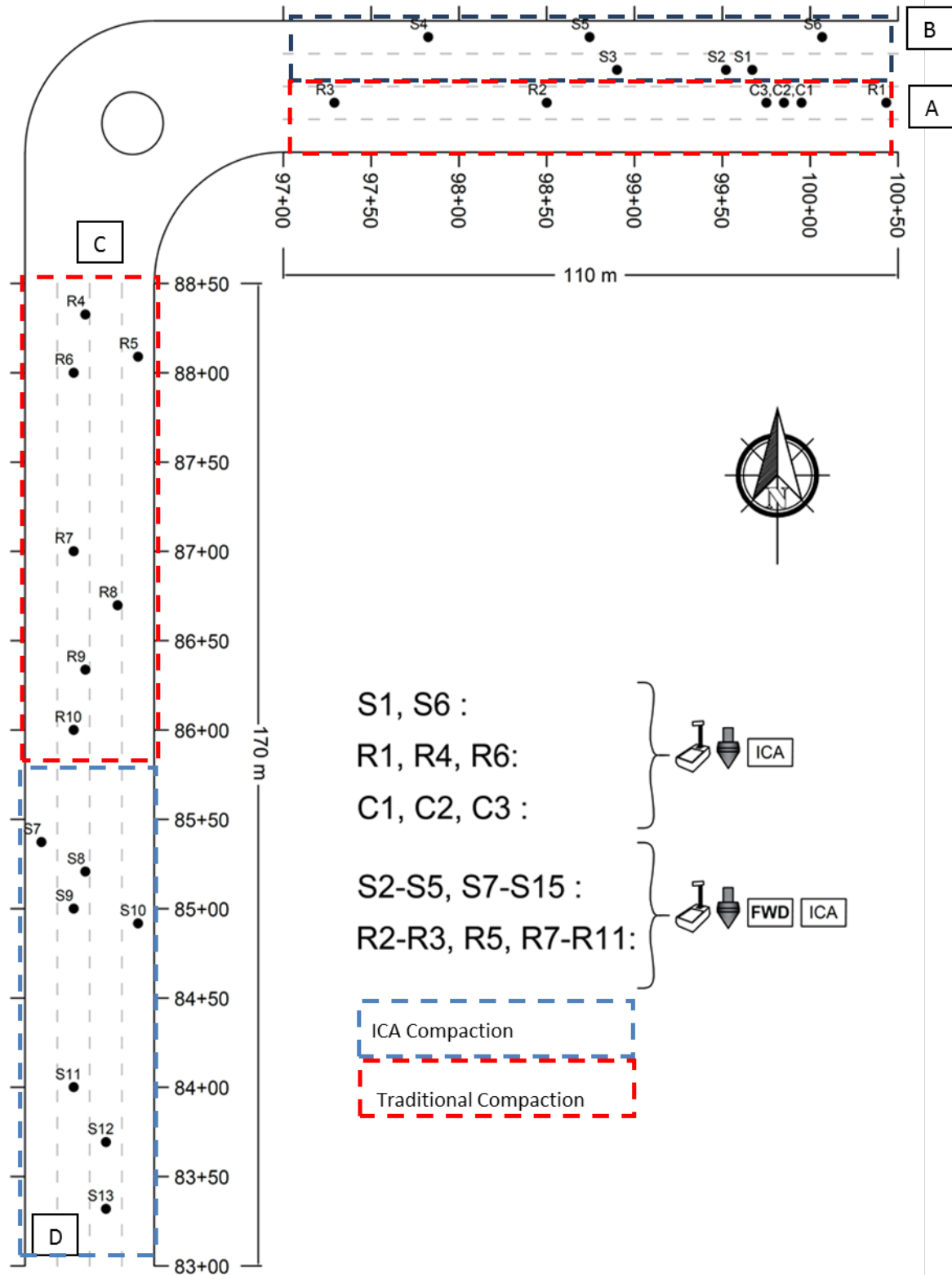
Figure 6.2. Location of test points at the I-35 Service Road project.

6.2. CHARACTERIZATION OF NATURAL AND STABILIZED SUBGRADE SOILS

Bulk samples of soil and lime were collected from the field during the construction work. CKD was collected from the plant of the construction company (Silver Star Company). Figure 6.3 shows the particle distribution (ASTM D422) of the natural subgrade soil. It can be seen that about 79% of the particles were finer than sieve No. 200. The LL and PI of this soil were found as 40% and 21, respectively. The soil was classified as CL (low plastisity clay) according to the USCS classification system. According to the AASHTO classification, the subgrade soil was A-6 type.

Standard Proctor tests were conducted on the soil-lime-CKD mix. This soil-lime-CKD mix was prepared simulating the curing procedure adopted in the field. In order to simulate the field condition, first the natural subgrade soil was air dried, processed and passed through ASTM sieve No. 4. Then, lime (3%) was added to the soil and mixed to uniformity under dry conditions. After that water (22% by weight of soil) was added to the dry soil-lime mix. It may be noted that the moisture content of the soil during the soil-lime mixing process in the field was measured by an NDG at several locations. The average moisture content was 22%. Figure 6.4 shows the soil-lime mixing process in the field. Figure 6.5 shows a photoghraphic view of the measurement of moisture contents and dry densities in the field.

The moist soil-lime mix was collected from the field and transferred to OU Broce Laboratory in ten plastic bags (approximately 50 Kg per bag). Since the soil-lime mix in the field was exposed to ambient conditions, the plastic bags were kept untied as shown in Figure 6.6a. The plastic bags allowed moisture exchange only from the top surface. Also, the depth of the moisten soil-lime mix in each plastic bag was around 280 mm to simulate the thickness of the loose soil-lime mix in the field before compaction. The plastic bags containing the mixes were

left open inside an environmental chamber where the relative humidity and temperature were controlled (Figure 6.6b). The average day and night temperature and humidity of the project location were collected for over a 14-day period from the website of National Oceanic and Atmospheric Administration (NOAA). The environmental chamber was programmed in such a way that the daytime ambient condition lasts for 15 hours and the nighttime ambient lasts for 9 hours.
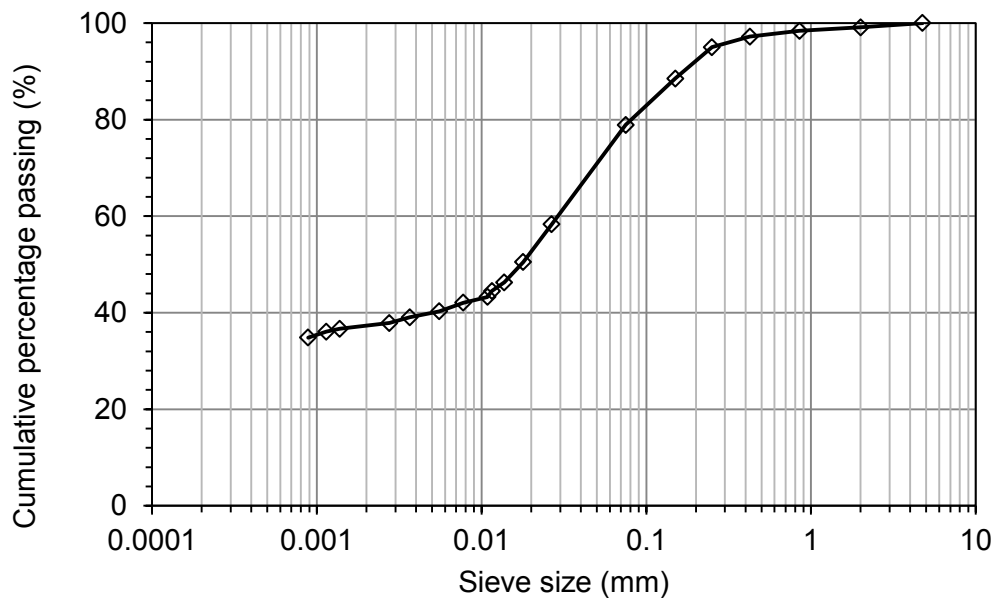
Figure 6.3. Particle size distribution of natural soil.

Figure 6.4. Pre-treatment of existing soil by 3% lime at the I-35 Service Road Project.

Figure 6.5. Measurement of moisture content and dry density during pre-treatment of existing soil with lime at the I-35 Service Road project.

Figure 6.6. Conditioning of soil-lime mix in the laboratory.

After 14 days, 12% CKD (by weight of dry soil-lime mix) was mixed with the soil-lime mix. This soil-lime-CKD mix was used for the standard Proctor test and also for the resilent modulus test. Figure 6.7 shows the moisture-density relationship for the soil-lime-CKD mix. The optimum moisture content and maximum dry density were obtained as 21.4% and 15.4 kN/m^3, respectively.
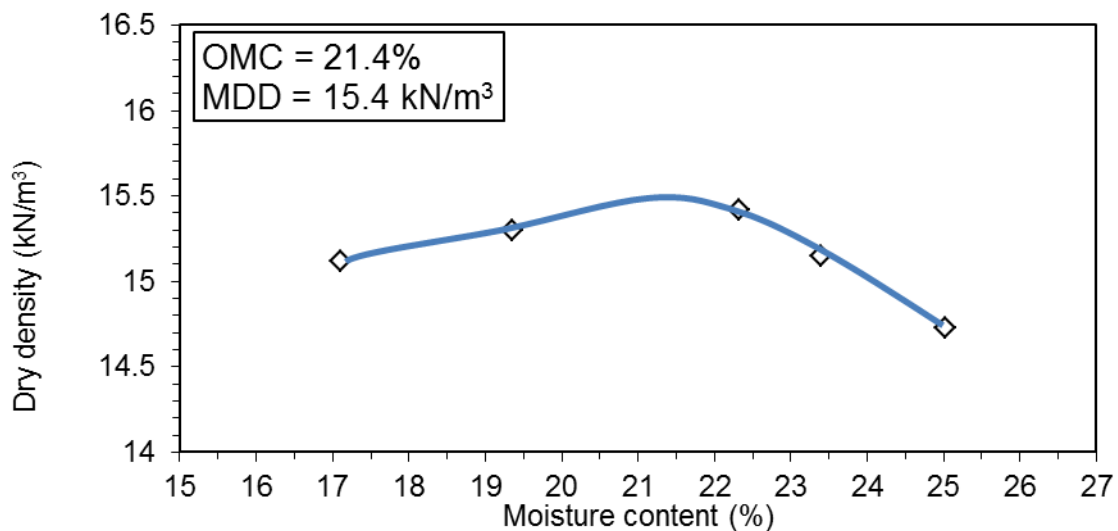
Figure 6.7. Standard Proctor test result for the soil-lime-CKD mix for I-35 Service Road project.

6.3. CALIBRATION OF THE ICA

The soil was pre-treated with lime and stabilized with CKD and then compacted using a pad-foot roller (Figure 6.8). The subgrade was then proof rolled using a single drum vibratory roller. This vibratory roller was equipped with the ICA. The ICA was calibrated on a 10-meter long calibration stretch prior to the proof rolling operation (Figure 6.9). The ICA measurements were recorded on the calibration stretch during proof rolling. The location of the calibration stretch is shown in Figure 6.2. Three points (C1, C2 and C3) spaced at three meter intervals were marked on the calibration stretch. The calibration points were on the east side of the east-west stretch (Section A). Moisture content and dry density were measured at these calibration points (Table 6.1). Initial and target M_r values were estimated using the regression models developed for this particular soil type and used to calibrate the ICA according to the procedure outlined in Section 2.

Figure 6.8. Initial compaction of soil-lime-CKD mix with pad-foot roller at the I-35 Service Road project.

Figure 6.9. ICA compaction of soil-lime-CKD mix with smooth drum vibratory roller at the I-35 Service Road project.

6.4. COLLECTION OF THE ICA MEASUREMENTS

The east-west and north-south sections were compacted on two separate days. Traditional compaction procedure was followed on Sections A and C. ICA compaction was carried out in Sections B and D. On Sections B and D, under-compacted regions were identified using the as-built maps generated by the ICA and remedial roller passes were applied to improve the level of compaction of the subgrade. ICA measurements were recorded throughout the entire compaction process on all sections.

6.4.1. East-west Stretch

In Section A, moisture content and dry density were recorded at three randomly selected points (R1, R2 and R3) right after the compaction of the stabilized subgrade by a smooth drum vibratory roller. Table 6.1 presents the degree of compaction and moisture content measured at the specified points in Section A. It can be seen that the degree of compaction varies between 95.5% and 101.3% in Section A.

In Section B, first traditional compaction was applied and the ICA measurements were recorded. The level of compaction was also monitored during the compaction process. After compaction, as-built maps were used to study the compaction achieved in Section B. It was found that several regions in Section B had a lower degree of compaction as compared to the target compaction. The moisture contents and dry densities that were measured at six test points (S1 to S6 shown in Figure 6.10 and Table 6.2) had low degree of compaction (92 - 96.7%). The dry density values are reported as degree of compaction in Table 6.2. Two additional roller passes were then performed over the entire length of Section B. The moisture content and dry density measurements were repeated at the six test points (S1 to S6). However, a minimal improvement in the ICA-estimated degree of compaction was observed (degree of compaction increased from 92% - 96.7% to 92.7% - 97.1%). While the ICA could accrurately estimate low/indequate compaction, the degree of compaction could not be improved with two additional roller passes. A possible reason for this could be the high level of moisture in the subgrade during compaction and probably two passes were not sufficient.

Table 6.1. Moisture content and dry density values at different test points on Section A in I-35 Service Road project.

Test points	Degree of compaction (%)	Moisture content (%)
C1	101.3	19.4
C2	99.9	20.6
C3	95.5	22.4
R1	100.1	21.2
R2	96.4	20.2
R3	97.4	18.4
Average	98.4	20.4
Std. Dev.	2.1	1.3
COV (%)	2.2%	6.2%

Note: Std. dev. = Standard deviation; COV- Coefficient of variation

Figure 6.10. NDG measurements on compacted subgrade at the I-35 Service Road project.

Table 6.2. Moisture content and dry density at different test points on Section B in I-35 Service Road.

Test points	Before remedial compaction		After remedial compaction	
	Degree of compaction (%)	Moisture content (%)	Degree of compaction (%)	Moisture content (%)
S1	95.0	23.4	96.1	24.0
S2	92.0	26.2	92.7	25.5
S3	96.7	22.1	97.1	21.5
S4	95.4	20.5	93.9	21.0
S5	96.3	22.5	96.2	23.7
S6	94.8	24.4	93.6	23.9
Average	95.0	23.2	94.9	23.3
Std. Dev.	1.5	1.8	1.6	1.5
COV (%)	1.6%	7.8%	1.7%	6.7%

Note: Std. dev. = Standard deviation; COV- Coefficient of variation

6.4.2. North-south Stretch

Traditional compaction was performed in Section C. Immediately after the compaction by proof roller, moisture content and dry density values were measured at eight randomly selected points (R4 to R10). Table 6.3 presents the degree of compaction and moisture content measured at the test points in Section C. It can be seen that the degree of compaction was between 91.0% and 97.7%.

In Section D, traditional compaction was first performed and the ICA measurements were recorded. The level of compaction was monitored during the compaction process. A total of seven under-compacted regions were identified. Test points (S7 to S13) were selected in these regions for further investigations. The moisture content and dry density were then measured at these locations (Table 6.4). The degree of compaction was between 82.5% and 93.1%.

Since it was observed in Section B that the two additional passes did not improve the degree of compaction by a considerable margin, four additional passes were provided on the entire length of Section D. The moisture content and dry density values were measured again at these seven locations (Table 6.4). It can be seen from Table 6.4 that the average degree of compaction increased by 1.5%. The range of degree of compaction in Section D improved from 82.5% - 93.1% to 87.0% - 98.1%. The degree of compaction in a severely under-compacted location, S14, improved from 82.5% to 93.1%, an increase of approximately 10%. Such severely under-compacted points otherwise could result in localized distresses and lead to premature failure of the pavement structure.

Table 6.3. Moisture content and dry density at different test points in Section.

Test points	Degree of compaction (%)	Moisture content (%)
R4	95.9	20.7
R5	91.0	21.8
R6	94.0	23.0
R7	94.7	21.5
R8	97.7	21.6
R9	97.0	19.8
R10	91.5	21.0
Average	94.5	21.3
Std. Dev.	2.39	0.92
COV (%)	2.5%	4.3%

Table 6.4. Moisture content and dry density at different test points on Section D in I-35 Service Road.

Test points	Before remedial compaction		After remedial compaction	
	Degree of compaction (%)	Moisture content (%)	Degree of compaction (%)	Moisture content (%)
S7	93.4	22.2	87.0	20.7
S8	89.5	20.7	93.4	21.9
S9	92.0	21.4	89.8	23.1
S10	93.1	21.9	89.5	20.8
S11	89.8	21.9	89.4	21.4
S12	82.5	20.8	93.1	23.0
S13	89.4	17.0	98.1	21.9
Average	90.0	20.84	91.5	21.8
Std. Dev.	3.42	1.66	3.41	0.89
COV (%)	3.8%	7.9%	3.7%	4.0%

6.5. RESILIENT MODULUS TEST ON THE STABILIZED SOIL

Based on the maximum dry density, optimum moisture content, and moisture content and dry density measured at test locations in the field (Table 6.1, Table 6.2, Table 6.3 and Table 6.4), it was planned to conduct resilient modulus tests at five different combinations of dry density and

moisture content. A graphical depiction of the range of moisture content and dry density measured in the field is shown in Figure 6.11. The moisture–density relationship for the stabilized soil is also shown in Figure 6.11 in order to compare the scatter of the field measured moisture content and dry density with the optimum moisture content and maximum dry density. Table 6.5 shows the target moisture content and degree of compaction for each of the five combinations. These combinations were selected so that a reasonable range of field moisture content and dry density could be captured in the laboratory. Three specimens were prepared for each combination and each specimen was tested with 15 different combinations of deviatoric stresses and confined pressures, as similar to the previously discussed projects. The resilient modulus tests were conducted immediately after the compaction of the specimen to simulate the field condition. Also, similar samples were tested after 7-day and 28-day curing periods.
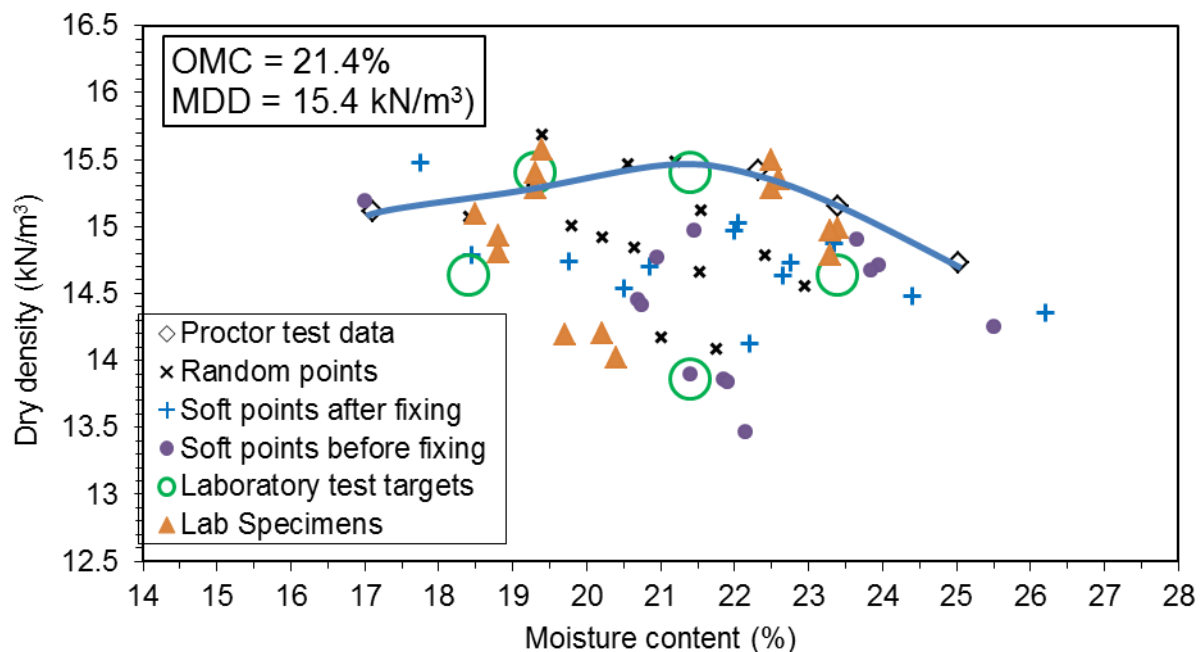
Figure 6.11. Comparison of field measured moisture content and dry density with moisture content and dry density of the M_r test specimens.

Table 6.5. Description of five different combinations for M_r test.

Combination designation	Degree of compaction (%)	Moisture content range	Moisture content (%)	Dry density (kN/m³)
I35SR-R-C1-21.4-100	100	OMC	21.4	15.4
I35SR-R-C2-19.4-100	100	OMC-2%	19.4	15.4
I35SR-R-C3-21.4-90	90	OMC	21.4	13.9
I35SR-R-C4-18.4-95	95	OMC-3%	18.4	14.6
I35SR-R-C4-18.4-95	95	OMC+3%	23.4	14.6

Note: I-35: Interstate 35, R- Resilient modulus, C- combination, 14.8- moisture content, 100-degree of compaction.

6.6. REGRESSION MODELS FOR RESILIENT MODULUS

6.6.1. 0-day Curing Period

The M_r regression models were developed using the M_{r-0} values following a similar procedure adopted for the previously discussed projects. The developed regression models are given in Equations 6.1 to 6.3.

$$k_1 = -3121.68 - 108.733(M_c) + 432.5896(\gamma_d) \tag{6.1}$$

$$k_2 = 1.803884 + 0.030014(M_c) - 0.14429(\gamma_d) \tag{6.2}$$

$$k_3 = -0.84907 - 0.01073(M_c) + 0.050347(\gamma_d) \tag{6.3}$$

Figure 6.12 shows the predictability of the developed regression models. As before, 80% resilient modulus values were used to develop the regression models and the remaining data (20%) were used to validate the model. It can be seen that the predictability of the models is excellent with a R^2 = 0.95 (for the data used to validate the model). Also, the model was seen to predict the resilient moduli with error within ± 10%.

57
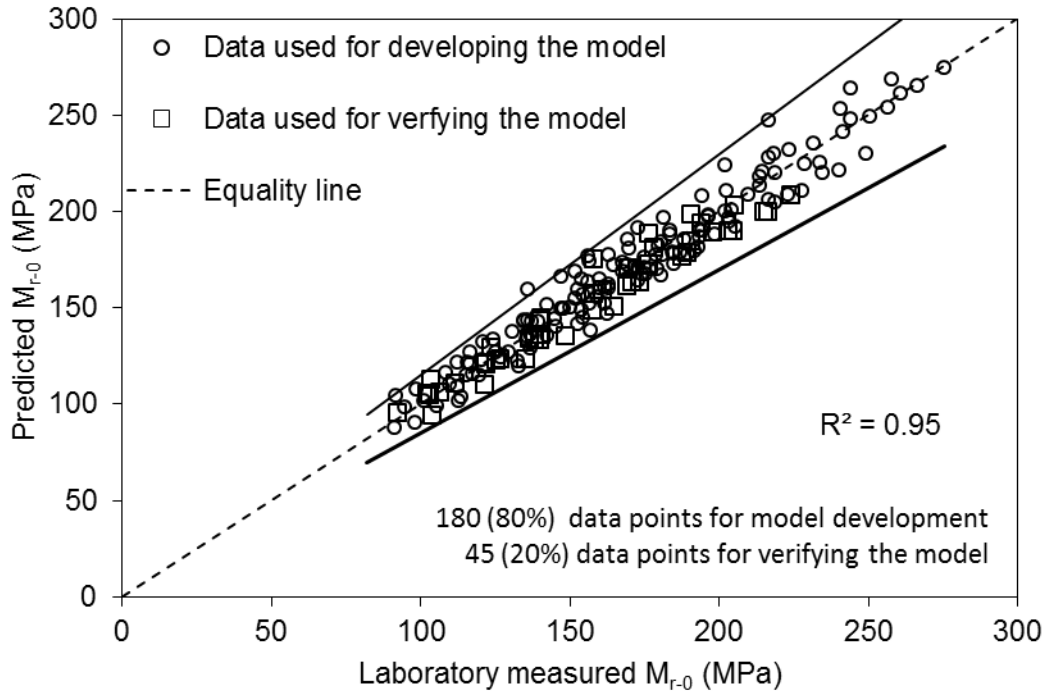
Figure 6.12. Comparison between regression model predicted M_{r-0} and laboratory M_{r-0} values.

6.6.2. 7-day Curing Period

To compare the ICA modulus with the FWD modulus, and since the FWD test was conducted seven days after compaction, a regression model was developed to convert 7-day FWD modulus (M_{f-7}) to 0-day equivalent FWD modulus (M_{f-0}). Regression models were developed using resilient modulus test results at 7-day curing period (M_{r-7}) and M_{r-0}. The following equation was used to convert M_{r-7} to M_{r-0}. The same equation was used to convert M_{f-7} to M_{f-0}.

$$\frac{M_{r-7}}{M_{r-0}} = -6.105(M_c) + 24.319\frac{{\gamma_d}^2}{MDD^2} - 0.047(M_{r-0}) \tag{6.4}$$

Figure 6.13 shows the predictability of the developed regression model. It can be seen that the predictability of the models is excellent with a $R^2 = 0.95$ (for the data used to validate the model). Also, the model was found to predict the resilient moduli with error within ± 20%.
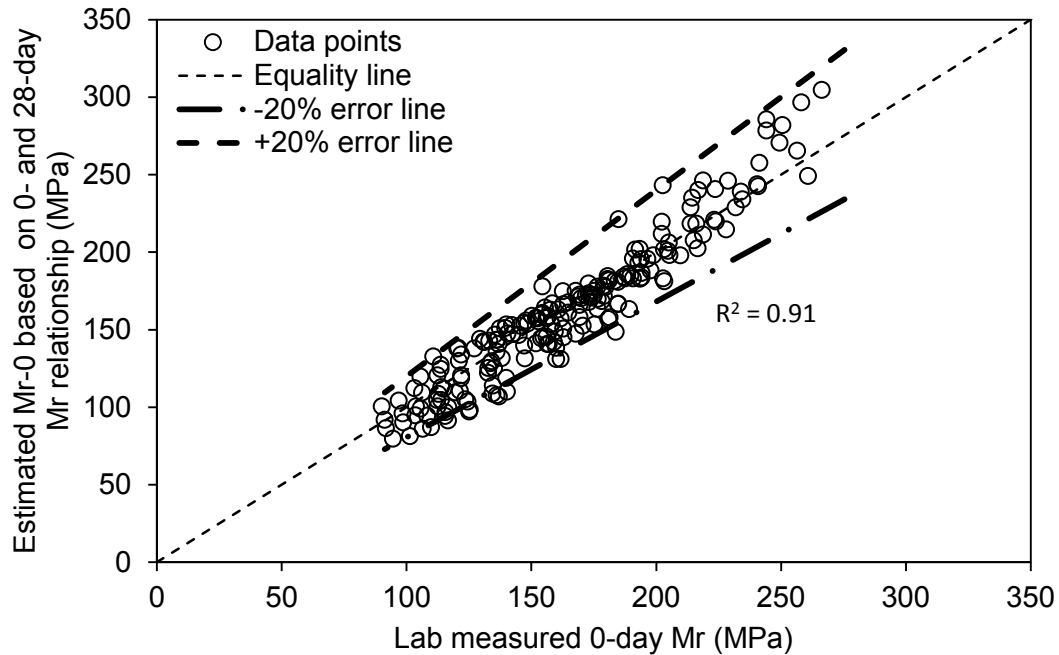
Figure 6.13. Comparison between M_{r-0} predicted by the regression model developed for converting M_{r-7} to M_{r-0} and laboratory M_{r-0} values.

6.7. VALIDATION OF ICA-ESTIMATED COMPACTION LEVEL WITH THE M_r

The ICA modulus values were validated by comparing them with the M_r values predicted using the regression models. First, the resilient modulus values were computed using the dry density and moisture content information from the 26 test points on Sections A to D at the test site (3 calibration points (C1- C3), 10 random points (R1 to R11) and 13 points in the under-compacted regions (S1 to S13)). The ICA calibration parameters were then adjusted using the modulus values predicted at locations C1 to C3. The ICA modulus was then estimated for the remaining 23 test locations. Table 6.6 presents a comparison between the M_{r-0} and the M_i for all 26 test points.

Figure 6.14 shows the relationship between the M_{r-0} and M_i values. It may be noted that densities and moisture contents measured at some points were outside the range of the

densities and moisture contents considered in the laboratory testing and regression model development. So, those points were not considered in the correlation as shown in Figure 6.14. A reasonably good correlation was found between M_{r-0} and M_i, with $R^2 = 0.63$.

Table 6.6. Comparison between the M_{r-0} and Mi values for the I-35 Service Road project.

Test points	M_{r-0} (MPa)	M_i (MPa)
C1	186.4	147
C2	167.9	150
C3	117.1	93
R1	162.1	131
R2	150.3	133
R3	175.1	179
R4	141.8	111
R5	89.5	72
R6	97.8	110
R7	122.5	115
R8	143.2	119
R9	158.3	172
R10	104.6	106
S1	109.3	118
S2	34.3	120
S3	133.1	117
S4	129.7	115
S5	121.2	85
S6	72.4	95
S7	44.3	157
S8	123.0	150
S9	83.4	115
S10	74.2	144
S11	72.5	178
S12	120.4	120
S13	192.0	164
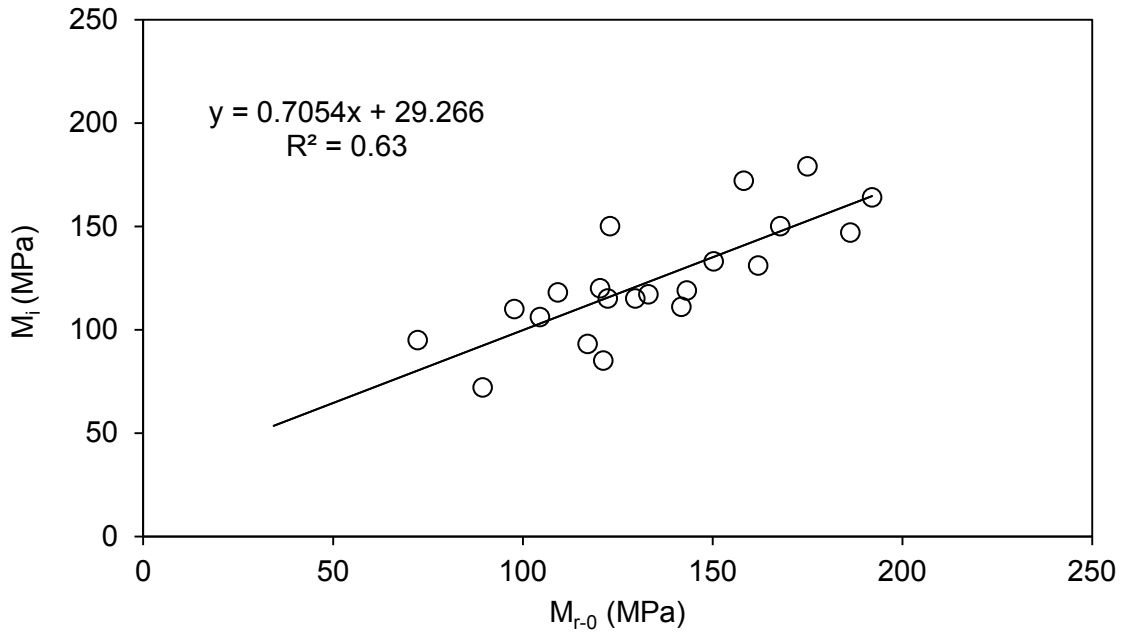
Figure 6.14. Comparison between M_i and M_{r-0} for I-35 Service Road project.

6.8. VALIDATION OF ICA-ESTIMATED COMPACTION LEVEL WITH THE DCP INDEX

In order to validate the ICA-estimated moduli with respect to DCP indices, DCP tests were conducted at randomly selected 15 (out of 26) points after the completion of the ICA compaction. Figure 6.15 shows DCP testing on the compacted subgrade. DCP indices were calculated using the 'penetration vs number of blows' relationships obtained at each point. Figure 6.16 presents the correlation between the inverse of DCP index (1/DCP index) and the ICA-estimated modulus. A reasonably fair correlation (R^2 = 0.50) was observed between the DCP index and M_i.

Figure 6.15. DCP test on the compacted subgrade at the I-35 Service Road project.
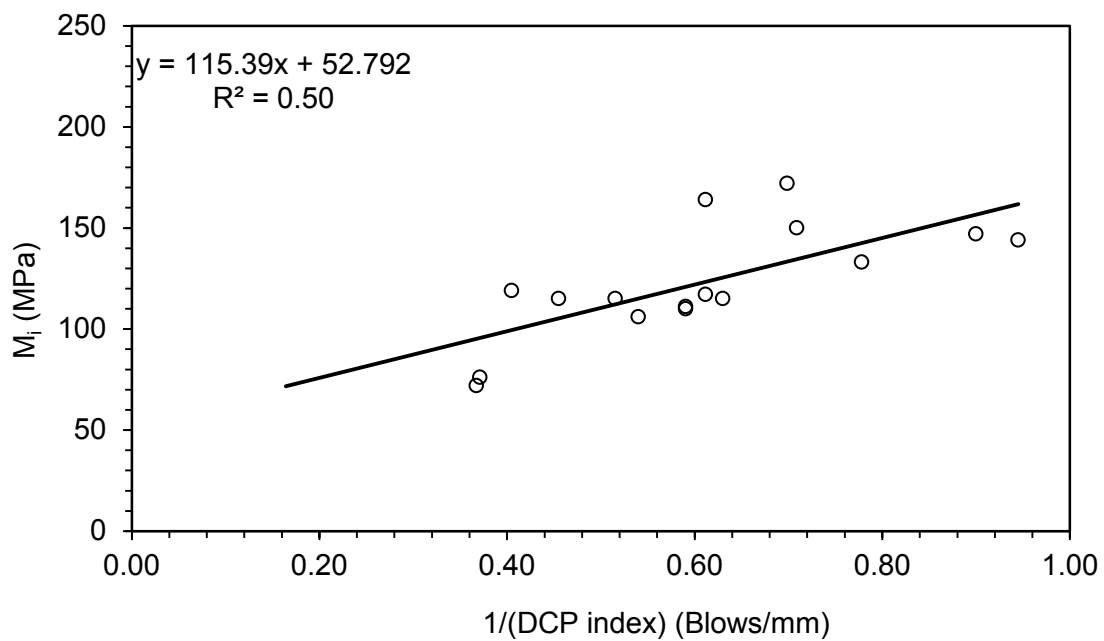
Figure 6.16. Correlation between the DCP indices and the ICA modulus.

6.9. COMPARISON OF ICA-ESTIMATED COMPACTION LEVEL WITH FWD MODULUS

In order to validate the ICA-estimated moduli with the FWD moduli, FWD tests were conducted at several test points on the compacted subgrade. The FWD tests were conducted seven days after the compaction (Figure 6.17). It should be noted that when the research team and the ODOT personnel visited the site after 7 days of compaction, several previously marked test points were found to be considerably wet and the remaining points were found to be very dry. FWD tests could not be performed at many wet points. The exact reasons for the source of this water were not known. Construction work related to water pipes was a possible reason. Also, a localized rainfall at the site could be another reason. Relatively smooth surface texture of the subgrade and the piles of dirt on the side of the subgrade seen in Figure 6.18 suggests water run-off during the 7-day curing period, a possible reason for localized wet spots.

Figure 6.17. FWD test on the compacted subgrade at the I-35 Service Road project.

Figure 6.18. Evidence of water run-off on the compacted subgrade before the FWD test.

Figure 6.19 presents a comparison between the ICA modulus M_i and FWD modulus M_{f-7}. It can be seen that no correlation exists between the M_i and M_{f-7} (R^2 = 0.1). The FWD modulus was found to be varying significantly. Because of this poor correlation, further analysis was not conducted on the FWD test results.

y = -0.0111x + 185
R² = 0.1

ICA modulus (MPa)

FWD modulus after 7 days curing (M_{f-7}) (MPa)
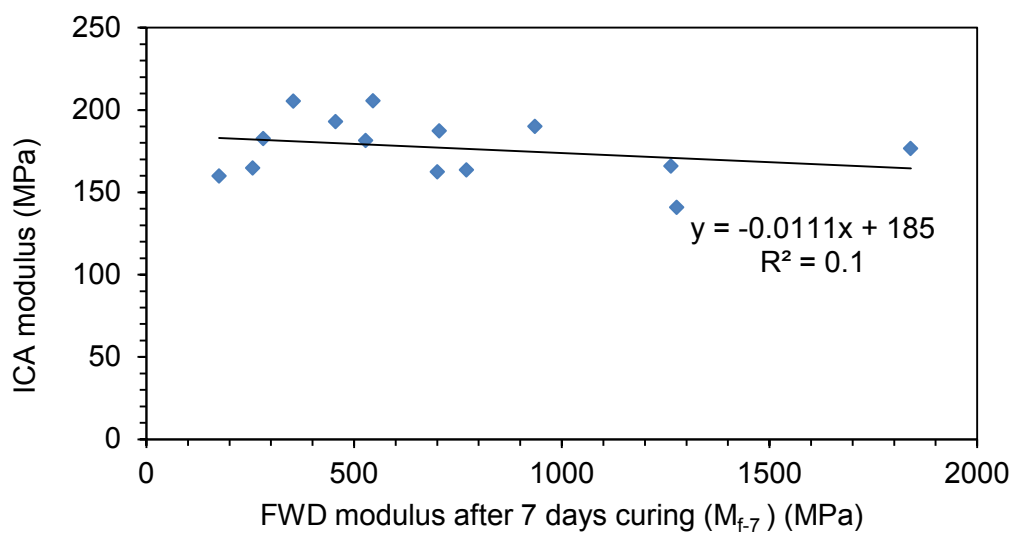
Figure 6.19.Comparison between ICA modulus and M_{f-7}.

6.10. IMPROVEMENT IN ICA-ESTIMATED MODULUS WITH REMEDIAL COMPACTION

As mentioned earlier, a total of 13 test points (S1 to S13) were identified as under-compacted regions in the two sections (Sections B and D). ICA moduli were estimated at these locations before and after remedial compaction. Table 6.7 presents a comparison between the ICA moduli estimated before and after remedial compaction. The average moduli calculated over a 1-meter vicinity of each test point and the corresponding standard deviation are presented in Table 6.7.

An important finding of this study is that the ICA was found to be able to identify under-compacted regions where the average modulus was below the target modulus (120 MPa). Figure 6.20 shows the improvement in moduli after remedial compaction. Significant improvement in the mean modulus and a decrease in the variation about the mean were observed in a majority of the test points. The improvement was significant at locations where the moduli were very low and where the remedial compaction was performed for a longer period of time (4 passes in Section D vs to 2 passes in Section B).

Table 6.7. Comparison of the ICA moduli before and after the remedial compaction.

Test Points	Before remedial compaction		After remedial compaction	
	Average (MPa)	Std. Dev	Average (MPa)	Std. Dev
S1	76	13	118	22
S2	75	12	120	10
S3	150	12	117	11
S4	143	10	115	7
S5	130	19	85	6
S6	110	12	95	17
S7	130	15	157	18
S8	86	20	150	6
S9	95	15	115	14
S10	107	9	144	10
S12	90	14	156	12
S13	110	17	178	8
S14	85	5	120	12
S15	110	9	164	4
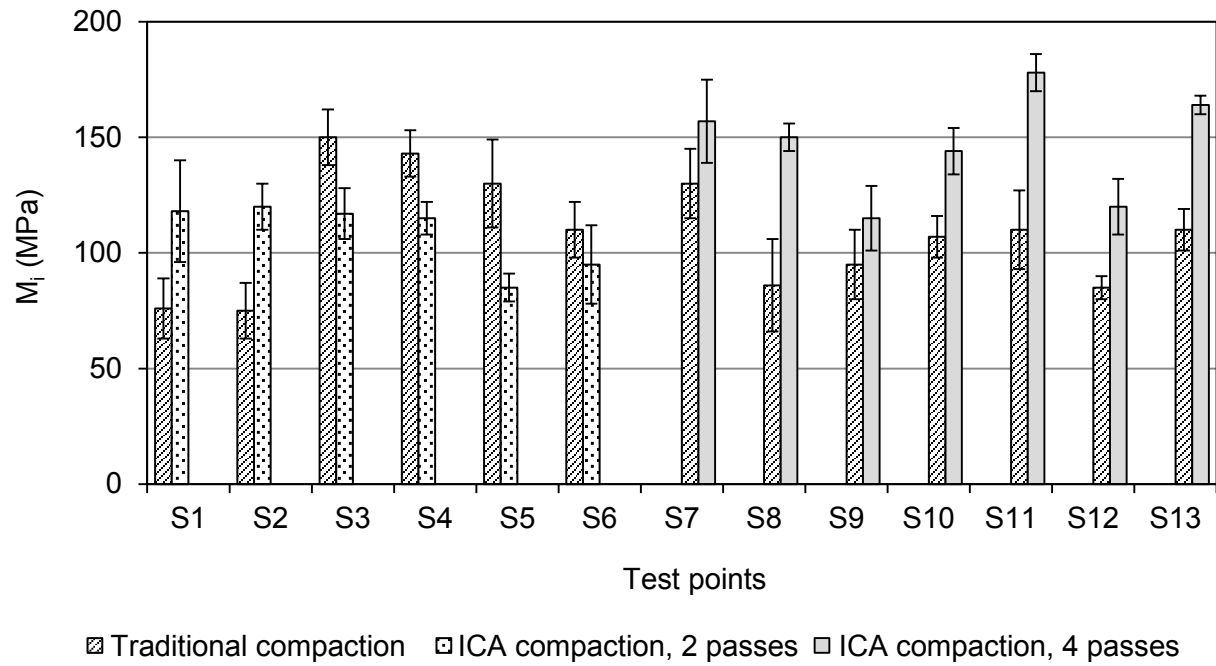
Figure 6.20. Bar chart showing improvement in the ICA moduli with 2 and 4 roller passes.

7. METHODOLOGY OF INTELLIGENT COMPACTION FOR ASPHALT LAYERS

Conventional quality control of asphalt pavement layers during compaction is usually performed by conducting volumetric analysis of cores collected from randomly selected locations. However, randomly selected locations do not adequately represent the entire compacted area and could leave under-compacted regions undetected. The feasibility of using the ICA in monitoring the level of compaction during construction of different asphalt layers was investigated in this project. The feasibility of performing remedial compaction to improve the compaction quality of the identified under-compacted regions was also investigated. The compaction quality was monitored by measuring the ratio (in percentage) of the compacted density to the maximum theoretical density, in real-time. This ratio, which is actually the relative density, is referred to as density (%) in this report. Under this scope of the study, the Intelligent Compaction was demonstrated at two different sites. The methodology adopted for the Intelligent Compaction on the asphalt layers is described below.

7.1. IDENTIFICATION OF SITE

The research team worked with the ODOT, Oklahoma Asphalt Pavement Association and other contractors for the site identification. As per the proposal, two projects were identified to demonstrate the capability of the ICA in improving the compaction quality of asphalt layers. The first demonstration deals with the compaction of asphalt base layer during reconstruction and widening of north-bound I-35, in Norman. The other project site involved the compaction of base and surface layers of a rural road in Shawnee, OK. The details of the sites are described under case studies in Section 8 and 9, respectively.

7.2. CHARACTERIZATION OF ASPHALT MIX

Representative bulk samples of asphalt mixes used in the construction were collected from the project site. In addition, information on the design of the asphalt mix used in the construction was collected from the plant. Depending on the type of construction, the collected asphalt mix was used to perform dynamic modulus test in the laboratory according to the test method AASHTO TP 79-09.

7.3. CALIBRATION OF THE ICA

The ICA was installed on the smooth drum vibratory roller. In both projects, a 9.14-m (30 ft) long stretch was marked as the calibration stretch. The paving contractor was requested to pave this calibration stretch first. Vibration and GPS data were collected during several roller passes over the calibration stretch. The vibration data were then used to train the ICA to recognize the power features in the vibratory signal. A preliminary calibration of the ICA was performed considering an approximate laydown density and a maximum final density based on the mix design information obtained from the contractor.

In order to adjust the calibration parameters, three core locations were marked on the calibration stretch at the end of the compaction work. Roadway cores were extracted from the marked locations and their densities determined in the laboratory according to the AASHTO T-166 test method. Final calibration of the ICA was performed by comparing the ICA-estimated density at the test locations with the density of the three cores. Further details of the calibration procedure can be found in the IACA User Manual in Appendix.

7.4. ICA MEASUREMENTS

During the compaction of the asphalt layer, the calibrated ICA was used to record the estimated densities and the GPS locations of the roller in real-time. After the compaction of each stretch, the as-built map displayed by the ICA was used to study the overall compaction achieved.

7.5. IDENTIFICATION AND REMEDIATION OF UNDER-COMPACTED REGIONS

During this traditional compaction, the density values were monitored in real-time, and as-built maps were generated after each stretch was compacted. The as-built maps were then used to study the compaction quality achieved and to detect under-compacted regions, if any. Additional roller passes with appropriate amplitude were applied to under-compacted regions to improve the level of compaction until the target density was achieved.

7.6. VALIDATION OF ICA-ESTIMATED COMPACTION LEVEL

The ICA-estimated density was validated by comparing the estimated density at select test locations with the density of the cores extracted from these location on the compacted layer(s). In addition, the ICA-estimated densities were compared with the NDG measured densities, wherever possible.

8. CASE STUDY 5: COMPACTION OF ASPHALT LAYERS (I-35 PROJECT)

8.1. IDENTIFICATION OF SITE

The ability of the ICA to estimate the density of asphalt pavements during compaction and its ability to improve compaction quality were demonstrated during the reconstruction and widening of north-bound I-35 in Norman, OK. A 640-m (2100-ft) long stretch was reconstructed as a full-depth asphalt pavement on the north-bound ramp of I-35 North near Main Street in Norman, OK. Two lanes and an access ramp were reconstructed. The location of the project site is shown in Figure 8.1. The construction at this site was carried out by Allen Construction, Oklahoma City, OK on September, 2013.

Intelligent Compaction was performed during the construction of an 89 mm (3.5-in) thick lift of the asphalt base layer. Figure 8.1 shows the cross-section of the constructed pavement . The asphalt base layer on which the Intelligent Compaction was performed is highlighted in Figure 8.1. During this demonstration, it was shown that real-time density measurements can be used to identify and remediate under-compacted regions of the asphalt layer.

8.2. CHARACTERIZATION OF ASPHALT MIX

The base layer on which the Intelligent Compaction was performed was constructed using an asphalt mix having a 19-mm nominal maximum aggregate size and a PG 64-22 OK binder. The asphalt mix also contained 25% reclaimed asphalt pavement (RAP). The properties of aggregates, asphalt binder and asphalt mix used in this project are provided in Table 8.1.

Intelligent compaction was performed in this layer

14'-0" Shoulder

14'-0" Shoulder

27'-0"

12'-0" N.B. Lane

12'-0" N.B. Lane

12'-0" N.B. Lane

CRL N.B.

30'-0"

12'-0" - 41'-6" Aux. Lane Varies At Ramps

●Var.

■10'-0" Shoulder

Construct Med. Barrier Des. 1-A

2" Superpave Type S4 (PG 76-28 OK)

3" Superpave Type S3 (PG 76-28 OK)

1-1/4 " Permeable Friction Course

2" Superpave Type S4 (PG 76-28 OK)

3" Superpave Type S3 (PG 76-28 OK)

N.B. Finish Grade

4" Superpave Type S3 (PG 64-22 OK)

Tack Coat

2" Superpave Type S4 (PG 64-22 OK)

3" Superpave Type S3 (PG 64-22 OK)

1'-6"

1'-6"

3'-1"

2'-8"

Approx. 1:6

Variable Slope to ramp

1:6

① ② ③

6" Edge Drain

3" Superpave Type S3 (PG 64-22 OK)

8" Agg. Base Type B

Separator Fabric

Prime Coat ④

Prime Coat ④

6" Edge Drain

8" & Var. Agg.Base Type B

Outlets connect to median structures as directed by the Engineer.

2% SLOPE

2% SLOPE

APPROX. 0.3% SLOPE

APPROX. 0.3% SLOPE

63'-9" & Var.

Limits of 8" Cementitious Stabilized Subgrade (Fly Ash Est. @ 15%)

66'-0" & Var.

Initial Grading Section

Survey I-35

Superpave S3 76-28 OK)

erpave 3 22 OK)

6"

arator ic

71

Figure 8.1. Cross-section of the pavement (north-bound I-35).
Table 8.1. Properties of aggregate, asphalt binder and asphalt mix.

Parameters	Value
Nominal maximum size aggregates	19 mm
Flat and elongated aggregates	0%
Los Angeles abrasion (%)	25.3%
Bulk specific gravity of aggregates	2.684
Type of asphalt binder	PG 64-22 OK
Specific gravity of asphalt binder	1.010
Asphalt binder content	4.3% (total); 3.2% (virgin)
Maximum theoretical specific gravity of asphalt mix	2.530
Voids in mineral aggregates	13.5%
Voids filled with asphalt binder	68.9%

8.3. CALIBRATION OF THE ICA

A double drum vibratory roller instrumented with the ICA was used for compaction of the base layer of the asphalt pavement. Calibration of the ICA was performed on a 9.14-m (30 ft) long stretch on the outermost lane. Three calibration cores (C-1, C-2 and C-3) were extracted after the pavement cooled down and their densities were determined, as explained in Section 7. Locations of these cores and other test points are shown in Figure 8.2. Table 8.2 presents the volumetric analysis of the cores and the corresponding ICA-estimated densities for the three calibration points. The density of the asphalt layer was also measured by a nuclear density gauge (NDG) and these readings are also shown in Table 8.2.
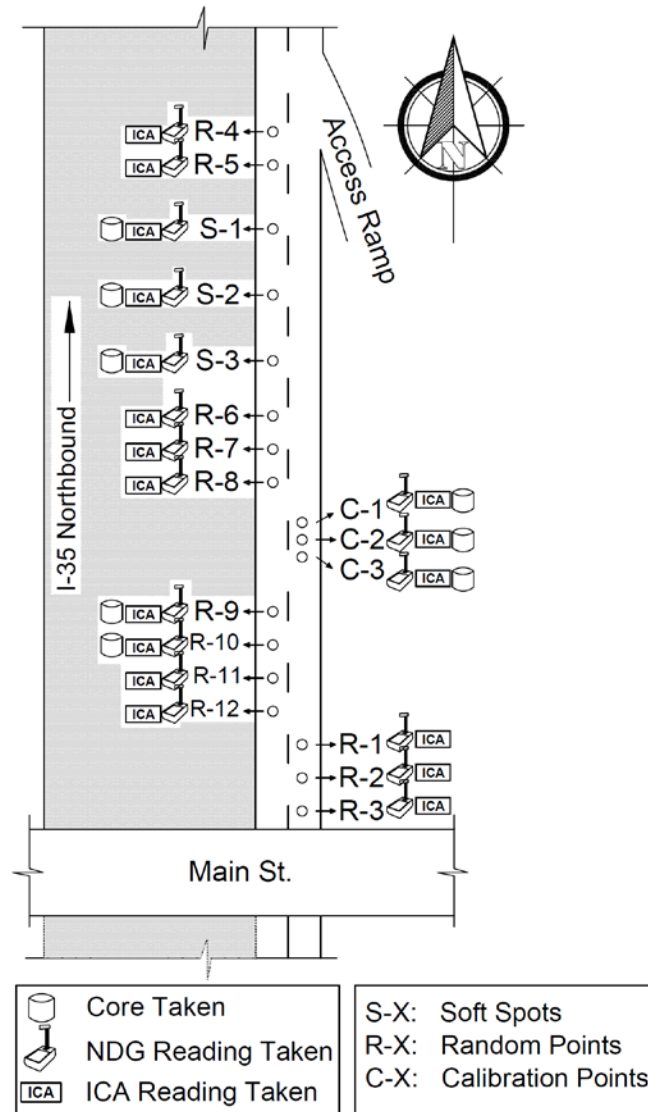
Figure 8.2. Locations of different test points in I-35 asphalt layer compaction project.

Table 8.2. Volumetric properties of cores and comparison of different densities at the calibration stretch for the I-35 project.

Calibration points	Core thickness (mm)	Air voids (%)	Density (percentage of maximum theoretical density)		
			Core	ICA	NDG
C-1	97	5.91	94.1	94.5	93.2
C-2	102	5.93	94.1	93.7	92.5
C-3	100	5.51	94.5	94.9	93.4

8.4. ICA MEASUREMENTS

The ICA measurements were recorded throughout the compaction process. The compaction of each stretch of the pavement was performed according to the rolling pattern established at the beginning of the project. The ICA records the roller vibrations, spatial locations of the roller, the surface temperature of the mat, and the estimated density throughout the compaction process. Verification of the ICA estimates was carried out by comparing the estimated density with the density of cores extracted from the compacted pavement at randomly selected locations.

8.5. IDENTIFICATION AND REMEDIATION OF UNDER-COMPACTED REGIONS

The use of the ICA in identifying and remediating under-compacted regions was studied at this site. The ICA-generated as-built maps were used to identify a region with inadequate compaction. In order to increase the compaction level, this region was compacted with additional passes and ICA measurements were collected again during these additional passes. Three points (S-1 to S-3 in Figure 8.2) were marked in this region after the completion of compaction. Twelve more random points were marked in the rest of the section. NDG tests were performed in all the 18 points (3 calibration points, 12 random points, and 3 soft points).

On the following day, a total of eight cores were extracted (3 calibration points (C-1 to C-3), 2 random points (R-9 and R-10), and 3 soft points (S1 to S-3)) for measurement of density.

Table 8.3 presents a comparison of the densities determined by different methods at each of the 18 test points. Figure 8.3 shows the improvement in density with the additional compaction. The average density at the three initially under-compacted points was increased by approximately 0.5%. This increment may not be large enough, but this project certainly verified the fact that the under-compacted regions can be identified and remediated using the ICA.

Table 8.3. Comparison between the densities determined by different methods.

Test points	Density (percentage of maximum theoretical density)			
	Core	ICA before remedial compaction	ICA after remedial compaction	NDG
R1	NA	95.70	NA	93.62
R2	NA	94.20	NA	94.73
R3	NA	95.20	NA	93.91
R4	NA	93.20	NA	92.57
R5	NA	93.30	NA	92.92
R6	NA	93.60	NA	93.37
C1	94.1	94.50	NA	93.18
C2	94.1	93.70	NA	92.51
C3	94.49	94.90	NA	93.37
R7	NA	93.60	NA	92.80
R8	NA	94.10	NA	92.23
S1	94.2	93.5	94.20	92.86
S2	94.7	94.6	94.80	93.30
S3	94.6	93.7	94.00	93.40
R9	NA	93.00	NA	91.18
R10	95.1	95.80	NA	93.21
R11	95.3	94.80	NA	94.06
R12	NA	95.40	NA	94.10
Lay-down density	86.3	86.1	NA	88

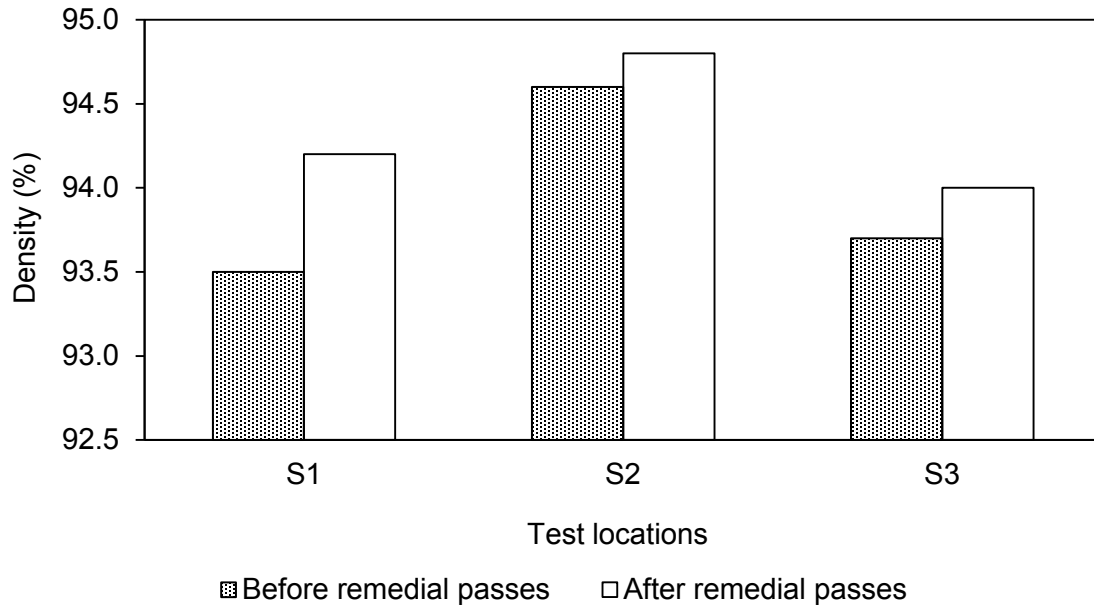*Note: NA- Not available or not applicable*

Figure 8.3. Improvement in the density with the ICA compaction.

8.6. VALIDATION OF THE ICA-ESTIMATED COMPACTION LEVEL

The correlation between the core densities and the ICA-estimated densities is shown in Figure 8.4. The R^2 and the standard error of estimate (SEE) for this correlation are 0.98and0.48% , respectively. The correlation can be considered as excellent with a low SEE and very high R^2. Figure 8.5 presents a comparison between the NDG-measured densities and the ICA-estimated densities. The R^2 and SEE values are 0.95 and 1.44%, respectively. It may be noted that the lay-down densities, which are significantly lower than the compacted densities, were also considered in the above-mentioned correlations. This consideration hypothetically increases the R^2. So comparing the SEE between the different correlations would be more appropriate. Since the ICA was calibrated with the core densities, a better correlation between the ICA-estimated density and core density than that between the ICA-estimated density and the NDG density was expected. Figure 8.6 shows the correlation between core density and NDG density. For this case the SEE was found to be 1.60%. As anticipated, this correlation is not as good as the

correlation between the ICA-setimated density and the core density. Thus it can be concluded

that the ICA can provide a better estimation of the level of compaction of the asphalt layer than
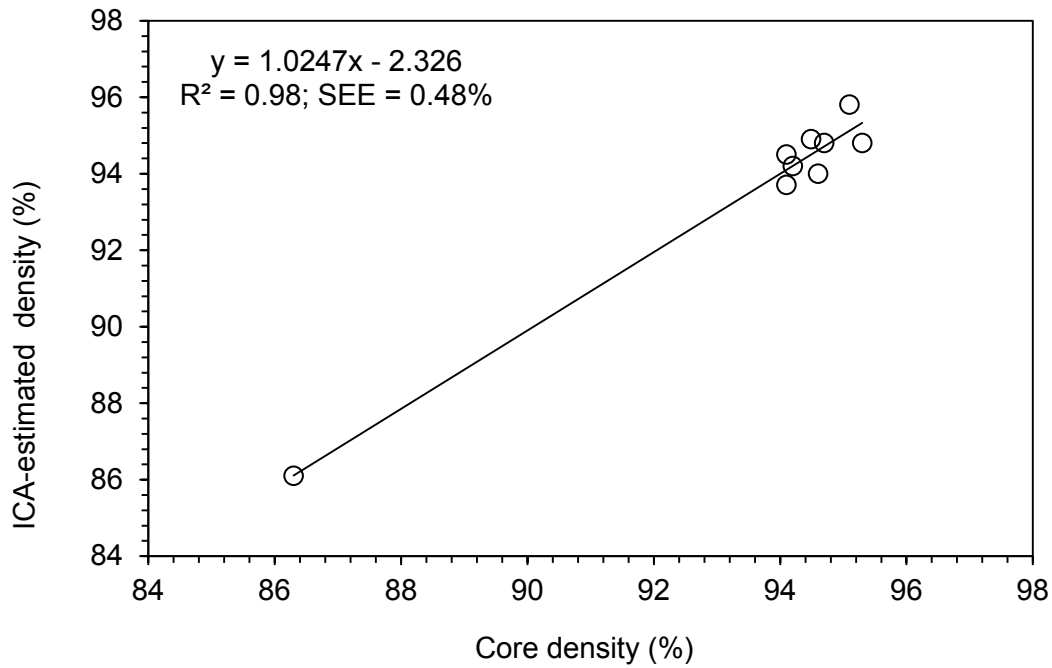
that which can be provided by an NDG.

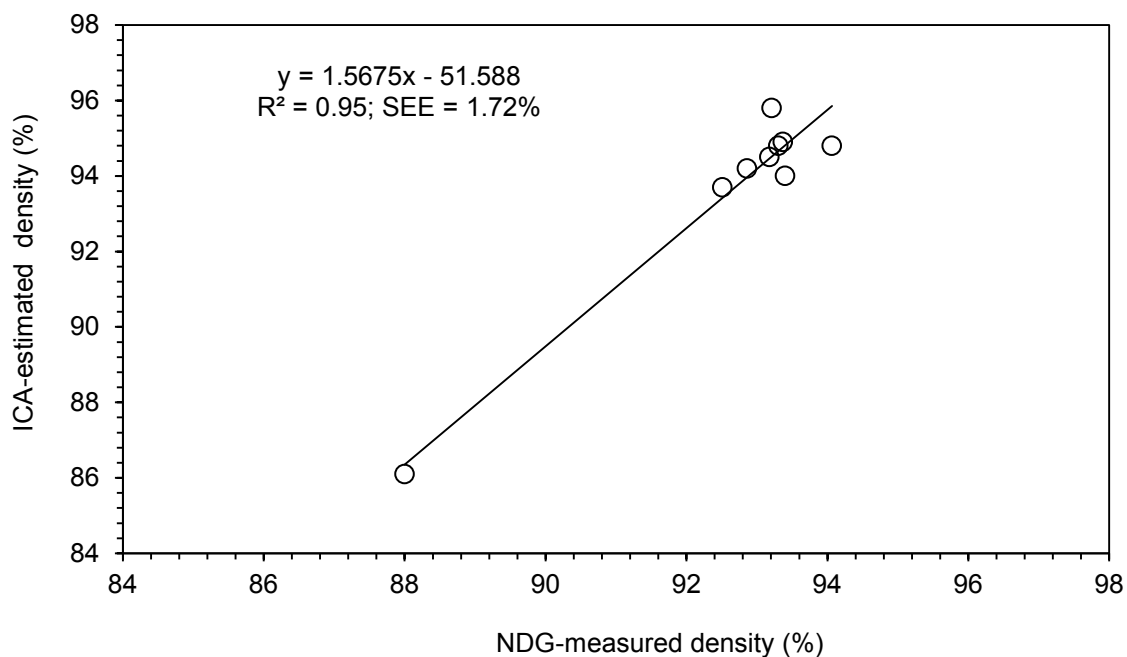Figure 8.4. Comparison between core densities and ICA-estimated densities.

Figure 8.5. Comparison between the NDG measured densities and ICA-estimated densities.
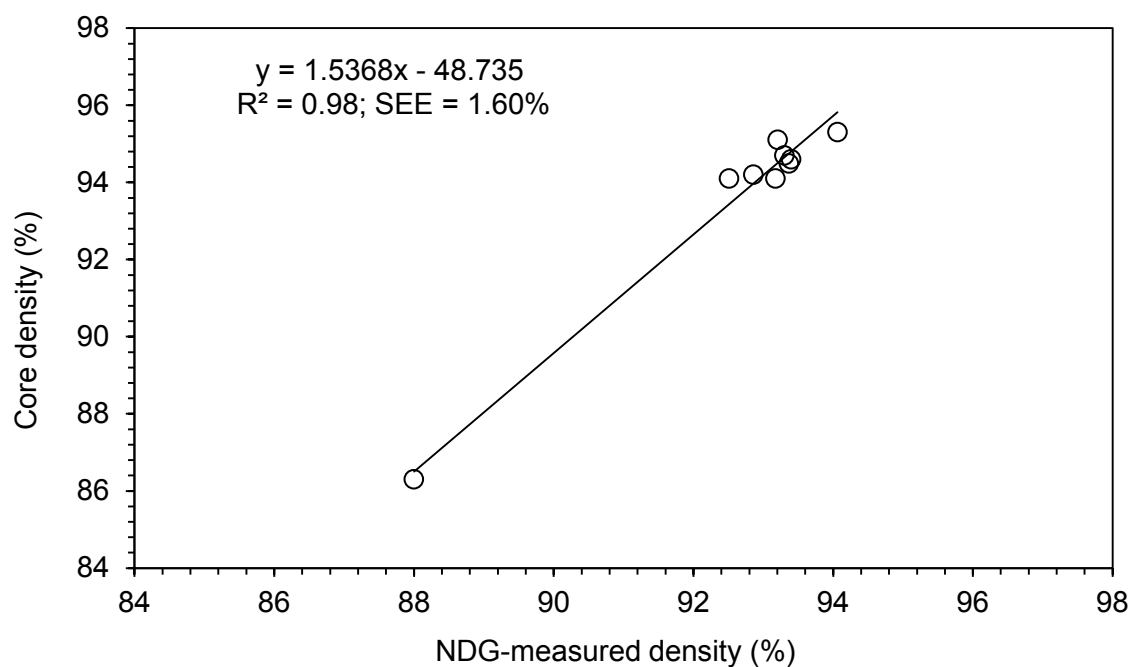

Figure 8.6. Comparison between the NDG measured densities and ICA-estimated densities.

8.7. APPLICATION OF THE ICA IN ESTIMATING DYNAMIC MODULUS

The ICA can be calibrated to estimate the dynamic modulus in real-time (Singh et al., 2011). In a previously conducted research project, it was concluded that the Light Weight Deflectometer (LWD) does not provide reliable measurements of pavement moduli (Commuri et al., 2013). Therefore, the ICA-estimated density was compared with the dynamic modulus estimated using core densities and dynamic modulus master curves that were developed for the mix used in the I-35 project.

In order to calibrate the ICA and estimate the dynamic moduli in real-time, it was necessary to obtain the equivalent dynamic modulus values at different test points in the field. Laboratory dynamic modulus tests were conducted according to the AASHTO TP 79-09 test method on specimens prepared using asphalt mixes collected from the I-35 project site. The test specimens were prepared by compacting them to air voids measured at different cores collected from the field. Results of the volumetric analyses of the cores collected from the project site are given in Table 8.4. It can be seen that the air void of the field cores range from 4.75 to 7.65%. Based on the volumetric analysis of the cores collected from the sites, it was decided to prepare dynamic modulus specimens for four different percentages of air voids. The selected air voids (target air voids) for dynamic modulus tests are 4%, 5.5%, 7% and 8.5% with a ±0.5% tolerance. Three specimens were tested for each air void. It may be noted that initially a large number of trial specimens were prepared and the test specimens were selected based on the target air voids. Each specimen was tested at 4 different temperatures (4, 21, 37 and 54 °C) and 6 different loading frequencies (25, 10, 5, 1, 0.5 and 0.1 Hz.), as specified in the test procedure.

Table 8.4. Volumetric analysis of cores collected from the I-35 project.

Test points	C-1	C-2	C-3	S-1	S-2	S-3	R-9	R-10
G_{mb}	2.381	2.380	2.391	2.383	2.396	2.394	2.406	2.410
G_{mm}	2.530	2.530	2.530	2.530	2.530	2.530	2.530	2.530
Relative density (%)	94.09	94.07	94.49	94.21	94.71	94.62	95.09	95.25
Air void (%)	5.91	5.93	5.51	5.79	5.29	5.38	4.91	4.75

The dynamic modulus test results were used to develop four dynamic modulus master curves, one for each target air void. The results from the three specimens tested for each target air void were averaged.

Dynamic modulus master curves were then constructed using the principle of time–temperature superposition. The reference temperature was specified as 21°C. The dynamic moduli results at various temperatures were shifted with respect to loading frequency until the curves merged into a single smooth curve. The dynamic moduli master curve as a function of frequency describes the loading rate dependency of the material. The amount of shifting at each temperature required to form the master curve describes the temperature dependency of the material (Bonaquist and Christensen, 2005). The following sigmoidal function (Equation 8.1) was fit to construct the master curves.

$$\log(E^*) = \delta + \frac{\alpha}{1+e^{\beta+\gamma(log\omega_r)}} \tag{8.1}$$

where E* = dynamic modulus; ω_r= reduced frequency; δ = minimum value of E*; $\delta + \alpha$ = maximum value of E*; and β, γ = parameters describing the shape of the sigmoidal function.

The developed master curves are presented in Figure 8.7. The shift factors and other fitting parameters for the master curves as a function of temperatures and air voids percentages are given in Table 8.5. As anticipated, the dynamic modulus decreases with the increase in air voids percentage. The master curves were then used to determine the asphalt layer dynamic

moduli at different locations on the compacted pavement. Figure 8.8 presents the comparison between the ICA-estimated dynamic moduli and laboratory dynamic moduli. It can be seen from Figure 8.7 that the ICA is effective in estimating layer modulus of the pavement during compaction. Further, the ICA-estimated modulus correlates well with the dynamic modulus of the pavement layer (R^2 = 0.73).
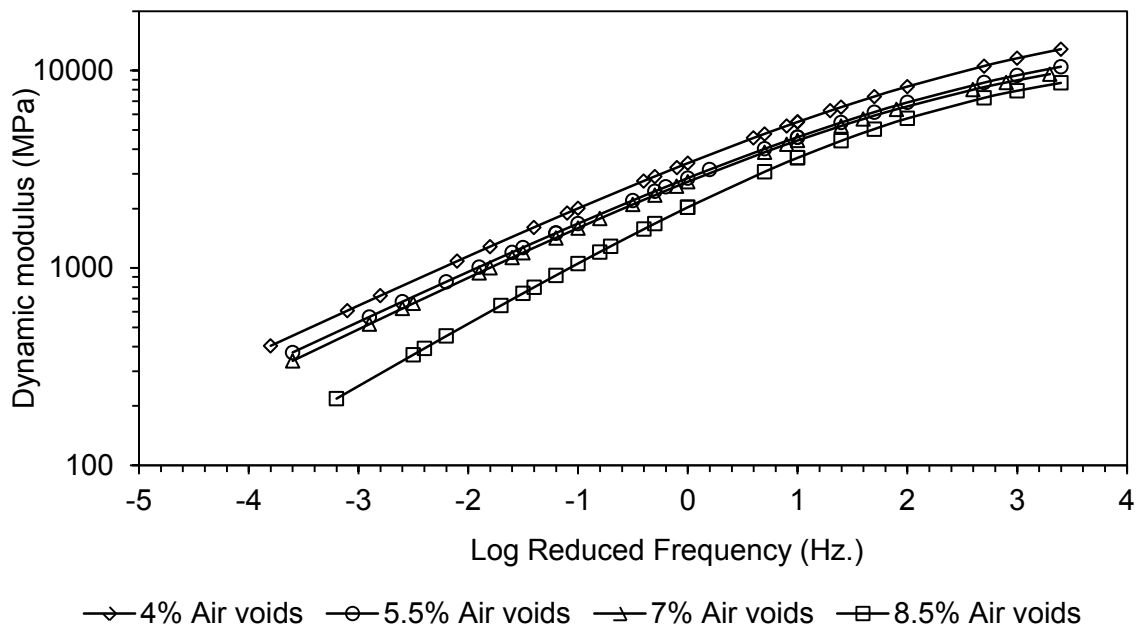

Figure 8.7. Master curves for four different target air voids for the I-35 project.

Table 8.5. Shift factors and fitting parameters used in developing the master curves for I-35 project.

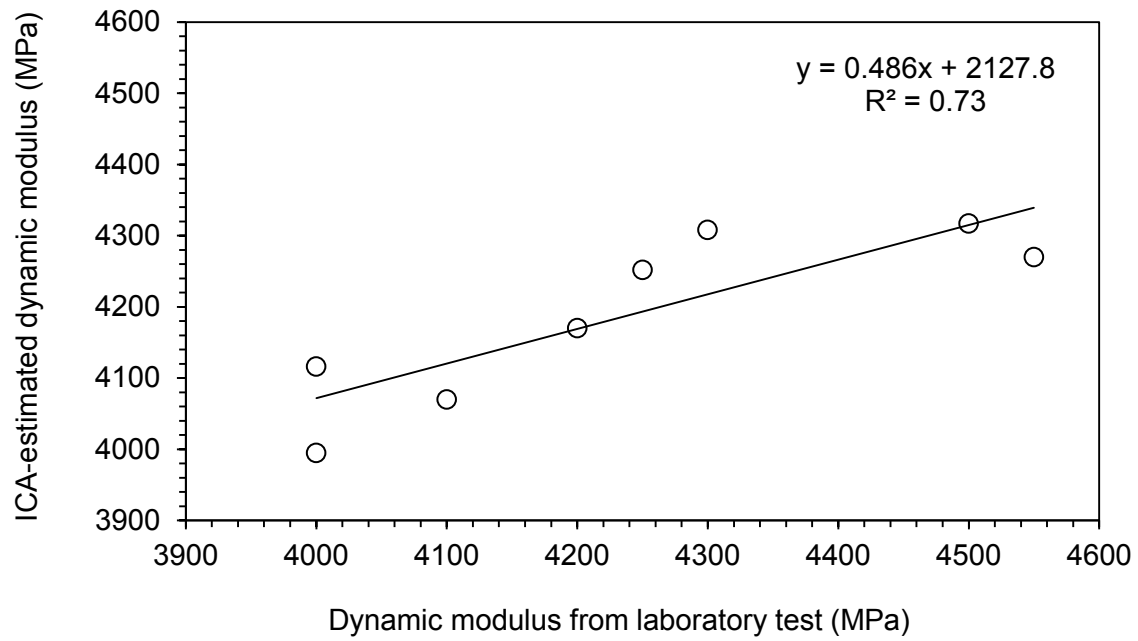|	Shift factors for different air voids and temperatures			
Temperature	4% AV	5.5% AV	7% AV	8.5% AV
4°C	2.00	2	1.9	2
21°C	0	0	0	0
37°C	-0.1	-1.2	-1.5	-1.4
54°C	-2.8	-2.6	-2.6	-2.2
Fitting parameters				
α	21990	16990	14990	11990
β	1.7	1.6	1.5	1.59
γ	0.6	0.61	0.63	0.75
δ	10	10	10	10

Note: AV = air voids percentage

Figure 8.8. Correlation between the ICA-estimated dynamic moduli and the laboratory measured dynamic moduli for the I-35 project.

9. CASE STUDY 6: COMPACTION OF ASPHALT LAYER (ACME ROAD PROJECT)

9.1. IDENTIFICATION OF SITE

This site is located on Acme Road (between NS Co Road 339 and Franklin Road) near Highway 177 in Shawnee, Oklahoma (Figure 9.1). Two lanes of Acme Road were paved with asphalt pavement. Intelligent Compaction was performed on the 76-mm (3-inch) asphalt base layer and also on the 51-mm (2-inch) surface layer. This project was selected as a representative of a low volume rural road in Oklahoma, and the asphalt layer was placed on the unstabilized granular layer, as shown in Figure 9.2. The construction at this site was carried out by Haskell Lemon Construction Company, Oklahoma City, OK on June, 2014.

9.2. CHARACTERIZATION OF ASPHALT MIX

The properties of aggregates, binder and asphalt mixes used in the base and surface layers are summarized in Table 9.1 and Table 9.2, respectively. The asphalt mixes of both layers contained a PG 64-22 OK binder. The nominal maximum aggregate size (NMAS) for the base layer was 25.4 mm (1 inch). The NMAS value for the surface layers was 12.7 mm (½ inch). Both the layers also contained a significant percentage of RAP. The base layer mix contained 25% RAP and the surface layer mix contained 35% RAP.

9.3. CALIBRATION OF THE ICA

A double drum smooth vibratory roller was used for compaction of both the base and surface layers. The ICA was calibrated separately for each layer. Calibration procedures for the two layers were identical and similar to the procedure discussed in Section 7. The ICA was calibrated on a 9.14-m (30 ft) long stretch on the base layer as well as on the surface layer. The

locations of the calibration stretches for both the layers are shown in Figure 9.3. Three cores

(C1, C2 and C3) were extracted from the calibration stretch of each layer, on the following day
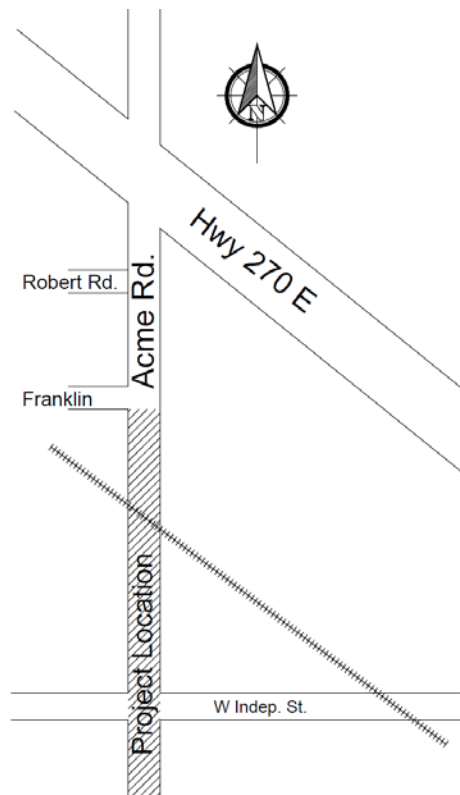
after compaction (Figure 9.4).

Figure 9.1. Location of the Acme Road project.

Figure 9.2. Unstabilized granular layer to support the asphalt base layer.

Table 9.1. Properties of aggregate, asphalt binder and asphalt mix used in the base layer.

Parameters	Value
Nominal maximum aggregate size	25.4 mm
Los Angeles abrasion (%)	23.7%
Effective specific gravity of aggregates	2.707
Type of asphalt binder	PG 64-22 OK
Proportion of RAP in the asphalt mix	25%
Specific gravity of asphalt binder	1.010
Asphalt binder content	4.0% (total); 3.0% (virgin)
Maximum theoretical specific gravity of asphalt mix	2.535
Voids in mineral aggregates	13.6%

Table 9.2. Properties of aggregate, asphalt binder and asphalt mix used in the surface layer.

| Parameters	Value
Nominal maximum aggregate size	12.5 mm
Los Angeles abrasion (%)	23.4%
Effective specific gravity of aggregates	2.693
Type of asphalt binder	PG 64-22 OK
Proportion of RAP in the asphalt mix	35%
Specific gravity of asphalt binder	1.010
Asphalt binder content	4.7% (total); 3.5% (virgin)
Maximum theoretical specific gravity of asphalt mix	2.495
Voids in mineral aggregates	15.2%
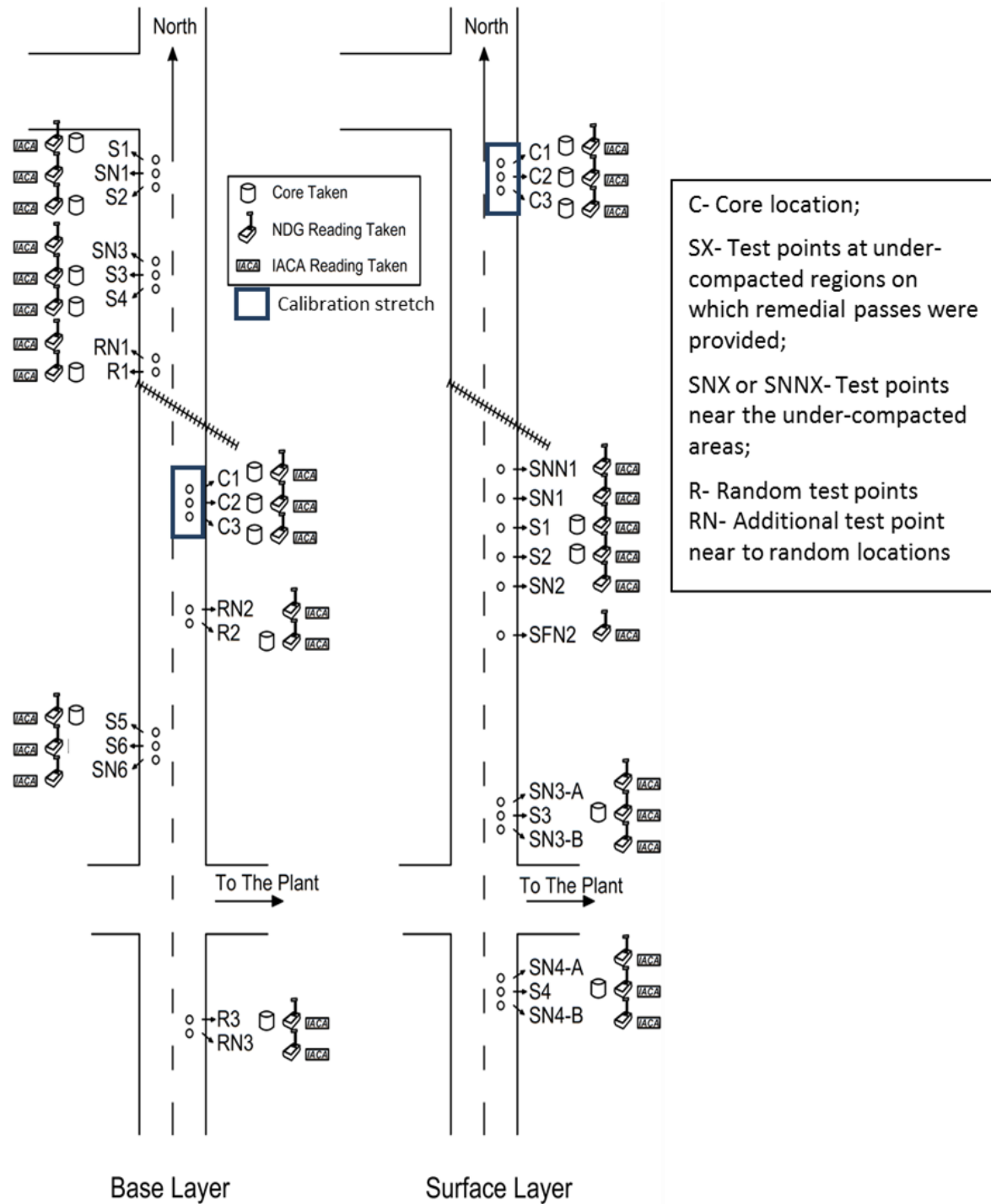
Figure 9.3. Location of test points on base and surface layers of Acme Road.

Figure 9.4. Extraction of roadway cores from Acme Road project.

9.4. ICA MEASUREMENTS

The ICA measurements were taken throughout the compaction of both the base and surface layers. The ICA recorded the roller vibrations, spatial locations of the roller, the surface temperature of the mat, and the estimated density throughout the compaction process. Verification of the ICA-estimated densities was carried out by comparing the estimated density with the density of cores extracted from the compacted base and surface layers at randomly selected test locations. Figure 9.5 and Figure 9.6 show compaction of the base layer and surface layer, respectively, using a smooth drum vibratory roller equipped with the ICA.

Figure 9.5. Recording ICA measurements during the compaction of the base layer.

Figure 9.6. Recording ICA measurements during the compaction of the surface layer.

9.5. IDENTIFICATION AND REMEDIATION OF UNDER-COMPACTED REGIONS

The performance of the ICA in identifying and remediating the under-compacted regions was tested on both the base and surface layers of this project. Under-compacted regions were identified at multiple regions both on the base and surface layers, as shown in Figure 9.3. Additional roller passes were provided to improve the level of compaction in those regions, wherever possible. ICA measurements were taken both before and after the remedial passes.

In the base layer, six under-compacted regions (S1 to S6) were identified. Remedial roller passes were applied on first 5 regions (S1 to S5). The roller operator could not provide additional passes on the last region (S6) because of time constraint. In the surface layer, four under-compacted regions were identified. However, remedial passes could only be applied on first two regions (S1 and S2) because of time constraint. It may be noted that as the Intelligent Compaction was not specified as a requirement, roller operator showed reluctance in applying additional passes outside the traditional procedure.

Figure 9.7 presents a comparison of the ICA density measured before and after the remedial passes. It is seen for the base layer that the density at the four regions (S1 to S4) was increased with the remedial passes. The density at Region S5 could not be increased because only one additional pass was provided on S5 as compared to two or three remedial passes on the other regions. It was difficult to keep the roller operator motivated towards the end of the day. The average density of the five regions improved from 90.9% to 92.2%. In the surface layer, the density was found to increase in one region (S1), while in the other region it remained almost the same. The average density improved from 93% to 93.2%.
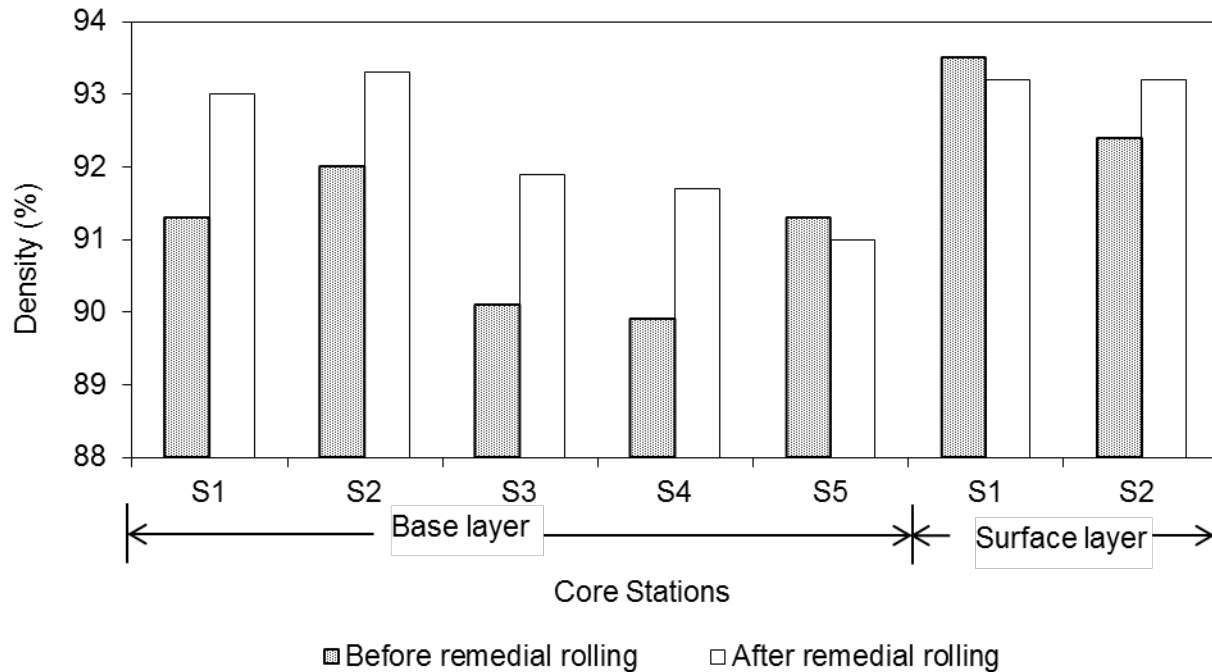
Figure 9.7. Improvement in ICA-estimated density with remedial roller passes at the under-compacted regions.

9.6. VALIDATION OF ICA-ESTIMATED COMPACTION LEVEL

In order to validate the ICA measured densities, roadway cores were extracted at various locations as shown in Figure 9.3. A total of eleven cores were extracted from the base layer and seven cores were extracted from the surface layer. Volumetric analyses were performed on all the cores. Table 9.3 and Table 9.4 present the results of the volumetric analyses of the cores. The core densities varied between 91.05% and 94.09% in the base layer, whereas it varied between 90.64% and 94.05% in the surface layer. The lay down density in the base layer was 88.10% and 86.5% for the base and surface layers, respectively.

A tabular comparison between the core densities and the corresponding ICA-estimated densities for the base and surface layers are presented in Table 9.5 and Table 9.6, respectively.

The correlations between the core densities and the corresponding ICA-estimated densities for the base and surface layers are given in Figure 9.8 and Figure 9.9. The correlations are quite reasonable for both the base (R^2 = 0. 85) and surface (R^2 = 0.93) layers. From these correlations, it can be concluded that the ICA could measure the density with a reasonable accuracy.

Table 9.3. Volumetric analysis of the cores collected from base layer in Acme Road project.

Parameters	Test points										
	C1	C2	C3	S1	S2	S3	S4	S5	R1	R2	R3
Wt. in air (A)	2567.2	2691.5	2790	2998.8	2570	2401.9	2393.2	2325.7	2335.4	2815.8	2677.8
Wt. in water (C)	1495.2	1565.2	1627.2	1731.2	1490.5	1393.2	1379.2	1344.4	1341.7	1620.8	1563.2
Wt. SSD (B)	2598.2	2700.6	2796.4	3010.7	2584.4	2418.5	2403.6	2337.1	2353.1	2829	2691.2
G_{mb}	2.327	2.371	2.386	2.344	2.349	2.343	2.336	2.343	2.309	2.331	2.374
G_{mm}*	2.536	2.536	2.536	2.536	2.536	2.536	2.536	2.536	2.536	2.536	2.536
Density (% of G_{mm})	91.78	93.48	94.09	92.42	92.64	92.38	92.12	92.38	91.05	91.90	93.61
% Air void	8.22	6.52	5.91	7.58	7.36	7.62	7.88	7.62	8.95	8.10	6.39
Core thickness (mm)	71.5	73	74	81	68	66	64	62.5	64	76	71

Table 9.4. Volumetric analysis of the cores collected from surface layer in Acme Road project.

Parameters	Test points						
	C1	C2	C3	S1	S2	S3	S4
Wt. in air (A)	1636	1421.8	1519.1	1656.9	1589.9	1695.1	1798.9
Wt. in water (C)	930.5	800.4	862.5	954.1	911.8	965.9	1030
Wt. SSD (B)	1641.4	1429.6	1527.2	1660.8	1593.3	1699.3	1803.1
G_{mb}	2.301	2.260	2.285	2.345	2.333	2.311	2.327
G_{mm}*	2.493	2.493	2.493	2.493	2.493	2.493	2.493
Density (% of G_{mm})	92.31	90.64	91.67	94.05	93.58	92.71	93.34
% Air void	7.69	9.36	8.33	5.95	6.42	7.29	6.66
Core thickness (mm)	45	42	43.5	43.5	45.5	44	47

*G_{mm} was provided by the contractor.

Table 9.5. Comparisons of ICA-estimated density and core density at test points on the base layer.

Test points	Density (%)		Difference between core and ICA densities (%)
	Core	ICA	
C1	91.8	91.5	0.3
C2	93.5	93.7	-0.2
C3	94.1	92.8	1.3
S1	92.4	93	-0.6
S2	92.6	93.3	-0.7
S3	92.4	91.9	0.5
S4	92.1	91.7	0.4
S5	92.4	91	1.4
R1	91.1	90.5	0.6
R2	91.9	91.1	0.8
R3	93.6	93	0.6

Note: Cores were not extracted at all the test points, as shown in Figure 9.3.

Table 9.6. Comparisons of ICA-estimated density and core density at test points on the surface layer.

Test points	Density (%)		Difference between core and ICA densities (%)
	Core	ICA	
C1	92.3	92.2	0.1
C2	90.6	91.5	-0.9
C3	91.7	92.8	-1.1
S1	94	93.2	0.8
S2	93.6	93.2	0.4
S3	92.7	92.7	0
S4	93.3	93	0.3

Note: Cores were not extracted at all the test points, as shown in Figure 9.3.
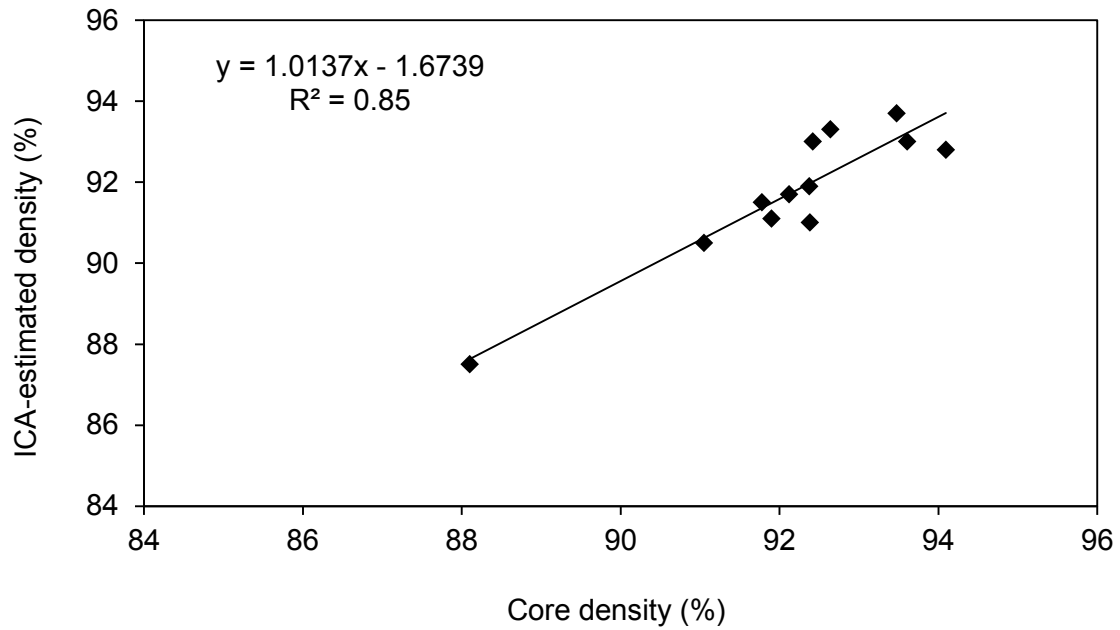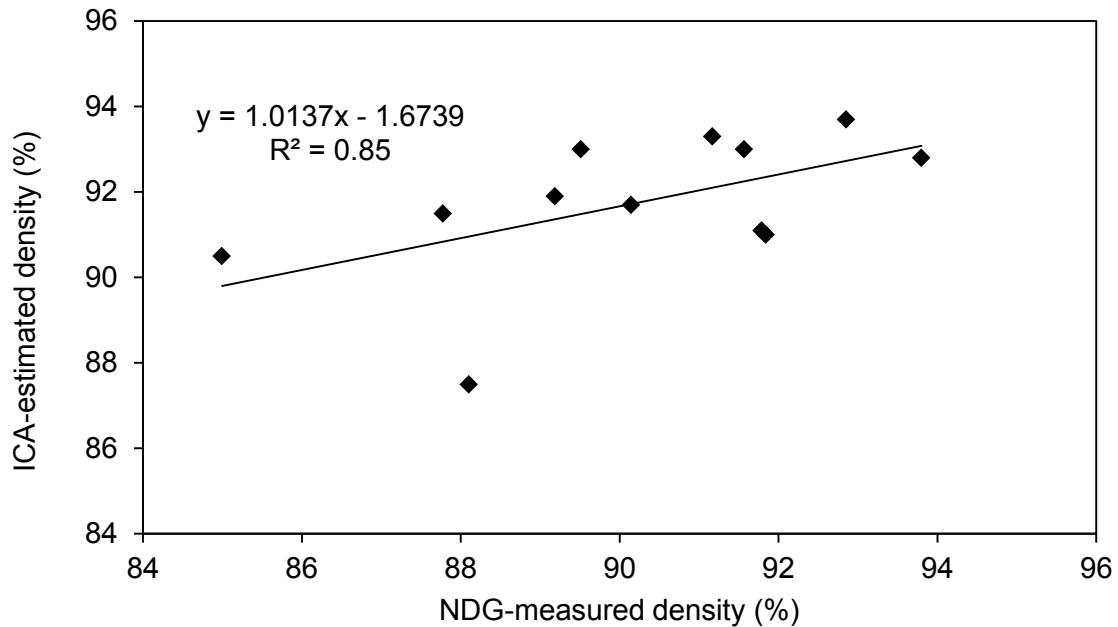
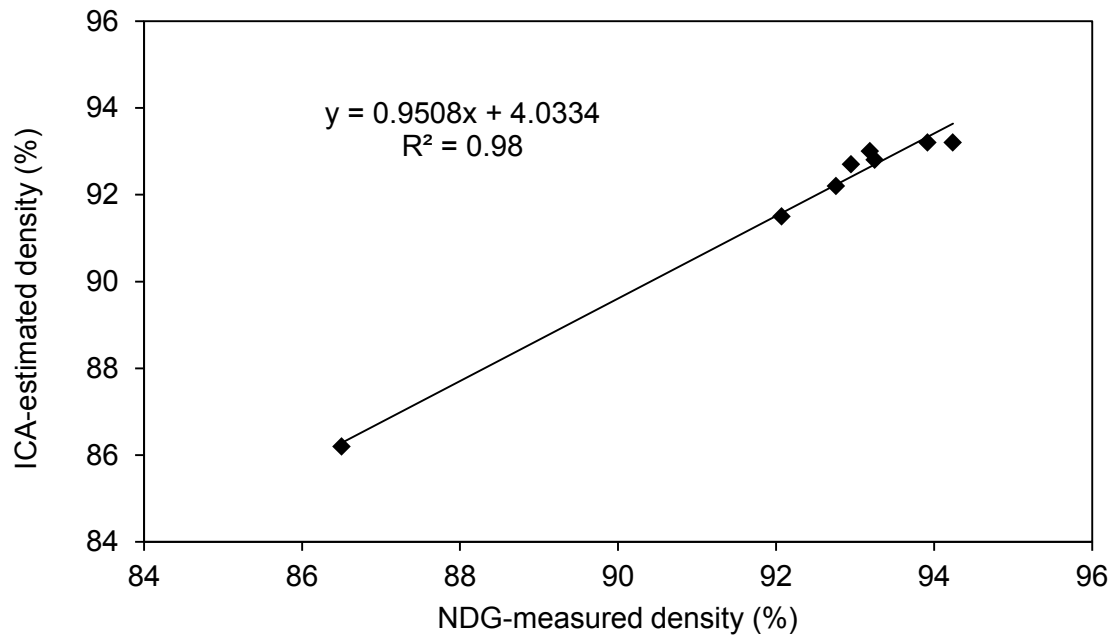Figure 9.8. Correlation between core density and ICA-estimated density for the base layer in Acme Road project.

.
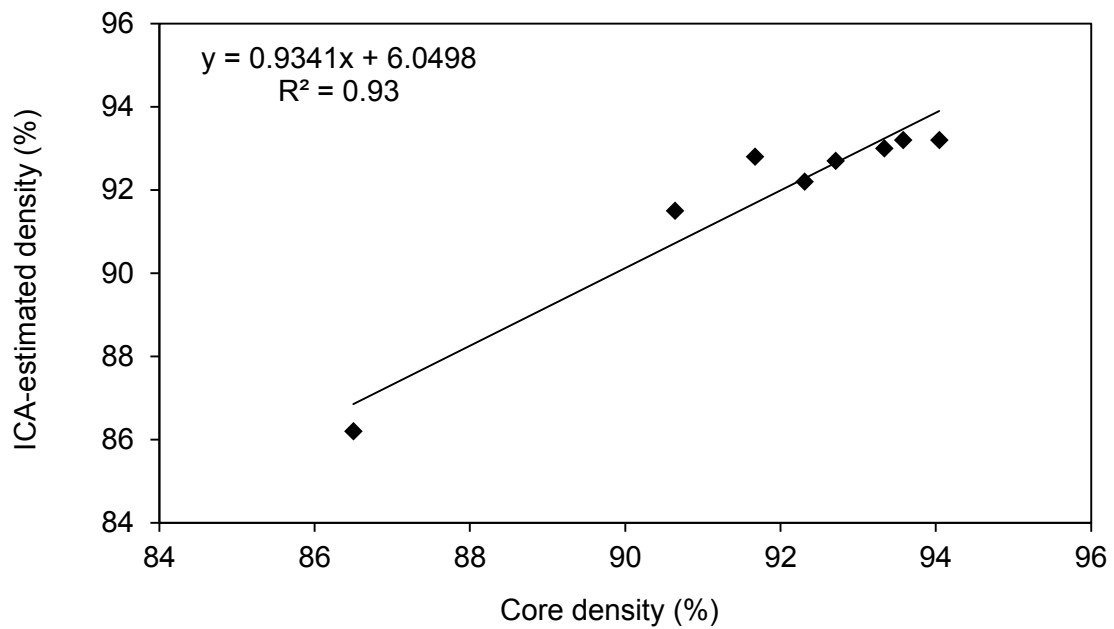
Figure 9.9. Correlation between core density and ICA-estimated density for the surface layer in Acme Road project.

It may be noted that the density was also measured at many test points by an NDG. A comparison between the NDG measured densities and the ICA-estimated densities for the base and surface layers is provided in Figure 9.10 and Figure 9.11, respectively. Reasonably good correlations were obtained between the NDG measured and ICA-estimated densities, with R^2 = 0.85 for base layer and 0.98 for surface layer, respectively.

Figure 9.10. Correlation between NDG-measured density and ICA-estimated density for the base layer in Acme Road project.

Figure 9.11. Correlation between NDG-measured density and ICA-estimated density for the surface layer in Acme Road project.

10. CONCLUSIONS AND RECOMMENDATIONS

10.1. CONCLUSIONS

Use of the Intelligent Compaction Analyzer (ICA) to estimate the resilient modulus of stabilized subgrade and the relative density of asphalt layers during compaction was evaluated in this project. In addition, the feasibility of identifying and remediating the under-compacted regions was studied.

Six case studies were considered in this project to demonstrate the ability of the ICA to estimate the level of compaction during construction and use these estimates to identify and remediate inadequate compaction. The first two case studies utilized compaction data collected during the construction of stabilized soil subgrade at two different locations. The data were used to refine a method by which the level of compaction of the subgrade layer could be estimated in terms of ICA modulus. This method was then used in Case Studies 3 and 4 to demonstrate the use of the ICA in improving the compaction of stabilized subgrades modified with Cement Kiln Dust (CKD). In Case Study 3, the use of the ICA in compaction of stabilized subgrade was demonstrated during the reconstruction and widening of I-35 in Norman, Oklahoma. In Case Study 4, the ICA was demonstrated during the extension of the I-35 Service Road in Norman, Oklahoma. In both of these case studies, a smooth steel drum vibratory roller equipped with the ICA was used to proof roll the subgrades that were initially compacted using pad-foot rollers. After calibration of the ICA, the ICA modulus of the subgrade was estimated and recorded continuously during the proof rolling process. Several test locations were marked on the compacted subgrade, and the moisture content and the dry density values were measured using a Nuclear Density Gauge (NDG). The method developed in Case Studies 1 and 2 was used to estimate the modulus at these test locations. The GPS readings of the test locations

were used to determine the ICA modulus at these locations. A comparison of the ICA modulus with the modulus determined through statistical means shows that the ICA can estimate the modulus during compaction with an accuracy level suitable for quality control in the field. As-built maps developed using ICA-estimated moduli were used to detect regions of inadequate compaction on the subgrade. Remedial rolling at those locations showed that the level of compaction of stabilized subgrade can be improved if the level of compaction was determined during compaction and under-compacted regions rectified.

In the last two Case Studies, the use of the ICA in improving the compaction quality of asphalt layers was demonstrated. The ICA was first installed on a dual steel drum vibratory roller and calibrated to estimate the density of asphalt layers being compacted on top of the subgrade prepared in the first demonstration. During the compaction process, the ICA-estimated density was recorded continuously over each roller pass. After the compaction of the stretch, test locations were marked on the compacted asphalt pavement and the density at these locations was recorded using a NDG. Cores were then extracted from these locations on the compacted pavement and their density was measured in the laboratory. A comparison of the ICA-estimated density at these locations with the density of the cores measured in the laboratory shows that the ICA can estimate the density with an accuracy level suitable for quality control purpose in the field. Similar to the previous case, after the stretch was compacted, the as-built map generated by the ICA was used to determine regions of inadequate compaction. Remedial rolling on these regions was carried out and the density at select locations was determined through extraction of cores. A comparison of these densities with the densities estimated by the ICA shows that the overall density improved as a result of remedial rolling. Further, the variance of these densities about their mean was smaller than the variance observed during the traditional compaction process.

The ICA moduli were validated by comparing them with the laboratory equivalent resilient modulus for the stabilized subgrade. The ICA moduli were also validated by comparing them with the FWD and DCP test results wherever possible. Natural subgrade soil and additives from each of the ICA demonstration sites were evaluated and their properties were studied in the laboratory. Separate regression models were developed for each demonstration site to correlate the resilient modulus with the moisture content, dry density and stress states. It was found that the ICA modulus and laboratory resilient modulus correlate well when the comparison was performed separately for each site, with limited data points. The coefficient of determination (R^2) was found to be between 0.60 and 0.65 at each test site. It is interesting to note that when the correlations between the ICA modulus and the laboratory resilient modulus was studied by combining the data points (81 data points) from all the stabilized subgrade compaction related projects, the correlation improved significantly as shown in Figure 10.1. The R^2 for this case is 0.89.
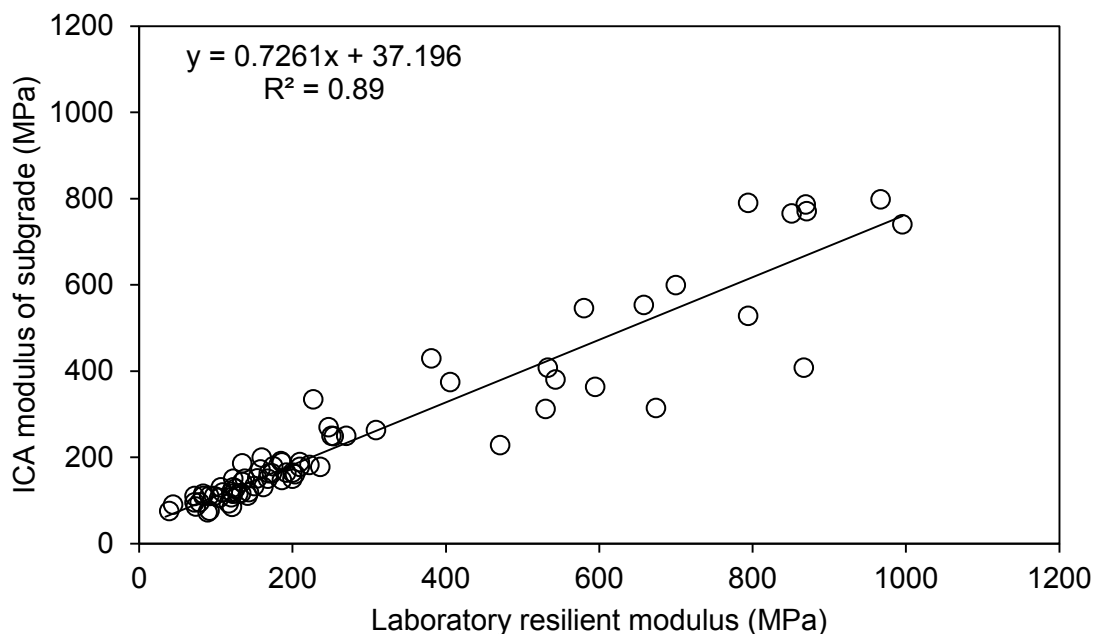
Figure 10.1. Correlation between ICA modulus and laboratory resilient modulus, data from four different projects (81 data points).

The other important finding from this study is that the ICA can be used to identify and remedy under-compacted regions during the construction of pavements. In both subgrade compaction projects (I-35 and I-35 Service Road projects), it was shown that the average modulus of the entire subgrade can be improved. The level of compaction in the entire project stretch was also more uniform when the ICA compaction procedure was followed.

In the asphalt layer compaction projects, the ICA was used in real-time monitoring of level of compaction in terms of relative density. The relative density is the ratio of the density at any location to the maximum theoretical density. The relative density was monitored throughout the compaction process. Under-compacted regions were identified during this process. Additional remedial passes were applied to improve the level of compaction on the identified under-compacted regions.

The ICA-estimated relative densities were validated by comparing them with the relative density of cores extracted from selected locations on the compacted asphalt layer. The coefficient of determination (R^2) was found to vary between 0.85 and 0.98. The correlation between the ICA-estimated density and density of the cores was studied by combining the data points (55 data points) from the two asphalt projects. The R^2 value was found as 0.93, as shown in Figure 10.2.

In a manner similar to subgrade compaction projects, the ICA can be helpful in identifying and remediating any under-compacted regions in asphalt layers as well. In both projects involving asphalt layer compaction (I-35 and Acme Road projects), it was shown that the average density of the asphalt layer can be improved. The level of compaction in the entire project stretch became uniform when the ICA compaction procedure was followed.
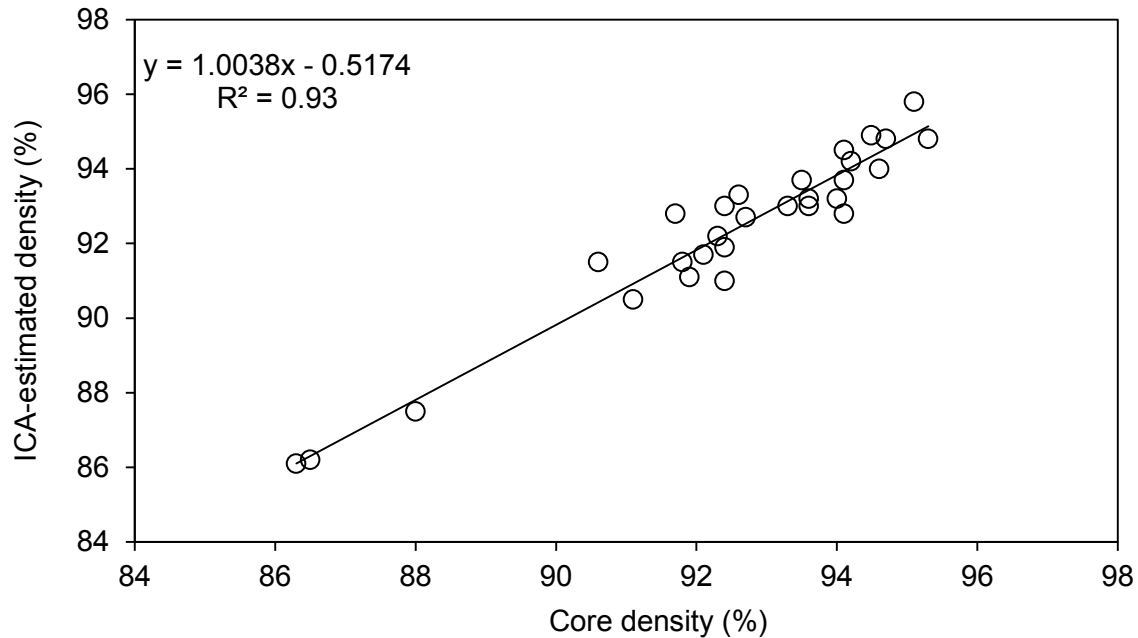
Figure 10.2. Correlation between core density and ICA-estimated density for the two asphalt layer projects (55 data points).

10.2. RECOMMENDATIONS

The case studies carried out in the current project demonstrated procedures for obtaining the level of compaction of stabilized subgrades and asphalt layers with the help of the ICA. It was shown that the ICA can estimate the subgrade modulus and asphalt layer density with a reasonable accuracy in real-time. Such estimates can provide guidance to the roller operator and aid in the improvement of the overall quality of compaction of both stabilized subgrades and asphalt layers. However, successful implementations of the ICA require a special provision or a specification, and shall be considered in the bidding process of the construction work. Since the Intelligent Compaction was not mandatory in the four projects considered in the current study, the research team encountered different problems during the demonstration of the ICA. Some of the problems encountered during the study are:

1) Difficulty in coordinating field test schedules with construction schedules as IC is not a requirement in the project specifications;

2) Selection of number and test locations is constrained by project schedules and weather conditions;

3) Availability of construction sites that meet project requirements such as layer thickness and length of the pavement for demonstration is an ongoing challenge;

4) Verification of the impact of IC-based construction on the performance of pavements is hard to ascertain unless the entire pavement is constructed using IC techniques and evaluated periodically;

6) Contractors and pavement professionals are still unclear on the functionality and benefits of IC techniques. Lack of information about specifications and incentives for implementation of IC is also a limiting factor in the early adoption of the technology.

Based on the experience gained from the current study, the following recommendations are made for studying the performance of ICA in greater detail and to further the early acceptance of Intelligent Compaction methods:

7) The necessary specification or a special provision shall be developed for Intelligent Compaction of both the stabilized subgrades and asphalt layers;

8) Intelligent Compaction shall be considered as a requirement in the bidding of the work;

9) Workshops and training programs shall be conducted for providing necessary training to the construction crews;

10) ICA technology shall be demonstrated on more construction sites varying with soil type, additive type and asphalt layer property to study the influence of these parameters on the ICA-estimated compaction quality parameters (ICA modulus of subgrade, density of subgrade, density of asphalt layer, dynamic modulus of asphalt layer);

11) Research studies shall be carried out to study the long-term benefits of the Intelligent Compaction;

12) The closed-loop control of vibratory compactors during Intelligent Compaction of subgrade and asphalt layers shall be considered in future projects.

REFERENCES

1. AASHTO T-166 (2010). "Standard Method of Test for Bulk Specific Gravity of Compacted Hot Mix Asphalt (HMA) Using Saturated Surface-Dry Specimens," AASHTO Standards, Washington, DC.

2. AASHTO T 307 (1999). "Standard Method of Test for Determining the Resilient Modulus of Soils and Aggregate Materials," AASHTO Standards, Washington, DC.

3. ARA (2004). "Guide for Mechanistic-Empirical Design of New and Rehabilitated Pavement Structures." NCHRP Project 1-37A. Transportation Research Board of the National Academies, Washington, DC.

4. ASTM D698-07e1 (2007). "Standard Test Methods for Laboratory Compaction Characteristics of Soil Using Standard Effort (12 400 ft-lbf/ft^3 (600 kN-m/m^3))," ASTM International, West Conshohocken, PA.

5. Barman, M., Nazari, M., Imran, S.A., Commuri, S., Zaman, M., Beany, F and Singh, D. V. (2014). "Application of Intelligent Compaction Technique in Real-Time Evaluation of Compaction Level During Construction of Subgrade," CD Rom, the 93rd Annual Meeting of the Transportation Research Board, Washington DC.

6. Briaud , J. L., Seo, J. (2003). "Intelligent Compaction: Overview and Research Needs," Texas A&M University. College Station, TX.

7. Camargo, F., B. Larsen, B. Chadbourn, R. Roberson, and J. Siekmeier (2006). "Intelligent Compaction: A Minnesota Case History," Proceedings of the 54th Annual University of Minnesota Geotechnical Conference, Continuing Education and Conference Center, St. Paul Campus, University of Minnesota, Eds. J.F. Labuz, G.S. Wachman & C.-S. Kao, pp. 109-128.

8. Chang, G., Q. Xu, J. Rutledge, R. Horan, L. Michael, D. White, and P. Vennapusa (2011). "Accelerated Implementation of Intelligent Compaction Technology for Embankment Subgrade Soils, Aggregate Base, and Asphalt Pavement Materials," Publication FHWA-IF-12-002. Federal Highway Administration, Washington, DC.

9. Commuri, S (2010). "Intelligent Asphalt Compaction Analyzer: Final Report for Assistant Agreement DTFH61-08-G-0002," Federal Highway Administration, Highways for LIFE Technology Partnerships Program, Washington DC.

10. Commuri, S., and Zaman, M. (2010). "Method and apparatus for predicting the density of asphalt," USPTO, 7,669,458.

11. Commuri, S. (2012). "Method and apparatus for compaction of roadway materials," USPTO, Patent 8,190,338 B2.

12. Commuri, S., and Zaman, M. (2008). "A Novel Neural Network-Based Asphalt Compaction Analyzer," International Journal of Pavement Engineering, vol. 9, No.3, pp. 177-188.

13. Commuri, S., and Zaman, M. (2009). "Calibration Procedures for the Intelligent Asphalt Compaction Analyzer," ASTM Journal of Testing and Evaluation, vol. 37, No. 5, pp. 454-462.

14. Commuri, S., Mai, A. T., and Zaman, M. (2011). "Neural Network-based Intelligent Compaction Analyzer for Estimating Compaction Quality of Hot Asphalt Mixes," ASCE Journal of Construction Engineering and Management, vol. 137, issue 9, pp 633-715.

15. FHWA (2009). "Accelerated Implementation of Intelligent Compaction Technologies for Embankment Subgrade Soils, Aggregate Bases, and Asphalt Materials," US FHWA Research Project DTFH61-07-C-R0032.

16. Jaselskis, J.E., Han, H., Tan, L., and Grigas, J. (1998). "Roller mountable asphalt pavement quality indicator," 1998 Transportation Conference Proceedings, pp. 192- 194.

17. Lambe, T.W., and Whitman, R.V., (1969). "Soil Mechanics," John Wiley and Sons, New York.

18. Maupin, G. W. (2007). "Preliminary field investigation of intelligent compaction of hot-mix asphalt," Final Rep. No. VTRC-08-R7, Virginia Transportation Research Council, Virginia DOT, Charlottesville, VA.

19. Minchin, R.E. (1999). "An asphalt compaction quality control model using vibration signature analysis," Ph. D Thesis, The Pennsylvania State University.

20. Mooney, M. A. and Rinehart, R. V. (2007). "Field Monitoring of Roller Vibration during Compaction of Subgrade Soil," Journal of Geotechnical and Geoenvironmental Engineering, 133(3), 257-265.

21. Mooney, M. A., Rinehart, R.V., Facas, N.W., Musimbi, O.M., White, D.J., and Vennapusa, P.K. (2011). "*Intelligent Soil Compaction System,*" Final report, NCHRP 21-09.

22. Peterson, P.L. (2005). "Continuous Compaction Control MnRoad Demonstration," Minnesota Department of Transportation, MN/RC – 2005-07.

23. Petersen, D., Siekmeier, J., Nelson, C., Peterson, R. (2006). "Intelligent soil compaction -technology, results and a roadmap toward widespread use," Transportation Research

Record No. 1975, Journal of the Transportation Research Board, National Academy Press, pp. 81-88.

24. Petry, T. M. and Little, D. N. (2002). "Review of Stabilization of Clays and Expansive Soils in Pavements and Lightly Loaded Structures – History, Practice, and Future," Journal of Materials in Civil Engineering, 14(6), pp. 447-460.

25. Proctor, R. R. (1933). "The design and construction of roller earth dams," Engineering News Record III, pp. 286-189.

26. Sandstrom, A. (1998). "Control of a compacting machine with a measurement of the characteristics of the ground material," USPTO # 5,727,900.

27. Siekmeier, J. A., Young, D. and Beberg, D. (2000). "Comparison of the Dynamic Cone Penetrometer with other Tests During Subgrade and Granular Base Characterization in Minneosta," Nondestructive Testing of Pavement and Backcalculation of Moduli, ASTM STP 1375, 3, West Conshohocken, PA.

28. Singh, D., Beainy, F.N., Mai, A.T., Commuri, S., and Zaman, M. (2011). "In-situ Assessment of Stiffness During the Construction of HMA Pavements," International Journal of Pavement Research Technology, Vol. 4, No. 3, pp. 131-139.

29. Swanson, D.C., Thomas, H.R., and Olaufa, A.A. (2000). "Compacted Material Density Measurement and Compaction Tracking System," USPTO # 6,122,601.

30. Thurner, H. F., (1978). "Method and a device for ascertaining the degree of compaction of a bed of material with a vibratory compacting device," USPTO 4,103,554.

31. White, D. (2006). "Field evaluation of compaction monitoring technology," Tech Transfer Summary, Iowa Highway Research Board, Iowa DOT Transportation, Ames, IA.

32. White, D. J. , Jaselskis, E. J., Schaefer, V. R., Cackler, E. T., Drew, I., and Li, L. (2004). "Field Evaluation of Compaction Monitoring Technology: Phase I," submitted to Iowa Department of Transportation, Iowa DOT Project TR-495.

33. Zambrano, C., Drnevich, V., Bourdeau, P. (2006). "Advanced Compaction Quality Control," Indiana DOT Final Report FHWA/IN/JTRP - 2006/10, Purdue University.

APPENDIX

INTELLIGENT ASPHALT COMPACTION ANALYZER[†]

User Manual

Version 2.0

University of Oklahoma
School of Electrical and Computer Engineering
Devon Engineering Hall, Room 432
110 W. Boyd St., Norman, OK 73019

Tel. 1 - 405 - 325 - 4302
Fax. 1 - 405 - 325 – 7066

http://hotnsour.ou.edu/commuri/Intelligent_Compaction.html

Email: scommuri@ou.edu

[†] *US Patent #**7,669,458***
Issued on March 02, 2010

The information disclosed in this document is protected under the United States Patent and Copyright Laws. Any duplication or publication of the material without express written permission from the University of Oklahoma or its authorized representatives is prohibited.

For further information, please contact:

The Office of Technology Development
University of Oklahoma
One Partners Place
David L. Boren Blvd., Norman, OK 73019
Tel. 1-405-325-4800

INTELLIGENT ASPHALT COMPACTION ANALYZER

User Manual

Version 2.0

1.0   Introduction

The Intelligent Asphalt Compaction Analyzer (IACA) is a roller-mounted device that can measure the density of an asphalt pavement during its construction. The IACA measures the vibrations of the drum of the vibratory compactor during the compaction process and estimates the density of the asphalt mat continuously, in real-time during the pavement's construction.

Quality control techniques currently used in the field involve the measurement of density at several locations on the completed pavement or the extraction of roadway cores. These methods are usually time consuming and do not reveal the overall quality of the construction. Furthermore, any compaction issues that are identified cannot be easily remedied after the asphalt mat has cooled down. The ability of the IACA to measure the level of compaction of the asphalt pavement during its construction will enable the roller operator to identify and remedy under-compaction of the pavement while avoiding over-compaction.

Key features of the IACA are:

- Neural network based intelligent analyzer that can estimate the density over the entire pavement.
- Display of mat density, surface temperature, roller position, speed and heading in real-time.
- Density is also displayed as a 'strip chart' to help identify the uniformity of compaction on a given stretch of the pavement.
- The displayed information is updated twice every second with a spatial resolution of better than 0.3 meters (1 foot).
- Intuitive, easy to use, calibration procedures that allow for accurate estimation of density of both full-depth, as well as overlaid asphalt pavements.
- Can be used to estimate the density of thick lifts (base and intermediate lifts), as well as thin lifts of asphalt pavement (surface course).
- Built-in utilities can be used to validate the density at a given location on the pavement against Nuclear Density Gauge (NDG) readings or density measured from a roadway core.
- As-built maps to plot the overall compaction for the entire roadway construction.
- Pass-by-pass density to detect under compaction and prevent over compaction of the pavement.

Table of Contents

Table of Contents

2.0   Installation Procedure

The Intelligent Asphalt Compaction Analyzer (IACA) consists of a rugged Tablet PC, GPS receiver, uniaxial accelerometer, and an infrared temperature sensor. The IACA should be mounted on a Volvo DD138HF or similar roller prior to its calibration and use. The installation procedure is described in this section.

2.1 Components

Check and verify the following components prior to installing the IACA on a Volvo DD138HF roller.

1) Rugged Tablet PC (Figure 1).
2) Trimble Pathfinder ProXT GPS receiver (Figure 2).
3) Raytek CI noncontact infrared pyrometer (Figure 3).
4) Summit Instruments 13200C 10g accelerometer (Figure 4).
5) Tablet PC mounting platform (Figure 5).
6) Mounting bracket (Figure 6).
7) Swivel arm (Figure 7).
8) Mounting Hardware (8 – 5/8 x 6 inch bolts, 8 – 5/8 inch nuts, 16 – 5/8 inch washers, 16 – 5/8 inch lock washers. Tie wraps).

**Figure 1. T8700 Rugged Tablet PC with integrated numeric keypad
(shown on mounting platform)**

Figure 2. Trimble Pathfinder ProXT GPS receiver

Figure 3. Raytek CI noncontact infrared temperature sensor

Figure 4. Summit Instruments 10g uniaxial accelerometer
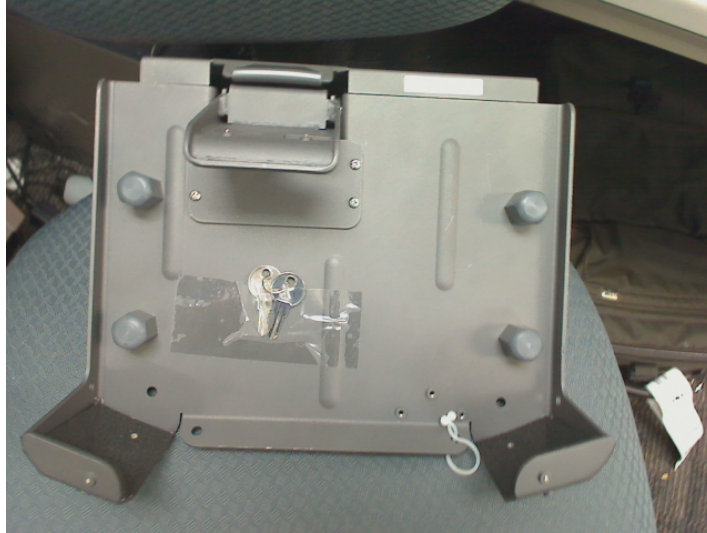
Figure 5. Tablet PC mounting platform with spring loaded latch

**Figure 6. Bracket used to attach the Tablet PC platform
to the rail on the roller**

**Figure 7. Swivel arm used to attach the Tablet PC platform
to the mounting bracket**

2.2 Installation

Figure 8. Mounting location labels on a Volvo DD118HF roller.

1 Find the best location on the drum to mount/glue the accelerometer. The closer to the drum the better and it should always be before the drum rubber mount to make sure the measured vibration is for the drum and not the roller body frame. Once the location is defined, clean it and use superglue to mount the accelerometer.

2 Mount the temperature sensor on its bracket and then glue it on a safe location on the frame pointing down towards the road surface.

3 Mount the GPS receiver on top of the roller. The GPS receiver has foam padding and a magnet that is good enough to stay in place without the need for glue or tape. Turn GPS receiver on. Write down the horizontal distance between the GPS and the accelerometer (offset distance) for later use during the post processing.

4

1. Mount the mounting bracket (Figure 6) to a convenient location on the rail. It is a good practice to use foam padding to absorb vibration. Mount the bracket by running the bar between the semicircular rods and tightening the bolts so that the bracket will not slide when the roller vibrates. Make sure the knob is facing inside the cab.
2. Attach the swivel arm (Figure 7) to the knob on the mounting bracket (Figure 6) and to the knob on the mounting platform (Figure 5) by inserting

the knobs into each side of the swivel arm and adjusting the tightening screw. Make sure the mounting platform is situated so that the ribbon cable is on top.

3. Insert the tablet PC in to the mounting platform. Do this by pulling the top bracket back and fitting the tablet PC in the space provided, and then bend the top bracket back down ensuring the tablet PC remains in place. Connect the power cord from the mounting bracket to the associated plug on the bottom of the tablet PC.

4. Connect the ribbon cable to the data acquisition on the tablet. There are three cables coming out of the back of the cradle labeled C1, C2 and C3. Connect the cable attached to the accelerometer to C1, the temperature sensor cable to C2. If needed, use straight serial cables to reach sensors.

5

1. Connect the power cable to C3 and to a 12V battery if available. Otherwise open the roller engine hood and connect to its battery. Use care when tapping to the roller's battery to avoid electric shocks and make sure polarities are correct.

2. Turn the tablet PC on by depressing the gray button on the top left hand side of the face of the tablet PC. Once this is on, connect the GPS null-modem cable to its associated port on the bottom of the tablet PC. **Wait until the tablet PC is ON before connecting the GPS using the null-modem serial cable.**

2.3   IACA Initialization

Boot up the Tablet PC by depressing the power button. After the Tablet PC has been powered up and the Windows XP operating system has been booted up, the IACA will be started automatically. The user interface to the application is shown in Figure 9 with different features being outlined.
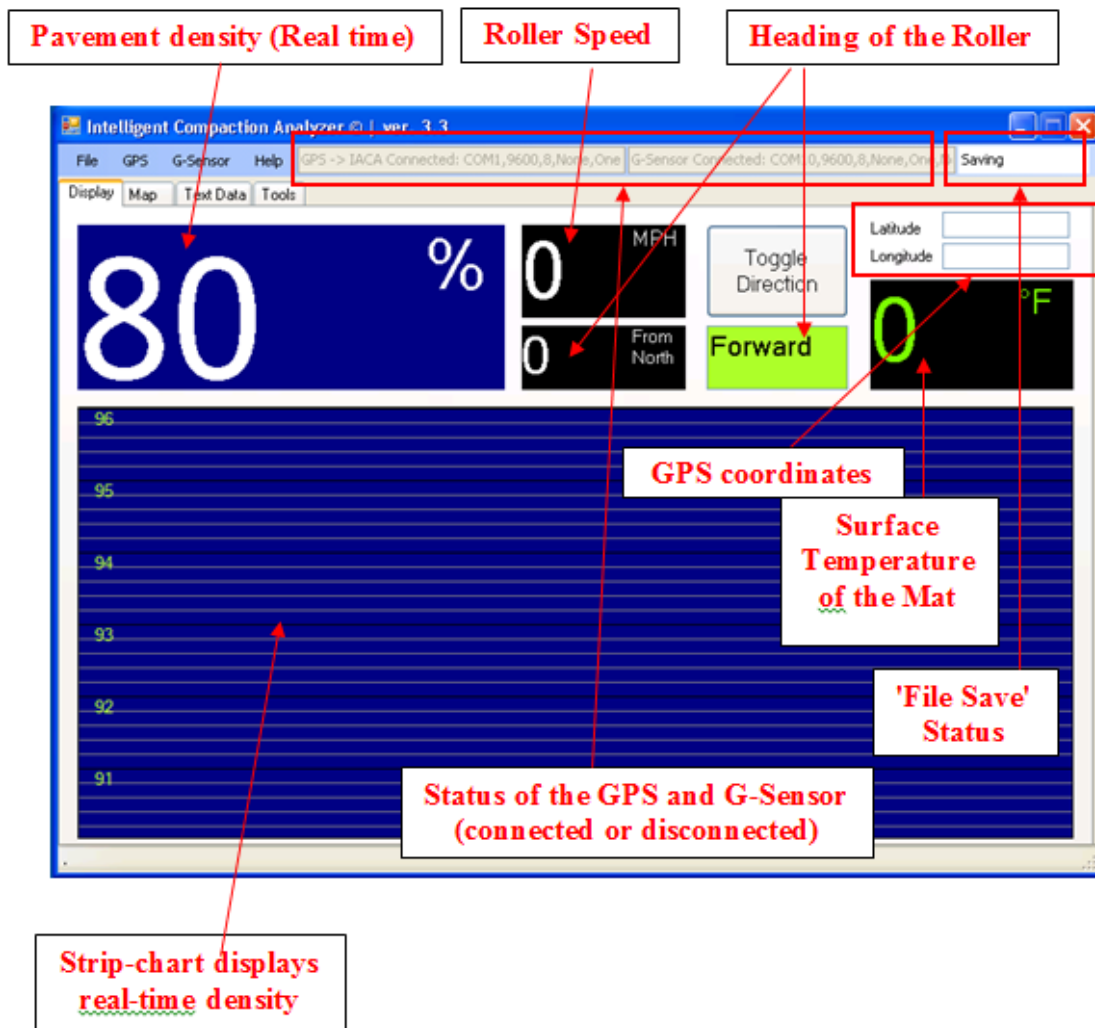
Figure 9. IACA user interface

3.0 Calibration of the IACA

The IACA is based on the hypothesis that the hot mix asphalt layer being compacted and the vibratory compactor form a coupled system whose vibrations are affected by the stiffness of the asphalt mat. As the compaction process unfolds, the stiffness of the asphalt mat increases and as a consequence the response characteristics of the roller are altered. These changes in the response can be used to determine the level of compaction achieved. In order to determine the level of compaction, the IACA should be trained to recognize the response of the roller during the compaction process. The calibration process described below is designed to train the IACA to recognize the vibrations resulting from different levels of compaction and to generate the density information based on the characteristics of the mix.

The calibration of the IACA is a two-step process. In the first step, the vibrations of the roller are captured over successive passes on a calibration stretch. These vibrations are analyzed and features corresponding to different levels of vibrations are extracted. The extracted features correspond to the amplitude of the vibrations at salient frequencies. These features are then used to train the neural network. After the completion of the training process, the neural network can classify vibrations of the roller during compaction as those corresponding to one of the predetermined levels of compaction. For the sake of calibration, the lowest level of vibration is assumed to correspond to the lay down density while the highest level of vibration is typically encountered when the target density is achieved.

In the second step of the calibration procedure, the calibration performed in step one is refined to improve the accuracy of the density measurements. After the calibration stretch is compacted, three cores are extracted from the completed pavement and the estimated densities at these locations are compared to the densities measured from the cores according to the AASHTO T-166 standard. The calibration parameters are then modified to minimize the error between the estimated and measured densities at these locations.

3.1 Selection of a pavement section for calibration of IACA

i)   First a control strip of approximately 100 feet (33 meters) long needs to be selected. Mark off a 30 foot calibration section in the middle of this control strip (Figure 11). The start and end of the calibration section need to be marked by GPS coordinates at the center line of the pavement. The GPS receiver is used to trigger the collection of the vibration data when the roller starts compacting this section of the pavement.

ii)   Mark test locations at the center of the lane at distances of, five feet, fifteen feet and twenty five feet from the beginning of the test section.

iii)   Stop the compaction process when no appreciable increase in the density is seen after the roller pass. After the final pass of the roller, three core locations are marked as shown in Figure 11. The GPS location of the cores is collected in the Tablet PC as explained in the section 4.0. Also, the density at the core and in the immediate vicinity of the core is recorded for each of the three cores using a hand held density gauge.

iv)   The cores marked in the previous step need to be extracted and their density is measured in accordance with the AASHTO T-166 method.

v)   The densities of the extracted cores are used to train and calibrate the IACA as detailed in the following sections of this manual.
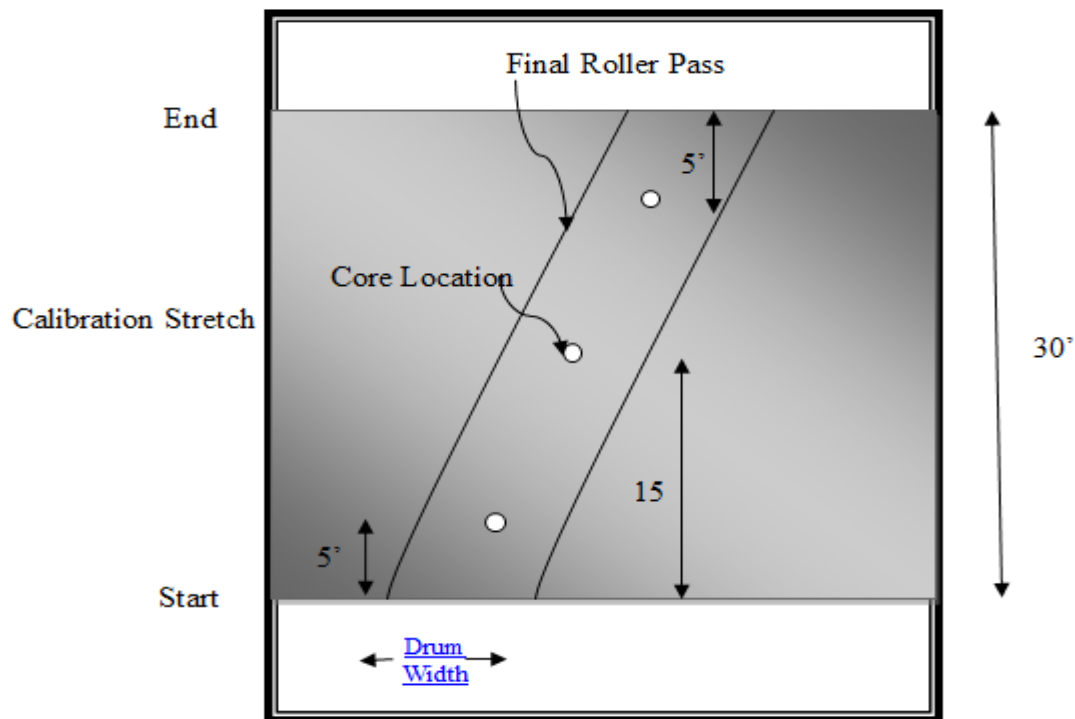
Figure 11. Selection of core locations after the final pass of the roller

3.2 Calibration procedure

1. Make sure that the GPS is updating by looking at the coordinates textbox on the display (see figure below).

2. Let the roller compact a couple of stretches (not passes) and make sure that the data is being saved by looking at the status textbox (see figure above).
3. Mark a calibration region of 30 feet as shown in the figure below:
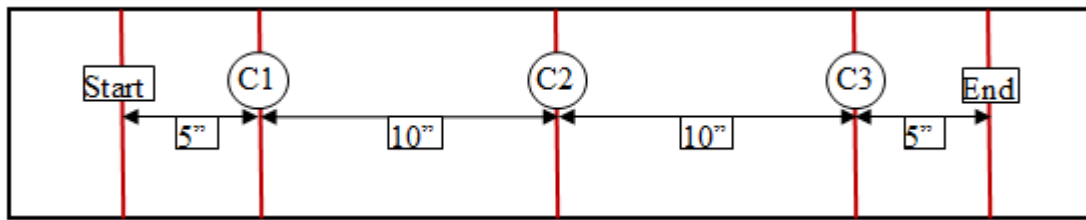
4. Make sure that the roller compacts all the passes without stopping and within 13 minutes. Also make sure that the roller stops for at least 1 minute before and after the calibration stretch for the roller to save data.
5. The last pass of the calibration region should be in the middle of the road.
6. In the tools tab of IACA, push "Start Point" button while the roller is aligned with the start line and the "End Point" button at the end of the calibration stretch.
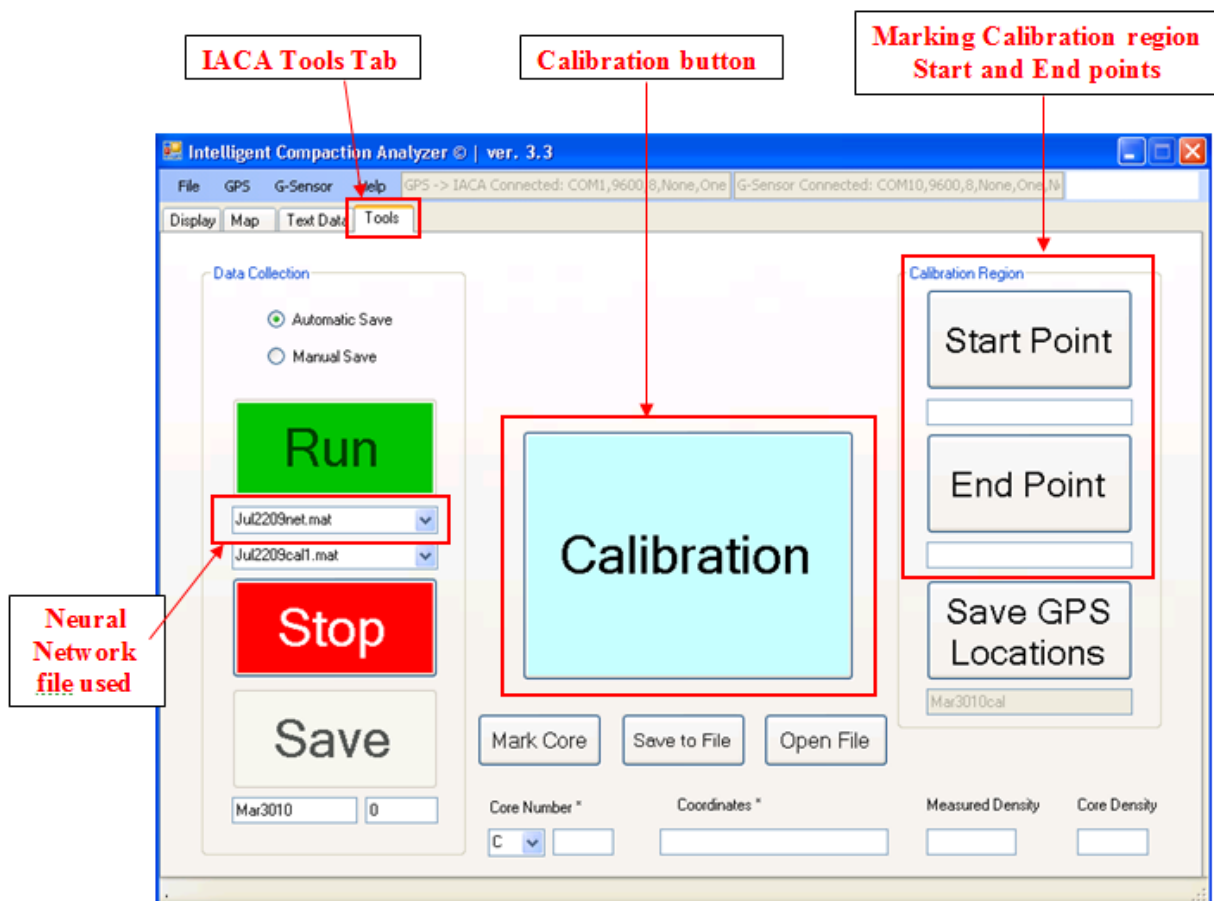
Figure 12. IACA Tools window

7. After the calibration region is compacted and the roller is stopped for the data to be saved (remember the file number), go to the tools tab and push the "Calibration" button (Figure 12). The following three windows appear on the screen.
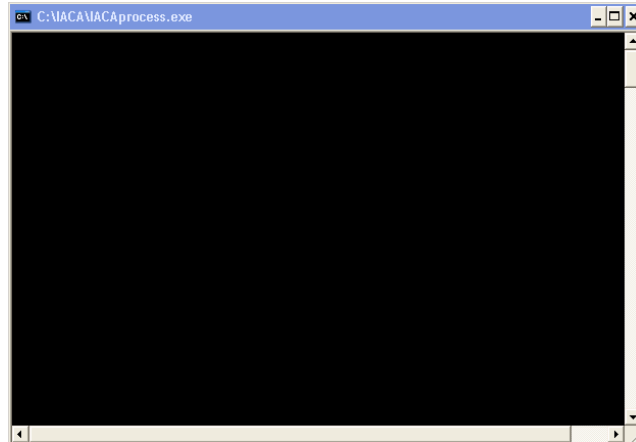
Figure 13. IACA command editor window
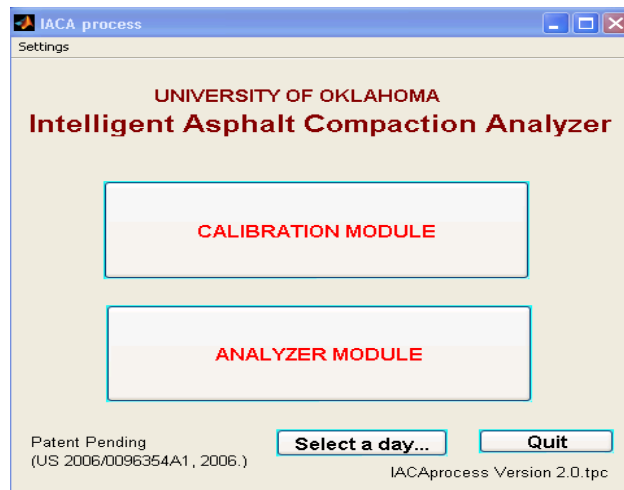
Figure 14. IACA process window
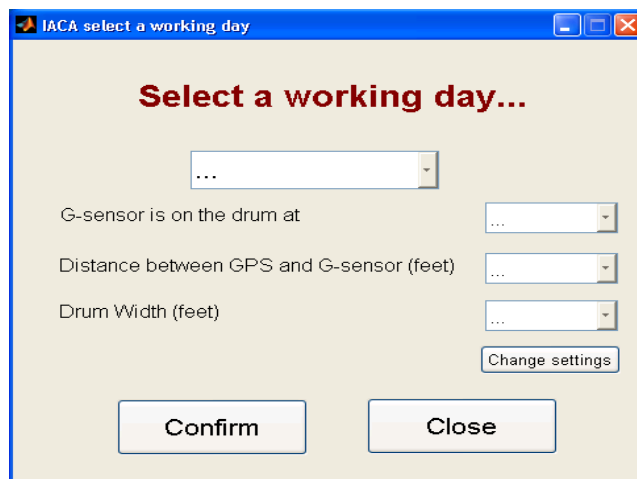
Figure 15. IACA Select a working day window

8. Select a working day as shown in the figure below.

After selecting the working day, enter the following parameters: G-sensor position on the drum (front or rear), distance between GPS and G-sensor (offset distance) in feet and drum width in feet (as shown in the figure below) and push "Confirm" button.

9. Push on the "CALIBRATION MODULE" button in the IACA process window of figure 14.

The following window appears after the successful initaialization of the calibration module. Click "OK".
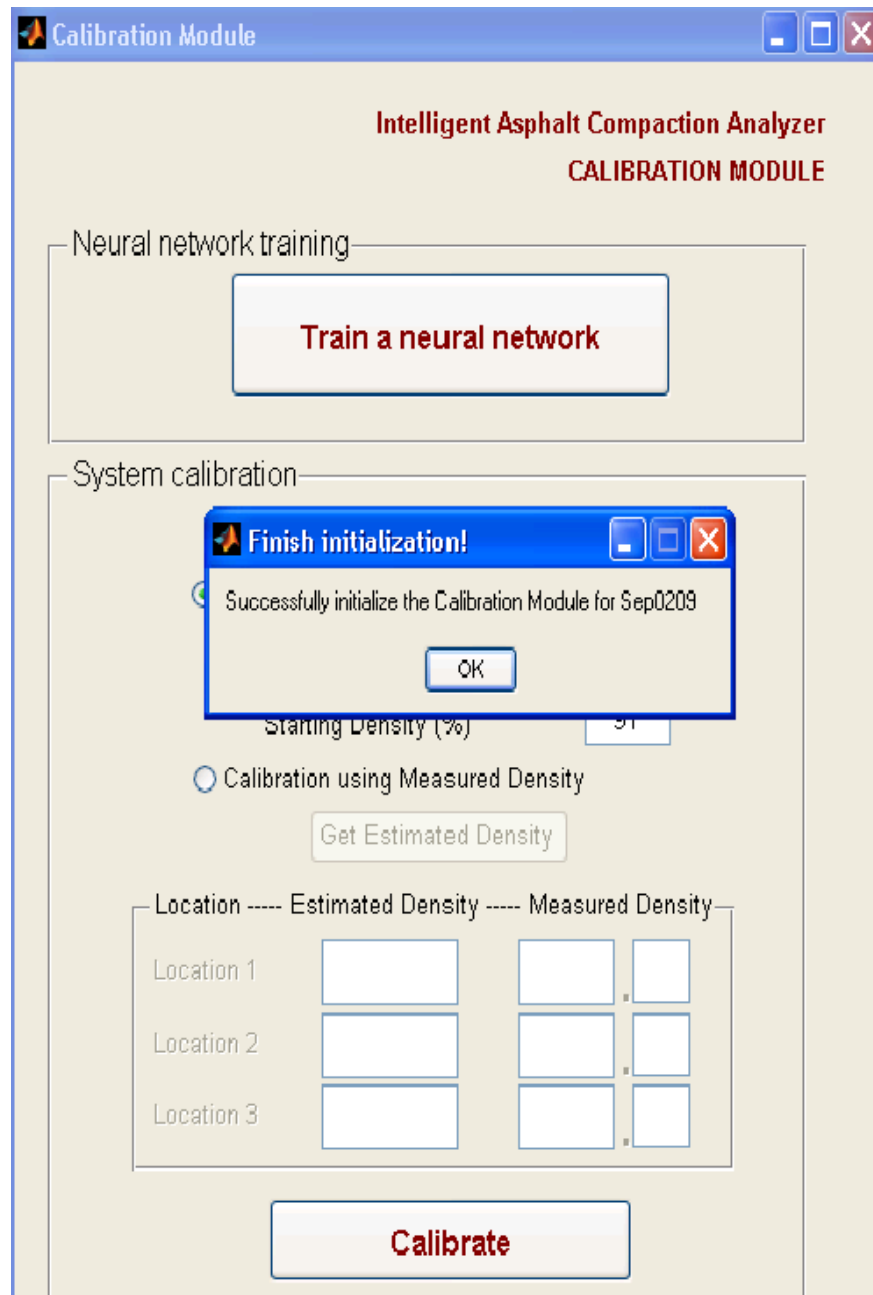
Figure 16. IACA Calibration Module window

10. Push "Train a neural network" button in the figure above.

11. After training is finished, select the theoretical maximum density as 96% and minimum density as 91% then push the "Calibrate" button. A new file named datecalRaw.mat is created and the new Calibration parameters are saved to it.
12. Close everything including the IACA application then open it again and make sure the right Neural Network is selected in the IACA Tools tab (see figure 12).
13. After you get the core densities of the calibration region from the lab, go back to the Calibration Module (figure 16) and change the selection from "Raw Calibration using Maximum Density" to "Calibration using Measured Density".
14. Push the "Get Estimated Density" button to get the estimated densities at the three core locations. Enter the corresponding Lab densities on the right side and push the "Calibrate" button (see figure below).


15. Close everything and then reopen IACA.

This completes the calibration procedure.

3.3 Validation of IACA Measurements

At the end of each day or whenever needed, GPS location of the cores should be collected to be able to correlate estimated density with the measured ones. The following steps describe core marking operation:

1. Remove the GPS receiver from the roller and reconnect it to the tablet PC if the cable was disconnected during the operation.
2. Disconnect the ribbon cable coming from the cradle to the data acquisition on the tablet PC.
3. Remove the tablet from the cradle and put the GPS receiver on top of the core to be marked.
4. On the Tools tab of the IACA GUI (figure 12), select a letter from the drop down menu as a core name for the day and type in the core number in the box next to it (see figure below).
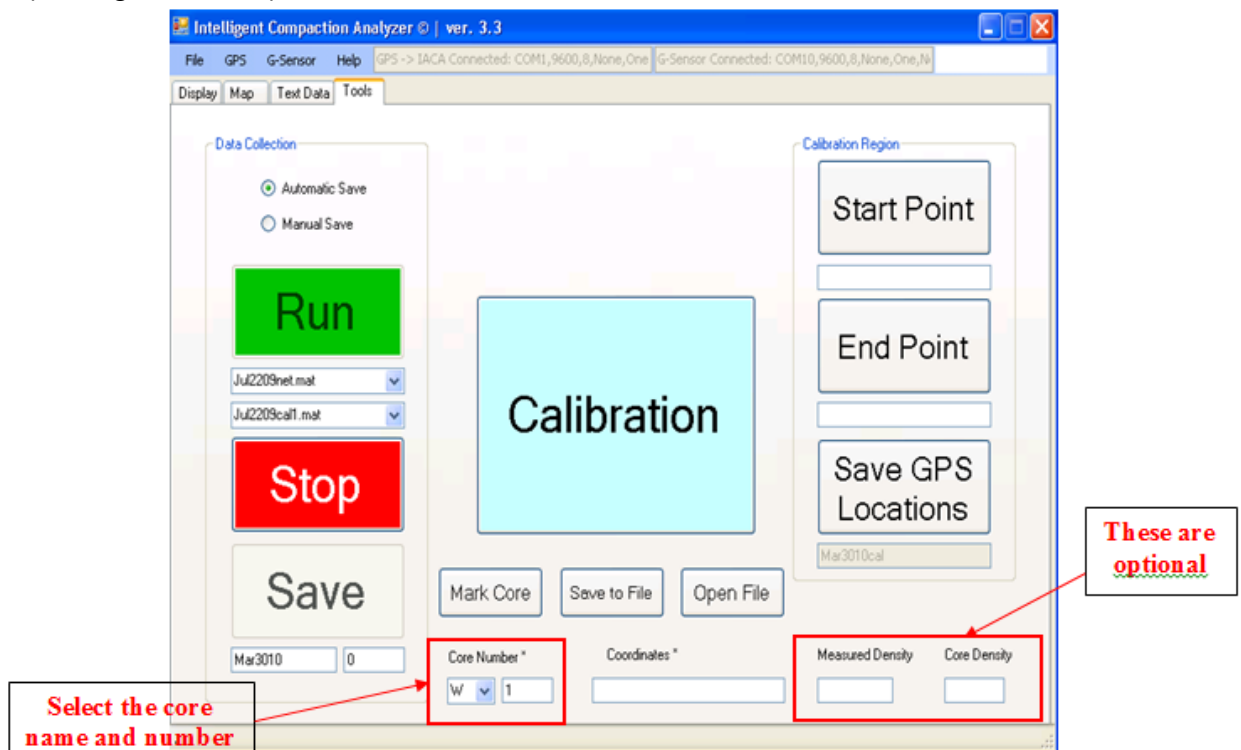
5. Push the "Mark Core" button to register the GPS coordinates in the box. The "Mark Core" button can be pushed as many times as the operator wants, without the data (GPS coordinates) being saved. Once the GPS coordinates are ready to be saved, the "Save to File" button should be pressed to automatically save or append the information to a text file named datecore.txt .
6. The "Measured Density" and "Core Density" boxes are optional information that can be filled in case the density measurement is available.
7. Repeat steps 4 to 7 for each core location.

4.0 Run Time Monitoring of Compaction

The calibrated IACA can be used to monitor the progress of compaction as well as to evaluate the quality of the construction. The capability of the IACA to influence the quality of compaction of asphalt pavements during their construction is described in this section.

4.1 Monitoring of the compaction process

To monitor the progress during compaction, select the 'Display' option in the IACA user interface (Figure 17). The interface shown in Figure 17, displays the roller position (latitude and longitude), the roller speed and heading, the surface temperature of the asphalt mat and the density of the pavement at the current location. The display is updated two times every second.
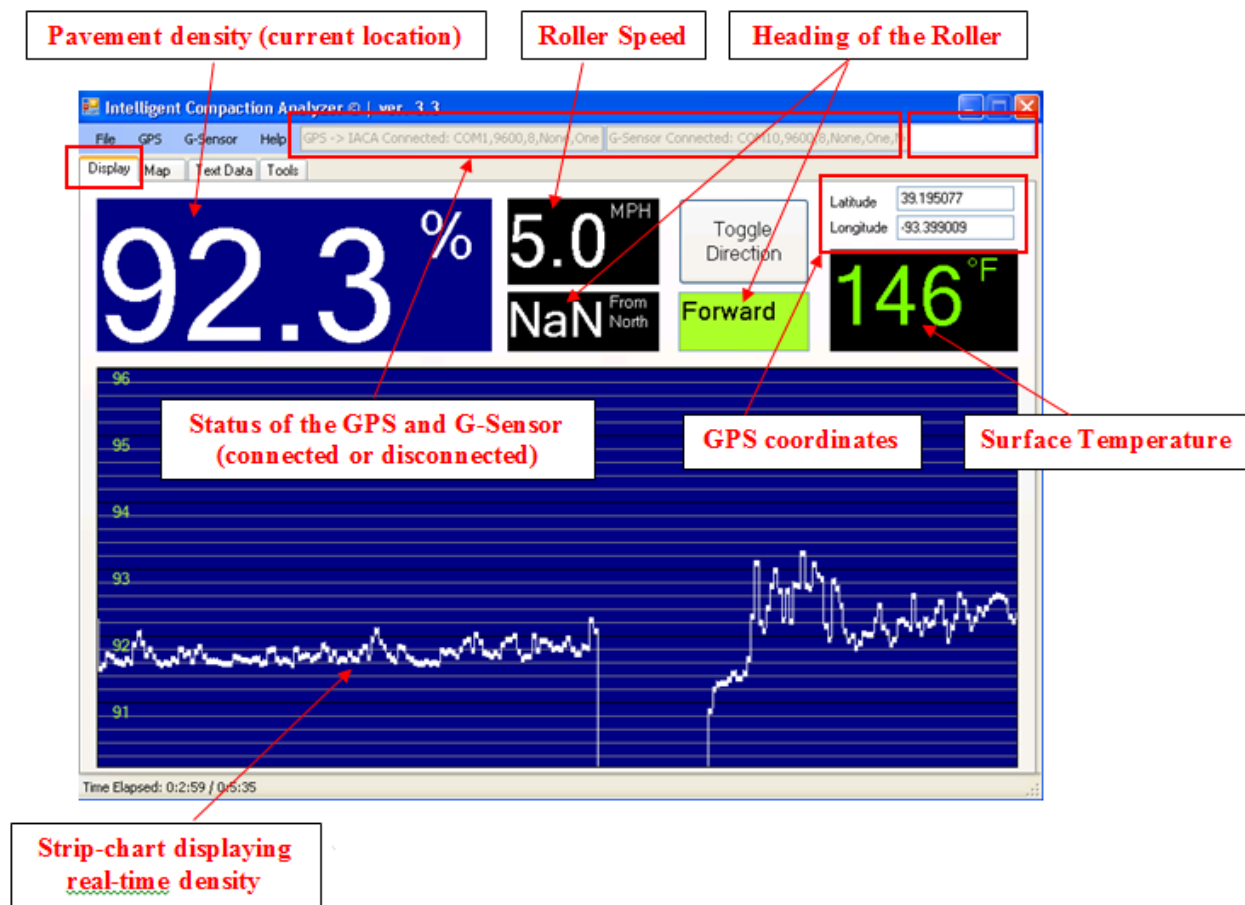

Figure 17. Real-time display of compaction density

The above figure also displays the density of the asphalt mat during the compaction as a 'strip chart.' This chart provides visual feedback on the uniformity of compaction to the roller operator.
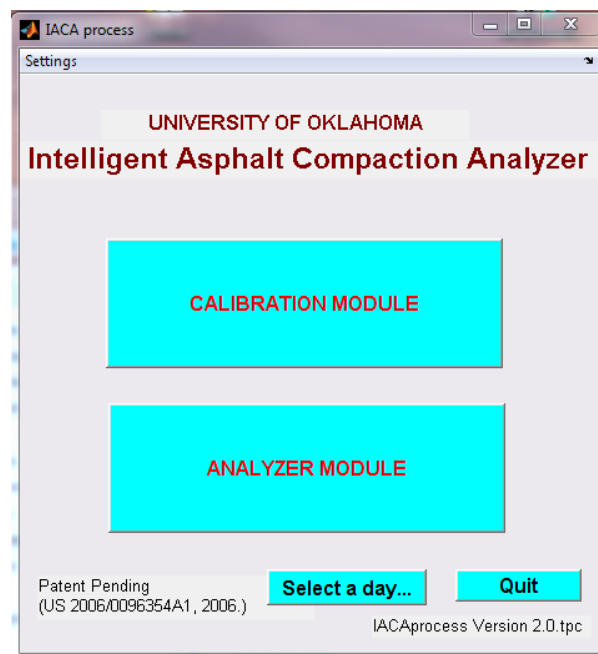
4.2 Compaction maps and tools for analysis

In addition to providing real-time information on the density achieved during compaction, the IACA can also be used to evaluate the overall quality of compaction over the entire project.

1. On the tools tab of the IACA GUI push the "Calibration" button and select a working day.
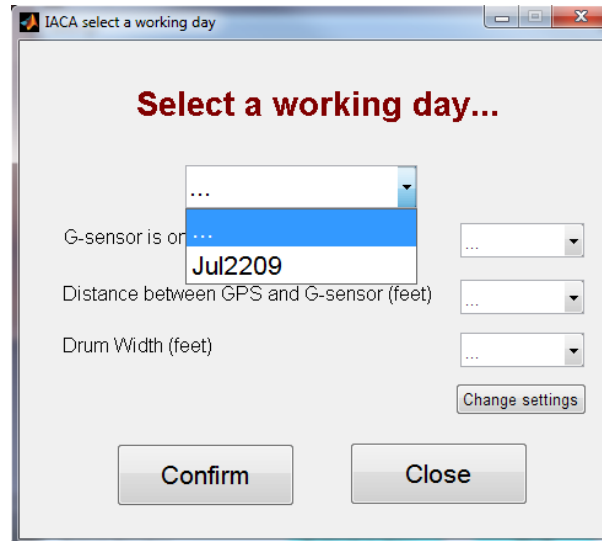
2. On the main window push "ANALYZER MODULE".

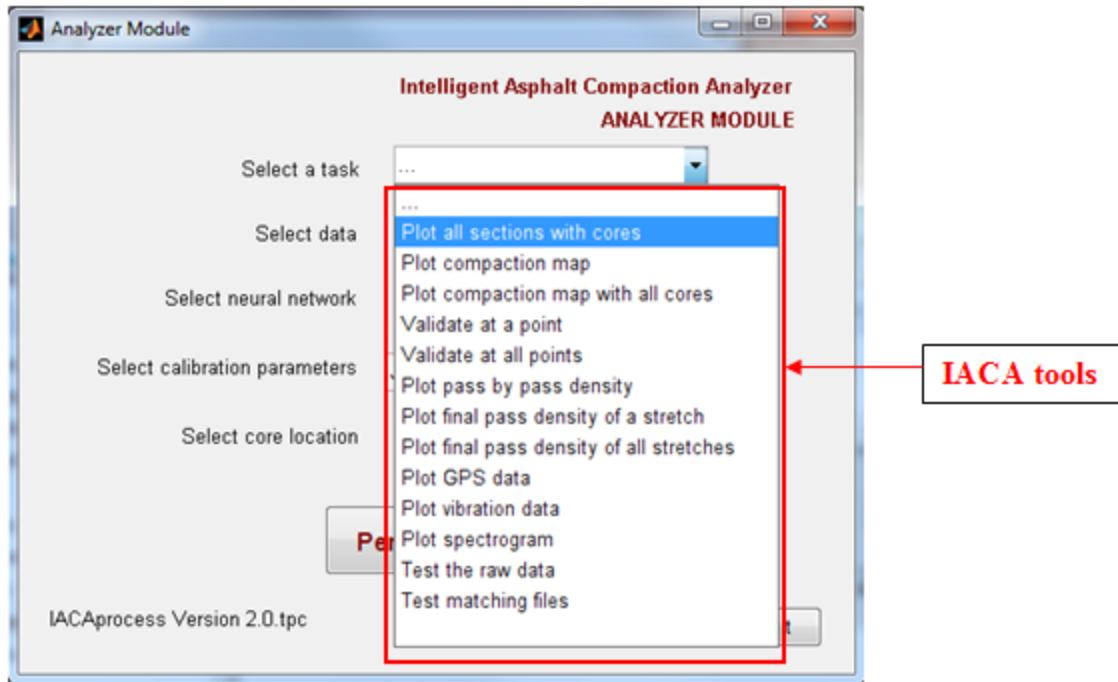3. On the Analyzer Module window select a task to be performed.

Figure 18. IACA Analyzer Module

There are a number of useful tools in IACA (as depicted in the figure above) which are helpful to understand the compaction process as well as to estimate the overall quality of the construction. A few of these tools are described below.

4.2.1 Generation of as-built maps

We can generate compaction map of a particular stretch using "Plot compaction map" tool in the IACA Analyzer module of figure 18. Once the tool is selected, we need to choose the stretch for which the map is required, neural network, calibration parameters and then push "Perform the selected task" button (see figure 19 below).
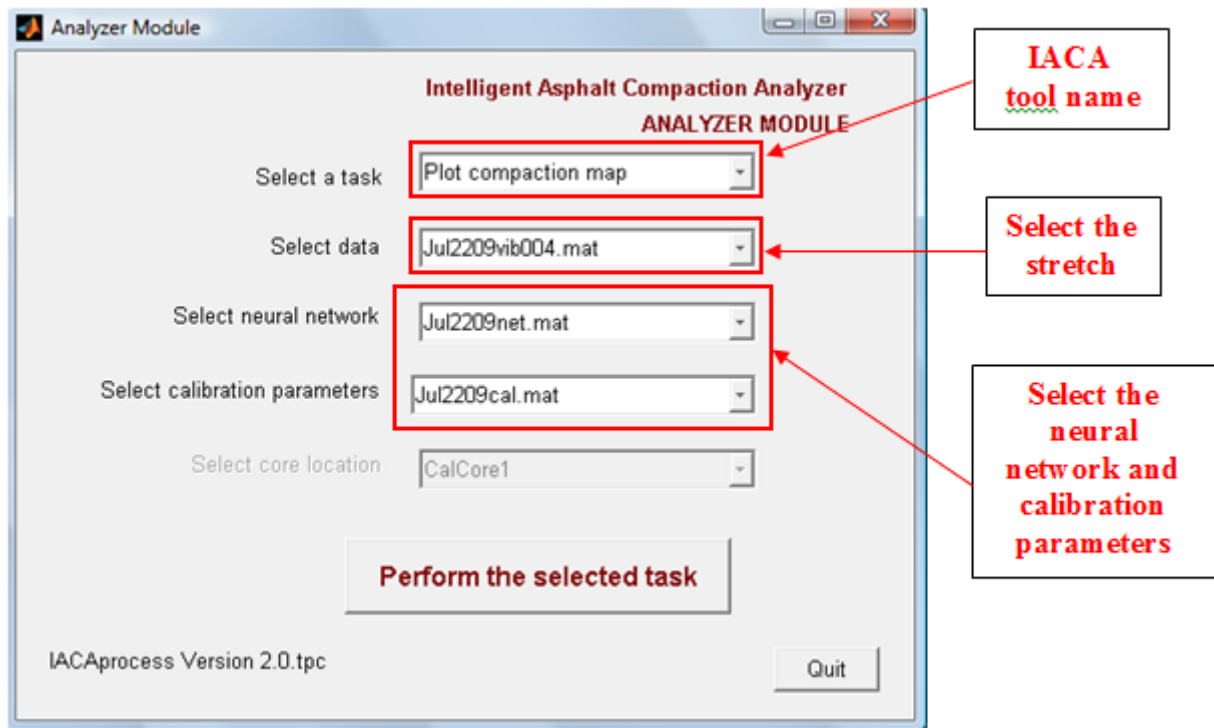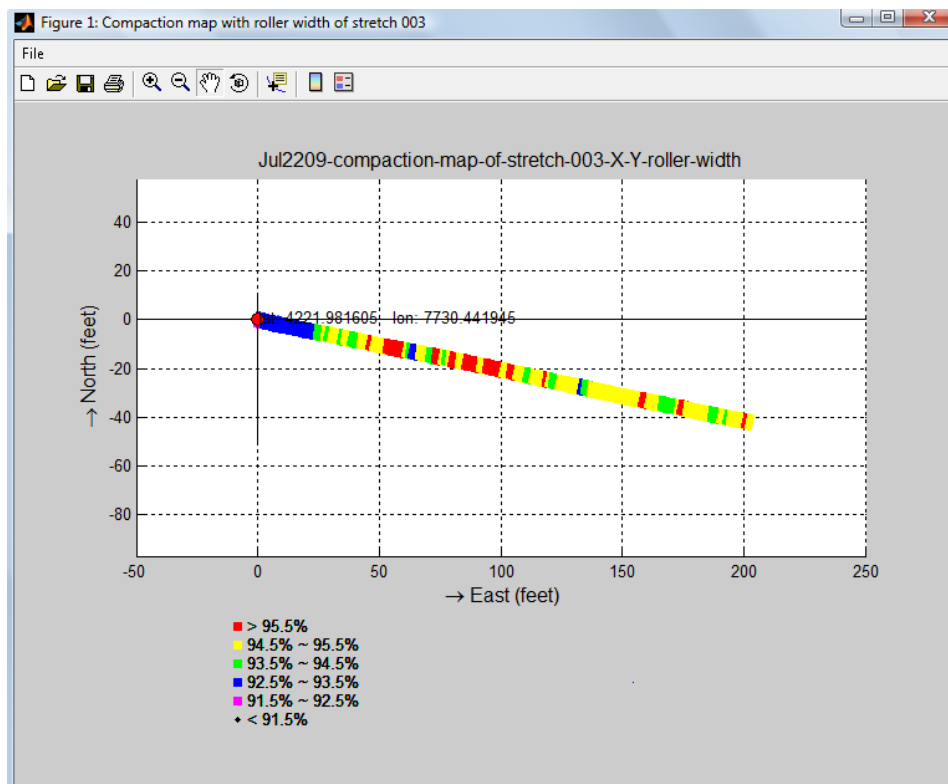
Figure 19. IACA "Plot Compaction tool"

An example plot is shown below.

In the above plot, each color corresponds to a different density level. So this map basically shows an outline of the approximate density achieved during the compaction of the stretch.

4.2.2 Plotting of GPS data

We can obtain a plot showing the compactor rolling pattern of a particular stretch by using the tool "Plot GPS data" in the IACA Analyzer module (figure 18). Once the tool is selected from the scroll down list, we need to choose the stretch for which the data is to be plotted and then push "Perform the Selected task" button (see figure 20 below).
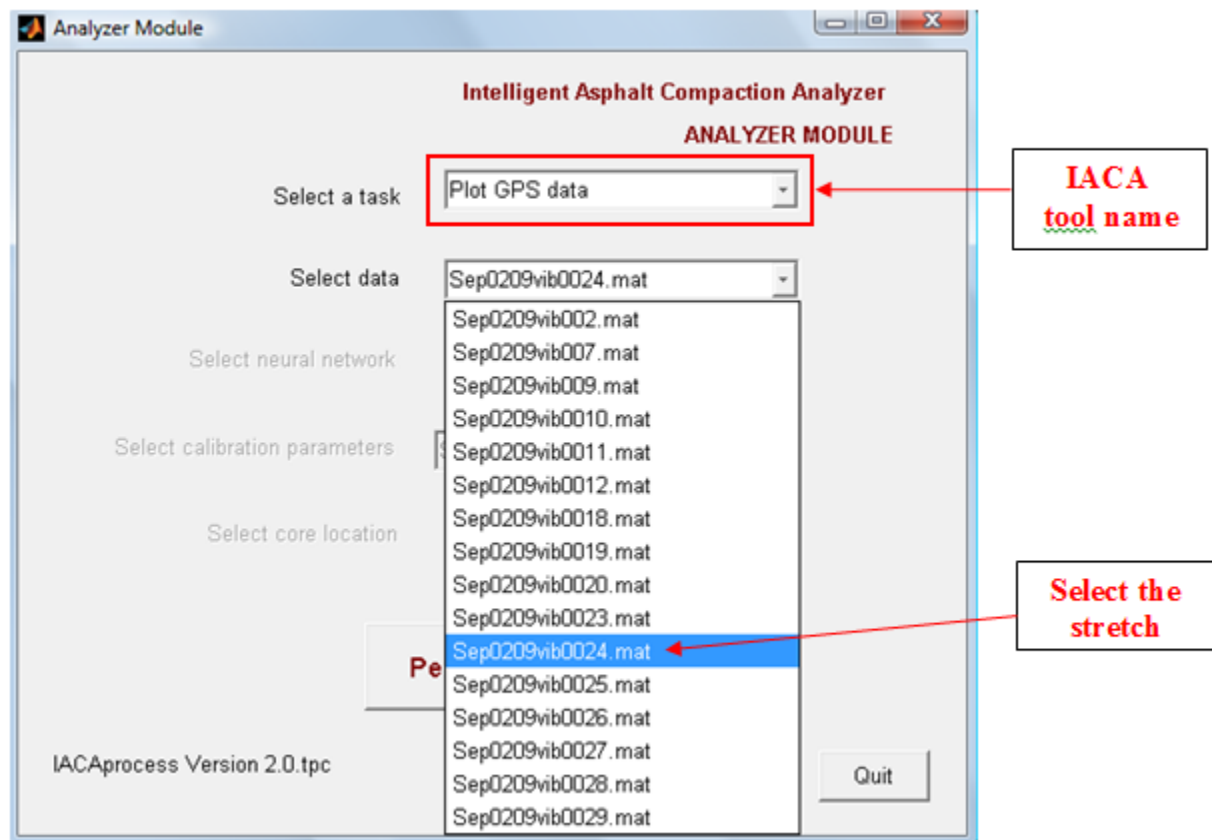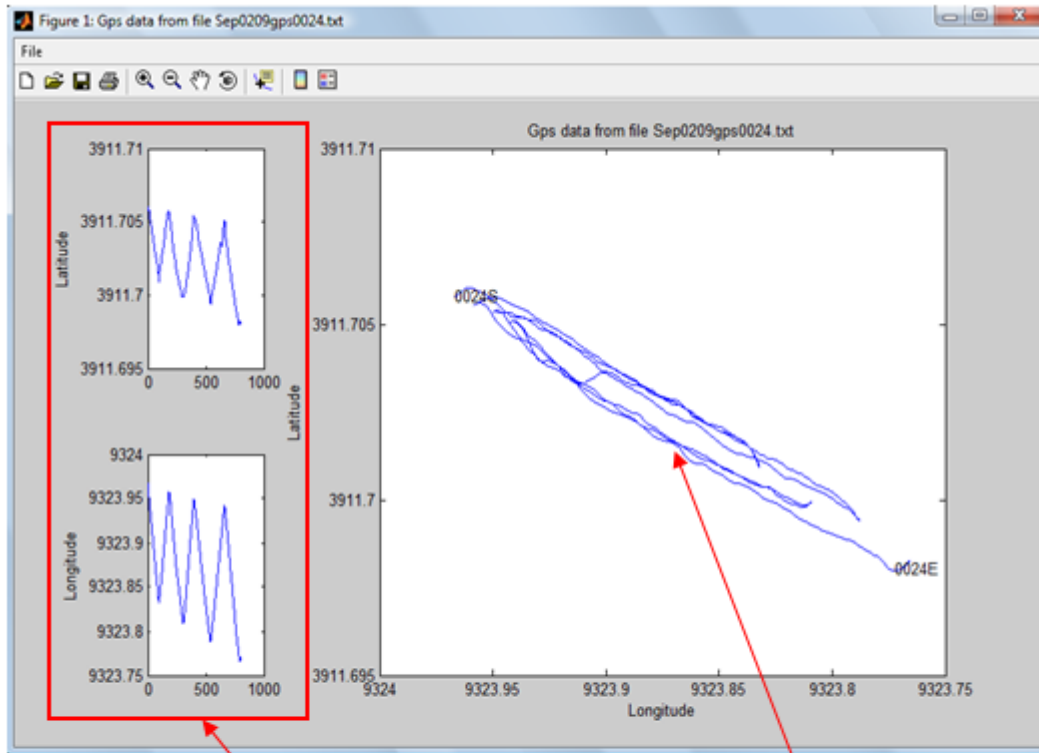

Figure 20. IACA "Plot GPS data" tool

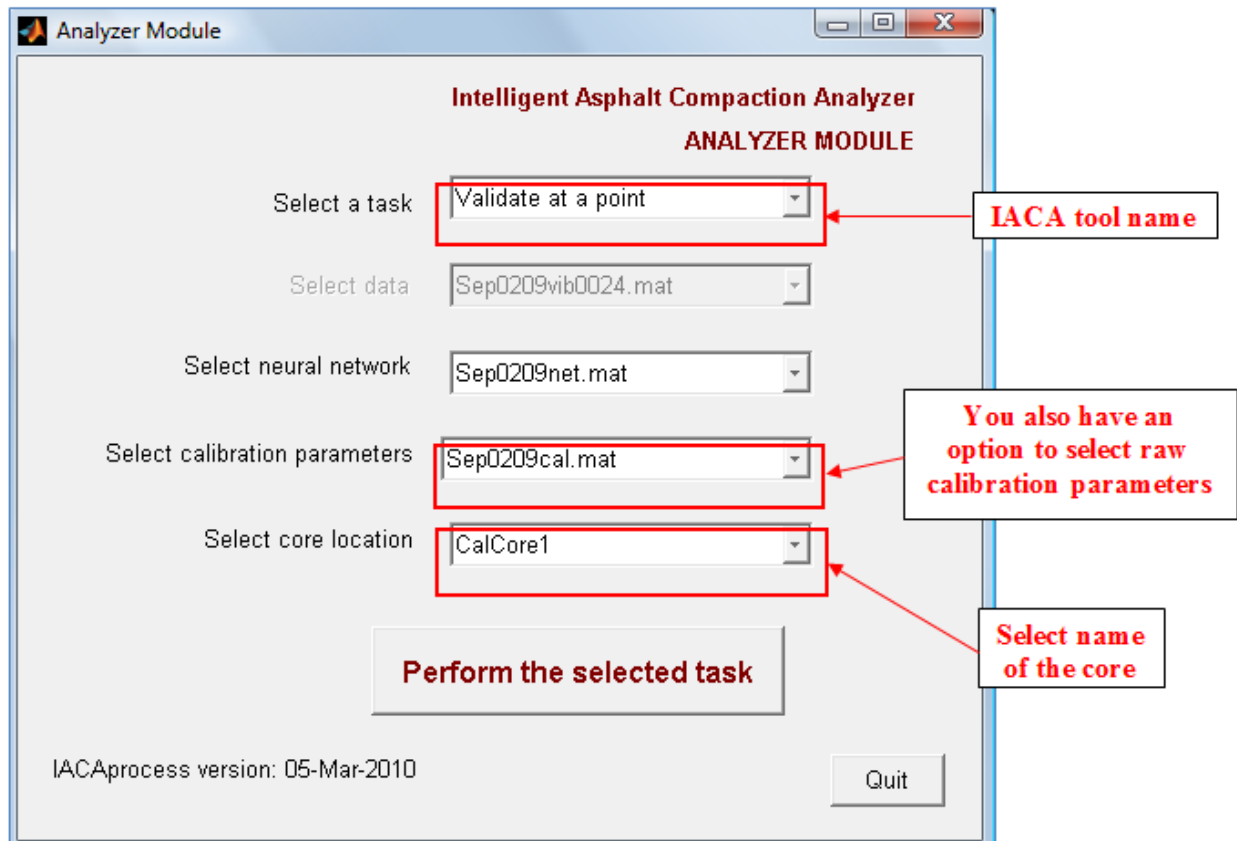An example plot is shown on the following page.

These plots indicate the number of passes taken by the roller during that stretch

This plot indicates the rolling pattern of the roller including the direction and position of it

4.2.3 Validate the compaction values at a point

Using the "Validate at a point " tool in IACA, we can estimate the density of a particular point or location on the pavement. Use the scroll down menu (as shown in the figure below) to select the core location and then push "Perform the selected task" button. This will generate a figure displaying the density during each pass for the selected core.
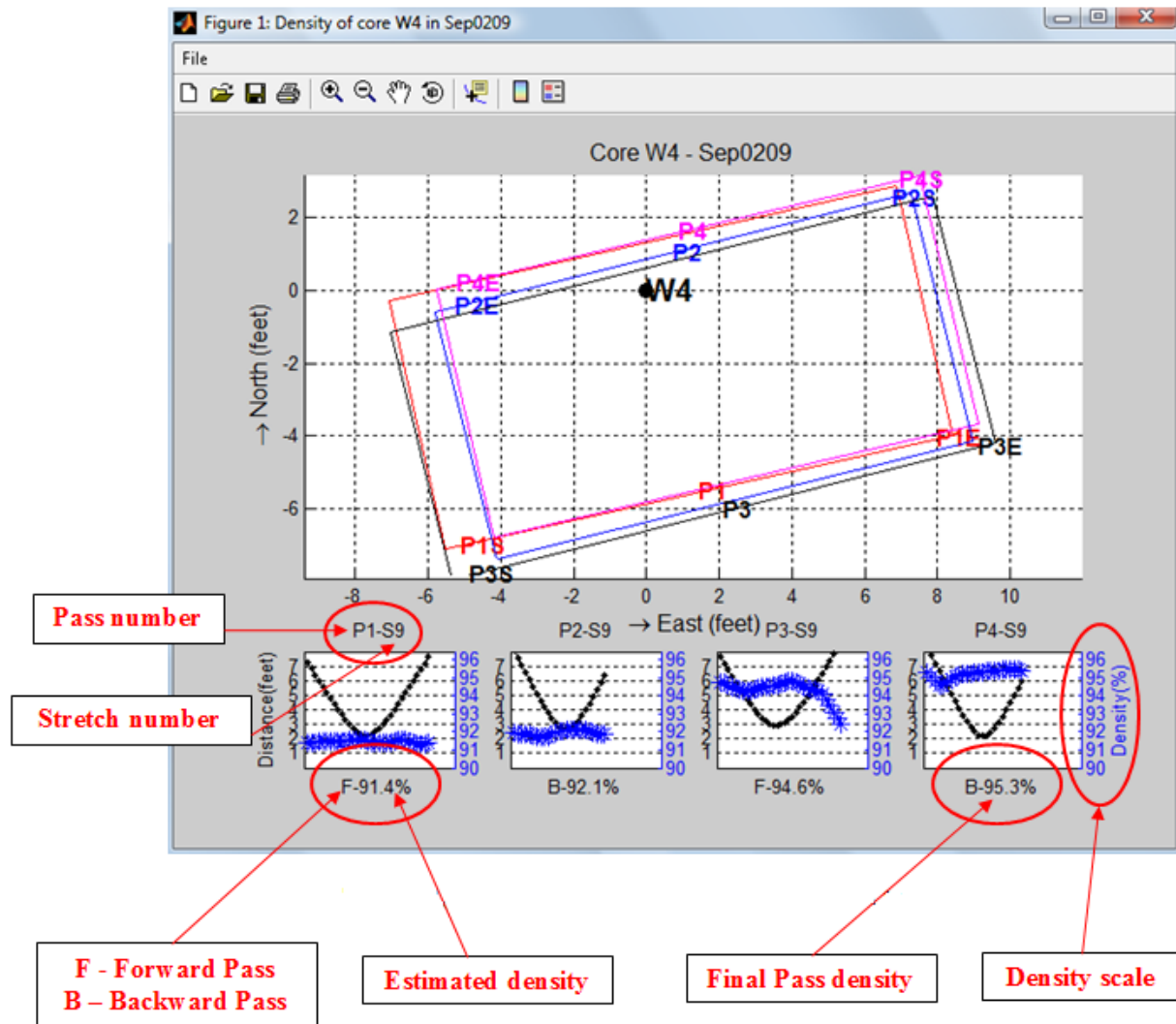
An example figure is shown on the following page.

Figure 21. Estimated Density of a core using IACA tool

5.0 Usage and Precautions

The IACA is capable of displaying the density of the asphalt mat continuously during its compaction. This information is also stored along with the GPS data and other relevant information for analysis of the quality achieved. While the accuracy of the measured densities have been found to be comparable to hand held devices used for in-situ testing of the density, a proper understanding of the technology and the calibration process is essential to obtaining accurate measurements. The following points must be kept in mind during the calibration and use of the IACA.

- Proper calibration is key to getting accurate measurements of density.

- The density obtained on compaction of an asphalt pavement depends on the mix, lift thickness, compacting equipment, and more importantly on the underlying layers of asphalt as well as the subgrade. Inability to obtain desired compaction can usually be traced to a poor asphalt mix or to insufficient preparation of the site.

- For accurate results, the IACA must be calibrated for each layer of the pavement under construction. Further, recalibration is warranted whenever there is an appreciable change in either the mix or the site characteristics.

- GPS sensors require a clear line of sight to the satellites for their proper functioning. Roadway construction under bridges and overpasses, as well as in cities with tall structures, poses a problem in determining the spatial location of the roller.

6.0 Removal and Care of IACA Components

The IACA and associated components have been designed for easy installation and removal. While it may be necessary to retain the equipment for a period of several weeks during the evaluation process, it is necessary to remove the computational platform (Tablet PC) and the GPS receiver at the end of each day's activities. The following steps must be followed to safely remove the Tablet PC and the sensor.

Step 1. Save all relevant files and terminate the IACA application on the Tablet PC.

Step 2. Power off the Tablet PC and disconnect connectors C1-C3. Also, carefully disconnect the ribbon cable connector and the GPS connector.

Step 3. Ensure that the compactor is turned off and securely parked. Remove the GPS receiver from the room of the compactor by gently prying the magnet off from the frame.

Step 4. Use the power adapter to charge the internal battery of the GPS sensor for future use.

Step 5. Carefully pack the Tablet PC taking care to not scratch or damage the PC display.

At the completion of the evaluation, the user is required to remove all the IACA components, place them in their original packages, and ship the IACA back to the University of Oklahoma.

The address for shipping is:

Attn. Dr. Sesh Commuri
University of Oklahoma
School of Electrical and Computer Engineering,
Devon Engineering Hall, Room 432
110 W. Boyd St., Norman, OK 73019

7.0 Troubleshooting

- Make sure the tablet PC is **ON** before connecting the GPS receiver.
- When charging the battery of the GPS receiver, please disconnect the battery from the receiver before connecting the charger.
- If the TabletPC is not receiving power, then check the fuse in the connector embedded in the power cable.